

Leg 188 Preliminary Report

Prydz Bay–Cooperation Sea, Antarctica: Glacial History and Paleoceanography

Shipboard Scientific Party

Ocean Drilling Program
Texas A&M University
1000 Discovery Drive
College Station TX 77845-9547
USA

April 2000

This report was prepared from shipboard files by scientists who participated in the cruise. The report was assembled under time constraints and does not contain all works and findings that will appear in the *Initial Reports* of the ODP *Proceedings*. Reference to the whole or to part of this report should be made as follows:

Shipboard Scientific Party, 2000. Leg 188 Preliminary Report: Prydz Bay–Cooperation Sea, Antarctica: glacial history and paleoceanography. *ODP Prelim. Rpt.*, 88 [Online]. Available from World Wide Web: <http://www-odp.tamu.edu/publications/prelim/188_prel/188prel.pdf>. [Cited YYYY-MM-DD]

Distribution

Electronic copies of this series may be obtained from the Ocean Drilling Program's World Wide Web site at <http://www-odp.tamu.edu/publications>.

DISCLAIMER

This publication was prepared by the Ocean Drilling Program, Texas A&M University, as an account of work performed under the international Ocean Drilling Program, which is managed by Joint Oceanographic Institutions, Inc., under contract with the National Science Foundation. Funding for the program is provided by the following agencies:

Australia/Canada/Chinese Taipei/Korea Consortium for Ocean Drilling
Deutsche Forschungsgemeinschaft (Federal Republic of Germany)
Institut National des Sciences de l'Univers-Centre National de la Recherche Scientifique
(France)
Ocean Research Institute of the University of Tokyo (Japan)
National Science Foundation (United States)
Natural Environment Research Council (United Kingdom)
European Science Foundation Consortium for the Ocean Drilling Program (Belgium, Denmark,
Finland, Iceland, Italy, The Netherlands, Norway, Portugal, Spain, Sweden, and Switzerland)
Marine High-Technology Bureau of the State Science and Technology Commission of the
People's Republic of China

Any opinions, findings, and conclusions or recommendations expressed in this publication are those of the author(s) and do not necessarily reflect the views of the National Science Foundation, the participating agencies, Joint Oceanographic Institutions, Inc., Texas A&M University, or Texas A&M Research Foundation.

The following scientists were aboard *JOIDES Resolution* for Leg 188 of the Ocean Drilling Program:

Alan K. Cooper
Co-Chief Scientist
Department of Geological and Environmental
Sciences
Building 320, Room 118
Stanford University
Stanford CA 94305
USA
Phone: (650) 723-0817
Fax: (650) 725-2199
E-mail: akcooper@pangea.stanford.edu
Home Phone/Fax: (650) 321-3644

Philip E. O'Brien
Co-Chief Scientist
Petroleum and Marine Division
Australian Geological Survey Organisation
GPO Box 378
Canberra, ACT 2601
Australia
Phone: 61-2-6249-9409
Fax: 61-2-6249-9920
E-mail: Phil.O'Brien@agso.gov.au

Carl Richter
Staff Scientist
Ocean Drilling Program
Texas A&M University
1000 Discovery Drive
College Station TX 77845
USA
Phone: 409-845-2522
Fax: 409-845-0876
E-mail: richter@odpemail.tamu.edu

Samantha R. Barr
LDEO Logging Trainee
Leicester University Borehole Research
Department of Geology
University of Leicester
University Road
Leicester, LE1 7RH
United Kingdom
Phone: (44) 116-252-3608
Fax: (44) 116-252-3918
E-mail: srb7@leicester.ac.uk

Steven M. Bohaty
Paleontologist (diatoms)
Department of Geosciences
University of Nebraska
214 Bessey Hall
Lincoln NE 68588-0340
USA
Phone: (402) 472-2648
Fax: (402) 472-4197
E-mail: sbohaty@unlserve.unl.edu

George E. Claypool
Organic Geochemist
8910 W. 2nd Avenue
Lakewood CO 80226
USA
Phone: 303-237-8273
Fax: 303-237-8273
E-mail: geclaypool@aol.com

John E. Damuth
Sedimentologist
Department of Geology
University of Texas at Arlington
PO Box 19049
500 Yates Street, Room 107
Arlington TX 76019-0049
USA
Phone: (817) 273-2976
Fax: (817) 273-2628
E-mail: damuth@uta.edu

Patrick S. Erwin
Paleomagnetist
Earth Sciences
Oxford University
Parks Road
Oxford, Oxfordshire OX1 3PR
United Kingdom
Phone: (44) 1865-272-047
Fax: (44) 1865-272-72
E-mail: patricke@earth.ox.ac.uk

Fabio Florindo
 Paleomagnetist
 Geomagnetism and Paleomagnetism
 Istituto Nazionale di Geofisica
 Via di Vigna Murata 605
 Rome, 00143
 Italy
 Phone: (39) 06-51-860-383/238
 Fax: (39) 06-5041-181
 E-mail: florindo@ingrm.it

Carl Fredrik Forsberg
 Physical Properties Specialist
 Norwegian Polar Institute
 Polarmiljøsentret
 N-9296 Tromsø
 Norway
 Phone: 47 77 75 06 53 or 47 77 75 05 00
 Fax: 47 777 50 501
 E-mail: carl.forsberg@npolar.no

Jens Grützner
 GEOMAR Research Center for Marine
 Geosciences
 Christian-Albrechts-Universität zu Kiel
 Wischhofstrasse 1-3, Gebäude 8/C
 Kiel, 24148
 Germany
 Phone: 49-431-600-2321
 Fax: 49-431-600-2926
 E-mail: jgruetzner@geomar.de

David A. Handwerker
 JOIDES Logger
 Department of Geology and Geophysics
 University of Utah
 1460 East 135 South
 Room 719
 Salt Lake City UT 84105
 USA
 Phone: 801-585-5328
 Fax: 801-581-7065
 E-mail: dahandwe@mines.utah.edu

Nicole N. Januszczak
 Sedimentologist
 Department of Geology
 University of Toronto at Scarborough
 1265 Military Trail
 Scarborough, ON M1C 1A4
 Canada
 Phone: (416) 287-7238
 Fax: (416) 287-7279
 E-mail: janus@scar.utoronto.ca

Alexander Kaiko
 Sedimentologist
 Department of Applied Geology
 Curtin University of Technology
 GPO Box U1987
 Perth, WA 6845
 Australia
 Phone: 61-8-9266-4459
 Fax: 61-8-9266-3153
 E-mail: Alexk@lithos.curtin.edu.au

Kelly A. Kryc
 Inorganic Geochemist
 Earth Sciences
 Boston University
 685 Commonwealth Avenue
 Boston MA 02215
 USA
 Phone: (617) 353-4085
 Fax: (617) 353-3290
 E-mail: kkryc@bu.edu

Mark Lavelle
 Inorganic Geochemist
 Geological Sciences
 British Antarctic Survey
 High Cross, Madingley Road
 Cambridge, CB3 0ET
 United Kingdom
 Phone: 44-1223-221-421
 Fax: 44-1223-362-616
 E-mail: mlavelle@esc.cam.ac.uk

Sandra Passchier
Sedimentologist
Geological Sciences
Ohio State University
130 Orton Hall
155 S. Oval Mall
Columbus OH 43210
USA
Phone: (614) 292-2605
Fax: (614) 292-1496
E-mail: passchier.1@osu.edu

James J. Pospichal
Paleontologist (nannofossils)
Department of Geology
Florida State University
Tallahassee FL 32306
USA
Phone: (850) 644-5860
Fax: (850) 644-4214
E-mail: jim@bugware.com

Patrick G. Quilty
Paleontologist (foraminifers)
School of Earth Sciences
University of Tasmania
Sandy Bay Campus
GPO Box 252-79
Hobart, TAS 7050
Australia
Phone: (61)3-6226-2814
Fax: (61)3-6223-2547
E-mail: p.quilty@utas.edu.au

Michele A. Rebesco
Sedimentologist
Geofisica della Litosfera
Istituto Nazionale di Oceanografia e di
Geofisica Sperimentale
Borgo Grotta Gigante 42/C
Sgonico, Trieste 34010
Italy
Phone: 39-040-2140252
Fax: 39-040-327307
E-mail: mrebesco@ogs.trieste.it

Kari O. Strand
Sedimentologist
Thule Institute
University of Oulu
Linnanmaa
PO Box 7300
FIN-90014
Phone: 358-8-553-3556
Fax: 358-8-553-3564
E-mail: kari.strand@oulu.fi

Brian Taylor
Physical Properties Specialist
Jacques Whitford and Associates
3 Spectacle Lake Drive
Dartmouth, NS B3B 1W8
Canada
Phone: (902) 468-0432
Fax: (902) 468-9009
E-mail: btaylor@jacqueswhitford.com

Kevin M. Theissen
Sedimentologist
Geological and Environmental Sciences
Stanford University
Building 320, Room 118
Stanford CA 94305-2215
USA
Phone: (650) 281-7998
Fax: (650) 725-0979
E-mail: theissen@pangea.stanford.edu

Detlef A. Warnke
Sedimentologist
Department of Geological Sciences
California State University, Hayward
25800 Carlos Bee Boulevard
Hayward CA 94542-3088
USA
Phone: (510) 885-4716
Fax: (510) 885-2526
E-mail: dwarnke@csu Hayward.edu

Patricia A. Whalen
Paleontologist (radiolarians)
Wolf Ridge
968-CR-206
Eureka Springs AR 72632
USA
Phone: (501) 253-5011
Fax: (501) 253-2031
E-mail: micropaw@ipa.net

Jason M. Whitehead
Paleontologist (diatoms)
Department of Geosciences
University of Nebraska
214 Bessy Hall
Lincoln NE 68588-0340
USA
Phone: (402) 472-2648
Fax: (402) 472-4917
E-mail: jm_whitehead@hotmail.com

Trevor Williams
LDEO Logging Scientist
Borehole Research Group
Lamont-Doherty Earth Observatory
Route 9W
Palisades NY 10964
USA
Phone: (914) 365-8626
Fax: (914) 365-3182
E-mail: trevor@ldeo.columbia.edu

SCIENTIFIC REPORT

ABSTRACT

Ocean Drilling Program (ODP) Leg 188 was drilled based on one of five linked proposals to decipher Cenozoic glacial history and paleoenvironments of Antarctica by drilling transects across the continental margin in five different regions. ODP Leg 178 (Antarctic Peninsula) was the first such proposal to be drilled. Three sites were drilled on Leg 188, with one each on the Prydz Bay continental shelf, slope, and rise. These sites provide records of the transition from East Antarctic preglacial to glacial conditions on the shelf (Site 1166); the variability of onshore erosion areas and glaciomarine depositional settings, during latest Neogene glacial–interglacial periods, on the slope (Site 1167); and the long-term, lower to upper Miocene transition from temperate to cold-climate glaciation, with superimposed short-term glacier fluctuations since early Miocene time (Site 1165). These sites document the paleoenvironments for select periods during Cenozoic and older times as Antarctica transformed from a temperate to polar setting.

INTRODUCTION

The Antarctic Ice Sheet and the ocean surrounding it are key components in the global climate regime from the early Cenozoic to the present. The steep climatic gradient generates the vigorous atmospheric and oceanic circulation of the Southern Hemisphere, and sea ice formation ventilates and provides nutrients to much of the world's oceans. Deep water mass formation around Antarctica is also a major sink for atmospheric carbon dioxide. The ice sheet is also the most likely governor of rapid eustatic sea-level change (Barrett, 1999). As part of the effort to understand the mechanics of Antarctic climate and its likely response to change, the Scientific Committee for Antarctic Research (SCAR) Working Groups on Geology and Solid Earth Geophysics have supported the Antarctic Offshore Stratigraphy Project (ANTOSTRAT), which has developed a series of Ocean Drilling Program (ODP) proposals for drilling on the Antarctic margin.

Because of its long history of sedimentation, Prydz Bay was seen as a place to investigate the long-term record of Antarctic glaciation. Also, the size of the Lambert Glacier–Amery Ice Shelf system that enters the bay in relation to the total drainage from East Antarctica (~20%) makes it a potential indicator of the state of the East Antarctic interior. It complements other ANTOSTRAT-identified regions that hold records of fast-responding coastal ice centers (Antarctic Peninsula), the West Antarctic Ice Sheet (Ross Sea), and coastal East Antarctica (Wilkes Land) (Barker et al., 1998). Leg 188 was designed to build on the results of Leg 119 by investigating the history of the Lambert–Amery system during key periods of the Cenozoic. In particular, the proposal aimed at dating the earliest arrival of glacier ice on the shelf,

documenting the number and timing of late Neogene expansions of the ice to the shelf edge, and extracting a climate record from the interbedding of continent-derived siliciclastics and marine biogenic sediments on the continental rise.

Investigations of Antarctic Cenozoic Climate History

Antarctic climate history has largely been deduced from oceanic proxy records, from fragmentary onshore outcrops and from several drilling campaigns around the margin. Modeling of ice sheet development has also been used to extend this fragmentary record and to provide a guide for further work, but it needs continual calibration with the geological record.

The main proxy records from marine sediments that have been used so far are eustatic sea level curves, Oxygen isotope ($\delta^{18}\text{O}$) records and ice-rafted debris (IRD) records. Sea-level curves are probably the most controversial; some workers claim a record of ice expansion extending back to the Mesozoic (Miller et al., 1999), whereas others doubt the validity of global correlation based on eustasy because of regional tectonic influences and a lack of precision in correlation (e.g., Miall, 1986). Short-term global eustatic changes during the Pleistocene are generally recognized as driven by ice volume changes, but the role of the Antarctic Ice Sheets even for the Pleistocene is not clear. The initial assumption that Antarctica ice extended to the shelf edge during the last glacial maximum (LGM) (Denton and Hughes, 1981) used in modeling postglacial sea-level rise has been shown not to be accurate in the Ross Sea (Licht et al., 1996), some coastal oases (Goodwin, 1992), and Prydz Bay (Domack et al., 1998).

Ice-rafted debris indicates the presence of floating debris-charged icebergs at a particular site, but its interpretation in terms of climate and glacial history is extremely complex because of the many poorly understood factors influencing the discharge and dispersal of debris-rich icebergs. IRD records can set a minimum age for the arrival of calving glaciers at the coast and the increase of icebergs associated with climatic cooling.

Oxygen isotope variations are the only measurement of global ice volume that is relatively continuous for the Cenozoic, with curves published and interpreted back to the Paleocene (e.g., Abreu and Anderson, 1998; Flower, 1999). Some researchers have used isotope curves to argue for the onset of glaciation in Antarctica as early as the Paleocene (Denton et al., 1991), whereas others argue for glacial onset in the early to middle Eocene (Abreu and Anderson, 1998). Major ice expansions have been inferred at 33.6 Ma, (Eocene/Oligocene boundary), 23.7 Ma (Oligocene–Miocene), 12 to 16 Ma (middle Miocene), and 2.7 Ma (late Pliocene) that marked the onset of Northern Hemisphere glaciation (Flower, 1999). For all the value of $\delta^{18}\text{O}$ curves, they are a function of both temperature and global ice volumes, making for ambiguity in the detailed interpretation of the record (Wise et al., 1992; Barker et al., 1999). The ability of isotope curves to resolve short-term changes is strongly dependent on finding sedimentary sections with sufficient resolution to avoid aliasing the signal and so becomes more difficult with increasing age of the section. Also, isotope curves are a measure of global ice volume and cannot provide information on the distribution of ice between the continents during periods of bipolar glaciation.

Neither can they indicate the distribution and interplay of ice and the ocean around different parts of Antarctica, information necessary for calibrating models of glaciation, or details of the Antarctic environment.

Deposits and landforms on the Antarctic continent provide a direct window into Antarctic climate history that can be very detailed (e.g., Quilty, 1991) but, by their nature, are fragmentary and difficult to correlate. Difficulties in the correlation of sediments in the Transantarctic Mountains have led to major disagreements over the extent of ice retreat during the Pliocene (Webb et al., 1984; Denton et al., 1991; Warnke et al., 1996). However, outcrops and landforms also indicate the possible complexities of responses by the ice to climate change with out-of-phase expansion of valley glaciers and the ice sheet first reported by Scott (1905).

Drilling of continental shelf sediments can provide a record of ice expansion onto the shelf and the evolution of shelf environments but must be considered in the light of both (1) depositional models for the facies present and (2) sequence stratigraphic models of facies stacking patterns and preservation (Fielding et al., 1998). Such concepts need to be applied to drilling of sections on the continental shelf and slope because of the strongly reciprocal nature of glacial–interglacial sedimentation on continental margins (Boulton, 1990). During major ice advances, the shelf tends to be eroded followed by the deposition of compact till, a difficult stratigraphic record to sample and interpret (Barron et al., 1991). At the same time, significant deposits are forming on the upper slope in trough mouth fans (Vorren and Laberg, 1997) or sediment transfers to the continental rise as turbidite deposits or contourite drifts (Rebesco et al., 1997).

A more complete picture of glacial history can be obtained by linking onshore outcrop data to the deep sea record through drilling key locations on the Antarctic shelf, slope and rise. Leg 188 was designed to provide such a transect, building on the work of Leg 119 (Barron, Larsen, et al., 1991) and linking studies of Cenozoic glacial sediments in the Prince Charles Mountains (Hambrey and McKelvey, in press) and around Prydz Bay (Quilty, 1991) to the oceanic record. Linking these data sources has the potential to provide a transect extending ~1000 km from the interior of East Antarctica to the continental rise along a single ice drainage system.

Aims of the Leg

Onset of Glaciation

Prydz Bay is at the downstream end of a drainage system that rises in the Gamburtsev Mountains in central East Antarctica (Fig. 1). Modeling studies of ice sheet development indicate that these mountains, if present in the Paleogene, would be the first area to develop extensive ice cover. Thus, Prydz Bay could contain the first sedimentary evidence of ice in East Antarctica. Evidence on the early development of the Antarctic Ice Sheet has been interpreted as indicating initiation of ice sheet growth from as early as the early middle Eocene to the early Oligocene (Abreu and Anderson, 1998; Barron et al., 1991). As yet, there has been no section drilled in the Antarctic that clearly spans the transition period from preglacial to glacial conditions. ODP Site

742 in eastern Prydz Bay reached glacial deposits interpreted by Barron et al. (1991) as late middle Eocene in age. Cooper et al. (1991) estimated that these sediments continued for 100 m below the total depth of Site 742, resting on an erosion surface on older sediments. A hole that drills this lower 100 m as well as the underlying sediments could establish the lower age limit for large-scale glaciation of Prydz Bay. Any preglacial Cenozoic sediments would contain paleontological and sedimentological evidence of the preglacial environment.

Major Events

Oxygen isotope records have been used to infer episodes of increased ice volume at 33.6 Ma, (Eocene/Oligocene boundary), 23.7 Ma (Oligocene/Miocene boundary), 12 to 16 Ma (middle Miocene) and 2.7 Ma (late Pliocene) that marked the onset of Northern Hemisphere glaciation (Flower, 1999). In Prydz Bay, an unconformity identified during Leg 119 (Solheim et al., 1991) may have formed in the late Miocene by a major ice expansion (Barron et al., 1991). Kuvaas and Leitchenkov (1992) studied the seismic facies of the Prydz Bay continental rise and slope and identified the initiation of drift sedimentation, which they suggested could have been related to initiation of the Antarctic Circumpolar Current after the opening of Drake Passage around the Oligocene/Miocene boundary or may relate to a major ice expansion during the Oligocene or Miocene. A hole drilled on the continental rise to intersect the base of the thick drift section could date the onset of drift formation and potentially record changes in rise sedimentation controlled by currents and continental sediment supply. The drift sediments should also contain a record of climate fluctuations reflected in the interplay of siliciclastic fed by the Lambert Glacier drainage system and biogenic sediment.

Late Neogene Fluctuations

A major change in Prydz Bay shelf progradation took place in the late Miocene to mid-Pliocene when a fast-flowing ice stream developed and excavated a channel across the shelf on the western side of Prydz Bay (Harris and O'Brien, 1996). Basal debris carried to the shelf edge was then deposited in a trough mouth fan on the upper slope (Fig. 2). This trough mouth fan probably contains a reasonably complete record of glacial history because it received siliciclastic sediment when the shelf eroded during major ice advances and hemipelagic material during interglacials and smaller glaciations (Vorren and Laberg, 1997). A history of major ice advances for the Antarctic is only just developing and, at present, relies on outcrop studies that have poor time control (Denton et al., 1991) and on seismic stratigraphic studies in which erosion surfaces are identified but the associated sediments have been sparsely sampled (e.g., Alonso et al., 1992). Identification of LGM grounding lines well in from the shelf edge in the Ross Sea (Licht et al., 1996) and Prydz Bay (Domack et al., 1998) means that not every glacial episode sees the full advance of the ice. A section drilled through the Prydz Channel Fan will record the episodes that did produce a major advance and so give insight into the mechanisms of ice sheet growth through multiple glacial cycles.

REGIONAL SETTING OF PRYDZ BAY

Bathymetry

Prydz Bay is a reentrant in the Antarctic margin between 66°E and 79°E. It is bounded on the southwestern side by the Amery Ice Shelf, on the southeast by the Ingrid Christensen Coast and by Mac. Robertson Land to the west, ending in Cape Darnley (Fig. 3). The eastern side of the bay has water depths from 200 to 300 m near the shelf edge forming Four Ladies Bank (Fig. 3). The bank surface slopes gently inshore and to the west. Along the Ingrid Christensen Coast, water depths reach 1000 m in the Svenner Channel. In front of the Amery Ice Shelf, the Amery Depression is mostly 600–700 m deep but reaches 1400 m in several closed depressions in the southwestern corner of the bay called the Lambert and Nanok Deeps (Fig. 3). The western side of the bay is crossed by a channel that runs from the Amery Depression to the shelf edge, where the seafloor is at 600 m below sea level. This feature is the Prydz Channel. It separates the Four Ladies Bank from Fram Bank, the shallow area around Cape Darnley (Fig. 3).

The continental slope on the eastern half of Prydz Bay is steep with submarine canyon tributaries and slump deposits (O'Brien and Leitchenkov, 1997). On the western side, contours bulge seaward in the Prydz Channel Fan (Fig. 3), which slopes smoothly from the shelf edge to its edge at ~2700 m water depth. The head of a submarine canyon (Wilkins Canyon) (Vanney and Johnson, 1985) is situated just west of the Prydz Channel Fan, north of Fram Bank (Fig. 3). It runs north from the shelf edge and then bends northeast from ~65°S. To the west of Wilkins Canyon is a ridge of drift sediment that separates it from Wild Canyon, which has its head on the continental slope off Mac. Robertson Land (Kuvass and Leitchenkov, 1992).

Circulation and Water Masses in Prydz Bay

The circulation in Prydz Bay is characterized by a closed cyclonic gyre adjacent to the Amery Ice Shelf (Fig. 4) (Smith et al., 1984; Wong, 1994). There is inflow of some cold water from the east near the West Ice Shelf and outflow near Cape Darnley. In contrast to the Ross and Weddell Sea basins, Prydz Bay holds a relatively small volume of highly saline deep water. It has been suggested that this is related to the geography and bathymetry of Prydz Bay (Smith et al., 1984). Because of its closed circulation and lack of significant bottom-water production, water masses in Prydz Bay play a limited role in current activity beyond the shelf.

Circulation on the Continental Rise

Kuvaas and Leitchenkov (1992) interpret the deposits on the continental rise offshore from Prydz Bay as the result of contour-current activity. These currents can be attributed to the activity of large Antarctic deep-water masses. Site 1165 is located within or near a large cyclonic gyre, between 60°E and 100°E (known as the Antarctic Divergence [AD]) (Fig. 4). Here, the eastward-moving Antarctic Circumpolar Current (ACC), driven by prevailing westerlies, meets the westward moving Polar Current (PC). A study of deep-water circulation showed eastward

flow north of 63°S and a band of westward-flowing water between the AD and the continental rise (Smith et al., 1984). Because of the proximity to the AD, sedimentation in this region may, at various times, have been subject to transportation via the ACC or PC or it may have circulated around the region in accordance with the gyre. The position of the AD may be a key control on the nature of bottom-current activity at this site.

Water Masses in the Prydz Bay Region

Circumpolar Deep Water (CDW) (0° to 2°C; 34.50 to 34.75 salinity), a large mass of cold, moderately saline water along with colder and more saline Antarctic Bottom Water (AABW) (0°C; 34.60 to 34.72 salinity), are the major bodies of deep water carried by the ACC (Smith et al., 1984). AABW is not actively formed in Prydz Bay, where waters are only moderately saline. This large water mass is primarily formed during winter on the margins of the Weddell and Ross Seas. Additionally, large ice shelves are undercut by inflowing water, and brines are winnowed out, making this Ice Shelf Water (ISW) a cold and highly saline component of AABW (e.g., Grobe and Mackensen, 1992). The overlying CDW also comprises a large portion of the water mass and its composition is influenced by North Atlantic Deep Water (NADW) flowing in from the north. Since NADW is a warmer water mass, changes in contribution to CDW have an impact on the development of sea ice in Antarctica.

Glaciology

The major glacial drainage system in the region is the Lambert Glacier–Amery Ice Shelf system. The system drains ~1.09 million km² representing ~20% of the East Antarctic Ice Sheet (Fig. 1) (Allison, 1979). The three largest glaciers are the Lambert, Fisher, and Mellor Glaciers that amalgamate in the southern Prince Charles Mountains to form the main Lambert-Amery ice stream (Fig. 1). They are joined by other glaciers of which the Charybdis Glacier is the largest. It flows from the western side of the northern Prince Charles Mountains (Fig. 1). Most glaciers flowing into the Lambert-Amery system originate more than 200 km from the present coast, although a few small glaciers join the Amery Ice Shelf from the western side.

The grounding zone was thought to be a sinuous line running approximately east–west; however, more recent Global Positioning System (GPS) and satellite image analysis has shown it to be in the southern Prince Charles Mountains, ~500 km upstream from the present seaward edge of the Amery Ice Shelf (Fig. 1). The ice reaches thicknesses of 2500 m in the Southern Prince Charles Mountains. This thins to ~400 m at the seaward edge of the Amery Ice Shelf, of which ~40% is snow that accumulates on the ice shelf and seawater ice that freezes onto the base (Budd et al., 1982).

Maximum ice velocities of 231–347 m/yr have been measured in the Prince Charles Mountains whereas velocities up to 1200 m/yr have been measured for the centerline of the Amery Ice Shelf (Budd et al., 1982). The seaward edge of the Amery Ice Shelf is presently moving northward but this is the result of spreading under its own weight rather than an advance

caused by an increase in mass balance (Budd, 1966). This spreading produces a major iceberg calving event approximately every 50 years; the last one being in 1963 (Budd, 1966).

The other source of glacial ice flowing into Prydz Bay is the Ingrid Christensen Coast where ice cliffs and numerous relatively small glaciers enter the bay. The largest are the Sorsedal that flows south of the Vestfold Hills and the glaciers that contribute to the Publication Ice Shelf. The bedrock swales of the Svenner Channel are seaward of these larger glaciers suggesting that they formed at their confluence with the Lambert during periods when the bay was occupied by grounded ice (O'Brien and Harris, 1996). The western side of Prydz Bay has only a few small glaciers that flow into the Amery Ice Shelf. The coast between the ice shelf and Cape Darnley provides only a small amount of ice because the ice divide is close to the coast.

GEOLOGY

Structure

Prydz Bay is a reentrant in the East Antarctic margin caused by a major crustal structure that extends 700 km inland called the Lambert Graben (Fig. 5) (Federov et al., 1982; Stagg, 1985; Cooper et al., 1991b). Mapping of marine seismic data indicates that the bay is underlain by a basin that is separate to the Lambert Graben named the Prydz Bay Basin by Stagg (1985; Fig. 6). Gravity, magnetic and seismic refraction data indicate maximum sediment thicknesses between 5 and 12 km (Cooper et al., 1991b). The Prydz Bay Basin is separated from the sediment underlying the outer shelf, slope and rise by a north-east plunging basement ridge that extends from the southwestern corner of Prydz Bay (Fig. I-6). This ridge and the basin sediments are extensively faulted with most faults in the southwest being normal down-to-basin faults. The northern end of the ridge is cut by east-west normal faults with large down-to-north displacement that may have formed as part of continental rifting process.

Prince Charles Mountains

Basement

The basement through which the Lambert Glacier and its tributaries flow is extensively exposed in the Prince Charles Mountains. Tingey (1991) distinguishes between the high grade metamorphic rocks of the northern Prince Charles Mountains and the lower grade rocks of the southern Prince Charles Mountains. The northern Prince Charles Mountains consist largely of layered and massive granulite to upper amphibolite facies intruded by charnokite plutons, granite, and pegmatite veins, and alkaline igneous dykes. Metapelites, marbles, skarns, metabasalts, metandesites, and metagabbros are all represented (Tingey, 1991). The southern Prince Charles Mountains have Archean granitic orthogneiss basement overlain by Archean quartzites that are intruded by pegmatites and tholeiitic dykes. These Archean rocks are overlain by Proterozoic greenschist facies metasediments, including conglomerates, sandstone, schists,

and phyllites that are intruded by Cambrian granite. Basement rocks in the Beaver Lake area are intruded by basic dykes including some lamproites (Tingey, 1982).

Phanerozoic Sediments

Geophysical data indicate that the Lambert Graben and Prydz Bay Basin contain several kilometers of sediment. The only outcrops are found at Beaver Lake in the northern Prince Charles Mountains, where a 270-m-thick section of coal-bearing, nonmarine sediments is exposed (Fig. 5; McLoughlan and Drinnan, 1997). The Amery Group is late Permian to Triassic in age (McLoughlan and Drinnan, 1997) and occupies a small fault angle depression on the western side of the Lambert Graben. These sediments are thought to be present within the Lambert Graben as well.

Cenozoic sediments are also present in the Prince Charles Mountains. In the northern Prince Charles Mountains at Beaver Lake some 800 m of diamictons and minor mudstone and sandstone is exposed in Pagodroma Gorge. Hambrey and McKelvey (in press) interpret these deposits, the Pagodroma Group, as glaciomarine fjord infillings that include in situ mollusks and reworked diatoms that suggest middle Miocene, late Pliocene and early Pleistocene ages (< 3.5 Ma) (McKelvey and Stephenson, 1990; Quilty, 1993; Hambrey and McKelvey, in press). Diamictites are also known from Fisher Massif and other parts of the Prince Charles Mountains at higher elevations than the Pagodroma Group. They are possibly of Miocene age (Hambrey and McKelvey, in press).

Prydz Bay

Basement

Coastal outcrops along the eastern side of Prydz Bay comprise high-grade Archean and Proterozoic metamorphic rocks. In the Larseman Hills, 60% of the basement consists of medium- to coarse-grained garnet-bearing gneiss and 10% a distinctive blue rich in cordierite (Tingey, 1991). Smaller outcrops of Proterozoic gneisses and Cambrian granites are scattered along the eastern coast south of the largest area of outcrop in the Vestfold Hills. The basement of the Vestfold Hills is mostly Archean gneisses, including metagabbros and pyroxenites cut by several generations of Proterozoic mafic dykes (Tingey, 1991).

Pre-Cenozoic Sediments

Pre-Cenozoic sediments are known from ODP Sites 740 and 741 (Fig. 7). Two sequences are present; a lower red bed unit and an upper, Aptian coal-bearing sequence (Turner, 1991; Turner and Padley, 1991).

The red bed sequence consists of sandstone interbedded with claystone and siltstone that may reach a thickness of 2–3 km in the center of the Prydz Bay Basin. The sediments are brown red to green gray in color. Sandstone units are as thick as 3 m and are medium to coarse grained, fining up to siltstone and claystone. Turner (1991) describes the sandstones as quartzose with 17% to

66% clay matrix. The matrix is a mixture of chlorite, sericite, biotite, and muscovite. X-ray diffraction (XRD) indicates the presence of illite-smectite and kaolinite in the clay fraction. The red-colored beds contain abundant iron oxide in the matrix; green units are richer in chlorite. Framework grains are predominantly quartz with 6% rock fragments mostly composed of rounded granite gneiss grains made up of quartz, muscovite, chlorite, and feldspar. Feldspars are mostly orthoclase and microcline with very little plagioclase. Turner (1991) interprets the sediments as deposits of floodplains in an actively subsiding basin where rapid uplift, erosion, and deposition preserved their immature composition.

The upper sequence of pre-Cenozoic sediments in the Prydz Bay Basin is composed of mid-Aptian sandstone, siltstone, claystone, and minor conglomerate and coal (Turner and Padley, 1991). Sandstone units are 2–3 m thick and white to gray with cross-bedding and thin conglomerates at their base and abundant plant fragments scattered throughout. Sand grains are predominantly quartz and feldspar with garnet, biotite, and illmenite accessories. Siltstones and claystones are rich in plant fragments with some ripple cross-laminations, and rootlets beds. They form coarsening-up sequences suggesting deposition in crevasse splay deposits in swampy, vegetated floodplains. Sandstone units were probably deposited in low-sinuosity fluvial channels. There are no indications of marine deposition. The presence of coal and abundant plant debris indicates a humid climate (Turner and Padley, 1991).

Cenozoic Outcrops

Cenozoic sediments are exposed in several small areas along the east coast of Prydz Bay (Quilty, 1993). The Larseman Hills features a thin, shallow marine sand containing shell fragments, Pliocene foraminifers and diatoms that suggest an age of between 2 and 3 Ma (Quilty, 1993). Of greater extent and significance are the Pliocene sediments of Marine Plain in the Vestfold Hills (Pickard, 1986; Quilty, 1993). They occupy an area of ~10 km² and reach thicknesses of 8–9 m. The sediment is diatomite, siltstone, and fine sandstone with sponge spicules, bivalves, and a diverse fauna of benthic organisms preserved in places (Quilty, 1993). The most spectacular fossils in the area are Cetacean skeletons, including dolphins and a right whale. Diatom assemblages suggest deposition in less than 75 m of water between 4.2 and 3.5 Ma (Quilty, 1993). The fossils present and preliminary isotope measurements led Quilty (1993) to infer warmer conditions during deposition than currently prevail. Water temperatures may have been as high as 5°C (Quilty, 1993).

Mac. Robertson Shelf

The area immediately to the south of Site 1165 is the Mac. Robertson Land Shelf, which may also have contributed to sedimentation on the continental rise. The Mac. Robertson Shelf is a narrow, rugged shelf west of Prydz Bay that is currently being eroded by iceberg scour and geostrophic currents (Harris and O'Brien, 1996). During the Pleistocene, coastal glaciers excavated U-shaped valleys to the shelf edge (Harris et al., 1996). The inner shelf is underlain by

Precambrian metamorphics and half grabens containing Mesozoic sediments (Truswell et al., 1999). The outer shelf is underlain by offlapping sediments ranging from Cretaceous to Paleogene as indicated by reworked microfossils (Truswell et al., 1999; Quilty et al., in press). Quilty et al. (in press) described Eocene and Oligocene foraminifers along with glauconite from surficial sediments on the shelf.

SEDIMENTATION IN PRYDZ BAY

Cenozoic

The Cenozoic sediments of Prydz Bay are extensively described in results from ODP Leg 119 (Barron, Larson, et al., 1989, 1991). Hambrey et al. (1991) recognized three major sequences composed chiefly of diamictites (Fig. 8). The upper sequence (PS.1 of Cooper et al., 1991a) is up to 250 m thick and flat lying (thickest under Four Ladies Bank) but thin to absent beneath Prydz Channel, Svenner Channel, and the Amery Depression. The second sequence lies unconformably beneath the upper one at Sites 739 and 742 and consists of steeply prograding foresets of massive and stratified diamictite with some evidence of slumping (Fig. 8) (PS.2A, Cooper et al., 1991a). The lowermost sequence is gently inclined massive clast-poor diamictite and bedded diamictite and poorly sorted mudstone. This sequence is richer in kaolinite than the overlying units. The lowermost sequence was dated as middle Eocene to early Oligocene, the upper sequence at Sites 739 and 742 was dated as late Miocene, Pliocene, and Pleistocene. Holocene siliceous, muddy ooze overlies the diamictite in places (Domack et al., 1991).

Hambrey et al. (1991) interpret the massive diamictites as mostly water-lain till formed by rainout from the base of glacial ice close to the grounding zone. They interpret some intervals with deformed bedding, particularly in the dipping, foreset units as debris flows formed from glacial debris with minor amounts of remobilized turbidites and ice-rafted sediment. Hambrey et al. (1991) describe some massive units with preferred orientation of clasts as possible subglacial till units, an interpretation supported by evidence of overcompaction of some intervals in the upper, flat-lying sequence (Solheim et al., 1991).

Hambrey et al. (1991) interpret the succession along the Leg 119 transect as indicating a history of earliest glaciation of the shelf in the Eocene to early Oligocene reworking preglacial Eocene sediments and depositing the lower, gently dipping sediments on the shelf. The ice then moved onto the shelf as a floating tongue and prograded the shelf edge in the early Oligocene. A major expansion of ice that Hambrey et al. (1991) regard as the largest pre-Quaternary expansion occurred during the late Oligocene to early Miocene.

Seismic data through the Leg 119 drill sites indicate that the flat-lying upper sequences pass seaward into foreset beds that prograde the continental shelf edge (Fig. 8; Cooper et al., 1991a, 1991b). Farther west where Prydz Channel crosses the shelf, the topsets are thin to absent and deposition has been concentrated on the upper slope in a trough mouth fan called the Prydz

Channel Fan (Fig. 9). Landward of Four Ladies Bank, the topsets pinch out and the Amery Depression is covered with a thin layer of till and glaciomarine clayey silts and sands and siliceous muddy ooze overlying Cretaceous and older sediments. Leitchenkov et al. (1994) suggested that the shelf prograded more or less evenly across the bay until some time from the late Miocene to Pliocene. A readily mappable erosion surface (pp12, Surface A of Mizukoshi et al., 1986) marks the development of Prydz Channel and the start of Prydz Channel Fan sedimentation at this time. The fan has been the major depocenter since then although the Four Ladies Bank has continued to receive topsets of till (Fig. 9).

The Prydz Bay continental slope and rise are underlain by thick (more than 6000 m) drift sediments, some in elongated ridges aligned along the margins of deep channels, others having no clear correlation with channels, but all of them elongate approximately orthogonal to the continental margin (Kuvass and Leitchenkov, 1992). The seismic geometry of these drifts suggests that they have been deposited as a result of the interaction of downslope mass flow and strong bottom (contour) currents. By analogy with other drift deposits on the Antarctic margin (Rebesco et al., 1997; Shipboard Scientific Party, 1999), the drifts are composed of alternating clastic- and biogenic-rich intervals that reflect alternations of glacial and interglacial conditions. Such records can be compared to the proximal records of the continental shelf and upper slope to understand the relationship between oceanographic conditions and the advance and retreat of the ice sheet.

The most conspicuous sediment drifts are developed in the western part of the Cooperation Sea between Wilkins and Wild Canyons and are referred to as the Wilkins and Wild Drifts (Fig. 3). Kuvaas and Leitchenkov (1992) recognized two major seismic unconformities (P1 and P2). Additional data and reinterpretation have allowed the mapping of a third surface younger than P1 and P2. Surface P1 within these sediments marks the transition from a lower homogeneous part of section, with mostly irregular reflectors, to an upper, heterogenous one in which a variety of well-stratified seismic facies are present. More distal data suggests that P1 may be as old as Cretaceous. Surface P2 marks a change to submarine canyons and to related channel and levee deposits and chaotic seismic facies. Kuvaas and Leitchenkov (1992) interpret this transition resulting from the onset of continental glaciation in the Eocene or the arrival of grounded ice sheets at the shelf edge in the early Oligocene, as indicated by ODP Sites 739 and 742 (Barron et al., 1991). This sedimentation change produced thick, prograding foresets above the P2 unconformity beneath the Prydz Bay outer shelf (Kuvaas and Leitchenkov, 1992).

Surface P3, above P2, represents the base of deposits containing abundant, well-stratified sediment drift facies, including sediment waves. Sediment wave geometry implies that strong, westerly flowing bottom currents played a significant role in drift formation. The changes at this level could have been related to initiation of the ACC after the opening of Drake Passage around the Oligocene/Miocene boundary or may relate to a major ice expansion during the Oligocene or Miocene.

Quaternary to Modern Sediments

The parts of Prydz Bay shallower than 690 m are extensively ploughed by iceberg keels (O'Brien and Leitchenkov, 1997) and so are covered with a layer of disturbed sediment. Surface sediments and their diatom floras are described in Harris et al. (1998). Areas deeper than this have undisturbed Quaternary sections. The Amery Depression inshore from grounding zone wedges in Prydz Channel is floored by fluted subglacial till and draped in places by clayey diatom ooze deposited since ice retreat in the last 12,000 years (Domack et al., 1998; O'Brien et al., 1999). The tills are dark gray pebbly sandy clays with high magnetic susceptibility in most of the Amery Depression but in the southwestern corner of the Bay, in the Lambert Deep, tills are brown-red with low susceptibility derived from pre-Cretaceous red bed sediments in the Lambert Graben (Domack et al., 1998). Prydz Channel seaward of the grounding zone wedges, is floored by smooth seafloor and iceberg scours draped by gray clays and diatom ooze. These draped iceberg scours are probably relict features from LGM low sea levels.

PRINCIPAL RESULTS

Site 1166: Continental Shelf (Prydz Bay)

Site 1166 is situated on the Prydz Bay continental shelf on the southwestern flank of Four Ladies Bank, ~40 km southwest of ODP Site 742, which was drilled on Leg 119 (Fig. 10). Prydz Bay is at the downstream end of a drainage system that originates in the Gamburtsev Mountains of central East Antarctica. The early development and growth of the Cenozoic Antarctic Ice Sheet is believed to have started in the early middle Eocene to early Oligocene, but, to date, drilling on the continent and the continental margin has not sampled a stratigraphic section that clearly spans and includes the transition period from preglacial to glacial conditions. Site 1166 was chosen to recover core from the Cenozoic sediments below the horizon reached at Site 742. This was intended to provide an age for the arrival of glaciers in Prydz Bay and a record of changes in paleoenvironments and biota with the onset of glaciation.

When the ship arrived in Prydz Bay, the drill site had to be moved to an alternate site because pack ice covered much of western Prydz Bay where the primary site was located. An additional 3-nmi displacement of the site was required because a large tabular iceberg was resting directly over the alternate site. The target sedimentary section (Fig. 11) was thinner and likely a bit younger near the base of the section at the final alternate site (i.e., Site 1166) than at the primary site. The drilling at Site 1166 was conducted safely and achieved the desired objective under the sometimes cold and stormy operating conditions.

Drilling at Site 1166 had to be halted temporarily about midway through the drilling because of a large storm with wind gusts exceeding 40 kt and swells greater than 2 m, the maximum limit for shallow-water drilling. During the storm, an iceberg approached within 0.6 nmi and the drill pipe had to be pulled out of the seafloor, without a reentry cone in place, and the ship moved

away from the site. Following the storm, the ship returned to the site and successfully reentered the hole to continue uninterrupted drilling to a total depth of 381.3 mbsf. Recovery at the site was 18.6%, with low recovery due partly to drilling through the upper section (135 mbsf) of diamictites, similar to those sampled at Site 742, and because of sandy fine-grain sediments in the lower part of the hole. Three full logging runs were obtained with excellent data from ~50 mbsf to the bottom of the hole.

The sedimentary section at Site 1166 comprises a diverse suite of strata that from the top down include glacial, early glacial, and preglacial rocks that consist of poorly sorted, sandy, and fine-grained sediments. The ages range from Holocene at the seafloor to Early Cretaceous(?) at the bottom of the hole, with many disconformities throughout. Age determinations have not been made for two units, pending palynologic analyses.

The sediments are divided into five lithostratigraphic units (Fig. 12). Lithostratigraphic Unit I is of late Pliocene to Holocene age and comprises four subunits. The uppermost subunit (Subunit IA; 0.0–2.74 mbsf) is a biogenic-rich clay interval with pebble-sized clasts. This unit is interpreted as an ice-keel turbate, based in part on iceberg furrows that occur in echo-sounder records in this area (O'Brien and Leitchenkov, 1997).

Below Subunit IA are two intervals of diamicton and one of poorly sorted clayey sandy silt. Subunits IB (2.79–106.36 mbsf) and ID (123.0–135.41 mbsf) are separated by a thin interval (Subunit IC; 113.30–117.22 mbsf) of biogenic-rich clayey silt. Subunit IB is predominately clayey silt with rock pebbles and clasts that include common fibrous black organic matter. Minor (<2 cm thick) sand and granule beds are present. Subunit IC is interbedded dark gray sandy silt with lonestones and greenish gray diatom-bearing clayey silt with dispersed granules. Biogenic-rich intervals are slightly bioturbated. Contacts with the dark silt are sharp. Subunit ID has interbeds of dark gray clast-poor and clast-rich diamicton. Clast lithologies vary and include gneiss, granite, and diorite rocks. The diamictons suggest subglacial deposition; the sandy silt with IRD is a glaciomarine unit deposited during interglacial periods.

Unit I has lonestones throughout. For Subunits IB and ID, the diamictons suggest subglacial deposition or deposition of a proglacial morainal bank. Sandy silt intervals with shell fragments and microfossils (Subunit IC) suggest current reworking and glaciomarine sedimentation during times of significant glacial retreat. The lonestones signify deposition of ice-rafted debris. In seismic reflection data, Unit I comprises the topset beds of the seaward-prograding sedimentary section of the outer continental shelf. The contact between lithostratigraphic Unit I and Unit II is an abrupt unconformity and was recovered (interval 188-1166A-15R, 8–11 cm). XRD data above and below the unconformity show shifts in relative abundances of mica, illite, kaolinite, hornblende, and plagioclase. The shifts suggest increased amounts of weathered terrigenous material within Unit I, just above the unconformity.

Unit II (135.63–156.62 mbsf) is late Eocene to early Oligocene diatom-bearing claystone with thin interbedded sands and lonestones. Carbonate contents range from 0.4 to 3.3 wt%. Sands are poorly sorted, and bioturbation is moderate. Rare fibrous black organic clasts are

present within the sand beds. The bottom of Unit II has rhythmically interbedded centimeter-thick sand and dark claystone. XRD shows gibbsite and kaolinite in Unit II, suggesting erosion of chemically weathered material formed in soils. Unit II is a glaciomarine sequence that records proglacial sedimentation during a marine transgression that infilled erosional topography. Site 742 (Leg 119), 40 km away, sampled similar or younger-age sediments that were interpreted as proximal, glacially influenced proglacial or subglacial deposits. The contact between lithostratigraphic Units II and III is abrupt and was also recovered (interval 188-1166A-17R, 77–78 cm).

Unit III (156.62–267.17 mbsf) consists of massive and deformed sands with a silty clay matrix. The unit is undated at present. Calcium carbonate content ranges from 0.4 to 8.4 wt%. The sands have a uniform fabric, are poorly sorted, and lack internal structure. Pebbles of quartzite and rare fibrous black organic fragments are widely dispersed throughout. Two cemented intervals are present in the sands and contain calcite cement. The lower part of Unit III is deformed and folded by soft-sediment deformation of sandy beds with black organic-rich material that includes pieces of wood. The coarse-grained sands record deposition on an alluvial plain or delta, and the deformed beds record some reworking of material from underlying organic horizons. A similar-looking sequence of carbonaceous material was drilled in the bottom 2 m of Site 742 and was interpreted as fluvial and possibly lacustrine. At Site 742, however, a sequence comparable to the homogeneous coarse sands was not recovered. The coarse sands of Unit III may record a preglacial alluvial plain or a braided delta of a glacial outwash system. The contact between lithostratigraphic Units III and IV was not sampled.

Unit IV (276.44–314.91 mbsf) comprises black highly carbonaceous clay and fine sandy silt with organic-rich laminae and rare to moderate bioturbation. The sandy silt contains abundant mica and some pyrite. Samples of the organic-rich material have organic carbon values as high as 9 wt% and have common occurrences of authigenic sulfides. Calcium carbonate content ranges from 0.3 to 3.7 wt%. Unit IV records deposition in a restricted marine or lagoonal environment.

Unit V (342.80–342.96 mbsf) consists of a small sample of undated finely laminated gray claystone that was captured in the core catcher within a thick no-recovery zone at the bottom of the hole. From resistivity and velocity log data, the unit may have a relatively large fine-clay content. The claystone was possibly deposited in a preglacial setting. The interpretation is based on tentative lithologic and seismic stratigraphic correlation with ODP Site 741, 110 km away, which recovered Early Cretaceous gray claystone (Barron, Larson, et al., 1989).

Micropaleontological analyses were done at Site 1166 for diatoms, radiolarians, foraminifers, and calcareous nannofossils (Fig. 13). Diatoms are present in limited intervals of the core and provide the primary biostratigraphic age estimates. Three distinct diatom assemblages were noted: Quaternary, Pliocene, and late Eocene–early Oligocene age. Extant Quaternary diatoms occur at 2.12–2.92 mbsf (age of <0.66 Ma). Quaternary to upper Pliocene diatoms occur in diamicts to at least 106.37 mbsf. Two layers of diatomaceous clay (~113.95 to 114.10 mbsf and ~114.50 to 115.15 mbsf) occur and have upper Pliocene diatoms: *Thalassiosira kolbei* (1.8–2.2

Ma) and *Thalassiosira vulnifica* to *Thalassiosira striata*–*T. vulnifica* Zones (2.2–3.2 Ma), respectively. Radiolarians give an age of >2.4 Ma for the lower bed. The boundary between lithostratigraphic Unit I and II is a major disconformity (~30 m.y.). Diatoms in Unit II between 135.73 to 153.48 mbsf are of early Oligocene–late Eocene age (~33 to 37 Ma). Diatoms were not recovered below Unit II, but several specimens of pollen, spores, dinoflagellates, and wood fragments were noted in lower intervals of the hole. Planktonic foraminifers are common above ~90 mbsf, and their ages generally agree with those for diatoms and radiolarians. Calcareous nannofossils are rare. Palynological samples were collected throughout the section for postcruise analysis to give ages for samples from the lower part of the hole.

Paleomagnetic stratigraphy is difficult because of limited core recovery, but a clear pattern of magnetic polarity intervals is recorded where the recovery is relatively high. A correlation to the geomagnetic polarity time scale (GPTS) is in progress using key biostratigraphic datums (Fig. 13). Downhole variations in the concentration-dependent and magnetic mineralogy-dependent parameters show that the main lithostratigraphic units have alternating high and low magnetic mineral concentrations and distinct magnetic signatures. Iron sulfide minerals are present below ~140 mbsf.

Interstitial water profiles document downhole sediment diagenesis and diffusional exchange with bottom seawater. From 0 to 150 mbsf, the oxidation of organic matter reduces sulfate values from 28 to 8 mM, and ammonium increases from 177 to 1277 mM. From 0 to 75 mbsf, alkalinity decreases from 4.5 to 1 mM, silica decreases from 800 to 200 mM, potassium decreases from 12 to 2 mM, and calcium increases from 10 to 22 mM. The profiles suggest diagenetic silicate reactions are occurring within the sulfate reduction zone. Between 150 and 300 mbsf, calcium and magnesium show minor changes in relative concentration (15 and 24 mM, respectively), suggesting diffusional processes are dominant.

Organic carbon (OC) contents of the sediments based on 14 samples (selected by dark color) vary according to lithostratigraphic unit. The diamictite (Subunit IB) has OC values of 0.4–1.4 wt%; the massive sand (Unit III) has OC values of 0.2–0.5 wt% except for one bed, near the base of the fluvial/deltaic sand section of Unit III with 9.2% OC; the carbonaceous claystone (Unit IV) has 1.5–5.2 wt% OC. Inorganic carbon was low (<0.1 wt%) throughout most of the recovered section. Gas analyses showed only background levels of methane (4–10 ppmv), and no other hydrocarbons were detected. Most samples are enriched in carbon relative to nitrogen, which suggests the input of land-plant organic matter, especially for samples with more than 1 wt% OC. Rock-Eval pyrolysis analysis shows that the pyrolyzable fraction of the organic carbon is low (hydrogen index values of 50 mg of hydrocarbon per gram of carbon or less), consistent with degraded plant material as the source of the carbon in the more carbonaceous (>2 wt%) samples. Samples with lower carbon contents (<1.4 wt%) may contain a recycled higher thermal maturity component. This recycled organic component is suggested by Rock-Eval T_{\max} values that approach 490°C as organic carbon decreases toward values of 0.5 wt%. The diamictites

(Unit I) have a greater proportion of recycled organic matter than the carbonaceous units (base of Unit III and Unit IV), which contain mostly first-cycle organic matter.

The majority of the sedimentary section has porosities between 20% and 40%, with the exception of Unit II, where the average porosity is 50%. *P*-wave velocities change abruptly at most lithostratigraphic boundaries. The measured shear strengths show that the sediments, especially Unit I, are overconsolidated, with an overconsolidation ratio of ~ 2 below 70 mbsf. The overconsolidation record implies at least one or two periods when sediments were either compacted by a 250- to 300-m-thick sediment column, now eroded away, or were loaded by a 330- to 420-m-thick glacier (nonbuoyant ice), during prior glaciations.

Wireline logging was done in Hole 1166A with excellent results (Fig. 14). Three runs were made using the triple combination (triple combo), sonic/geological high-sensitivity magnetic tool (GHMT), and Formation MicroScanner (FMS) tools from 33 mbsf to the bottom of the hole at 385 mbsf. Six logging units are recognized, and all stratigraphic units have distinctive signatures and appearance, especially in the resistivity, sonic velocity, and FMS data. The deeper parts of the hole (logging Units 4b, 5a, 5b, and 6, equivalent to lithostratigraphic Units III [lower part], IV, and V) with preglacial to early glacial units have large gamma-ray fluctuations indicative of heavy mineral K, Th, and U contents associated in part with the high organic carbon values here. These units also have lower velocity, density, and resistivity than the thick overlying deltaic sands of lithostratigraphic Unit III. All log traces show abrupt shifts at the logging Unit 3/4 and 2/3 boundaries (equivalent to lithostratigraphic Unit II/III and Unit I/II boundaries) that appear from cores to be unconformities. The diamictons with interbedded glaciomarine clays and silts of lithostratigraphic Unit I have generally high and variable magnetic susceptibilities that suggest high variability in magnetite concentrations. FMS images clearly show the variability in the lithostratigraphic units, the presence of lonestones, and the deformation of the organic-rich silt-sand horizons (lithostratigraphic Unit III) (Fig. 15). The resistivity and velocity logs, along with seismic reflection profiles, give evidence for a marine transgression from the alluvial sands (Unit III) to the glaciomarine diatom-bearing claystones (Unit II).

Logging while drilling (LWD) was done in Hole 1166B to test the Power Pulse and Compensated Dual Resistivity tools and record spectral gamma-ray and resistivity data in the uppermost 42 m of the sediment. This interval could not be covered by wireline logging because of pipe position. Resistivity values increase in linear segments from near zero at the seafloor to the 3.5(?) Ω m values measured by the wireline logs at the base of the pipe.

Site 1166 achieved a primary objective of Leg 188 by recovering a set of cores, albeit limited, that record brief intervals in the history of Antarctic paleoenvironments for the Prydz Bay region, extending back through the early stage of glaciation to preglacial times (Fig. 16). Drilling during Leg 119 in Prydz Bay recovered a record of early proximal glaciation at Sites 739 and 742 but had not captured the transition to warmer climates as would be indicated by the presence of local vegetation. Correlation of Site 1166 to Site 742, which is 40 km away, by comparison of downhole logs and regional seismic stratigraphy shows that Units I and II at Site

1166 are equivalent to (or older than) similar units at Site 742. Below the level of Unit II, however, Site 1166 samples are stratigraphically lower and record a more temperate alluvial facies than seen at Site 742. The lower part of Unit III (i.e., the deformed organic-rich sands and silts) may have been sampled in the last 2 m of core at the bottom of Site 742, but confirmation of this awaits further comparison of the two drill sites. If the organic units are the same, then a thick section of sands (Unit III) is missing at Site 742. The deepest unit at Site 1166 (Unit V) lies below a regional seismic unconformity that can be traced to Site 741, ~110 km away, where similar gray claystones like those of Unit V were also sampled. The age of the claystone at Site 741 is Early Cretaceous, which is preglacial.

The paleoenvironmental record inferred from the cores at Site 1166 shows a systematic uphole change from preglacial warm to full-glacial cold climates, such as that envisioned for the Prydz Bay region in Figure 16. The rich carbonaceous strata (undated Unit IV), which overlie Unit V, record a time of more temperate climatic conditions when vegetation existed on Antarctica. The sands (undated Unit III) of the alluvial plain environment may be the transition into the progressively colder climates that are recorded in the proglacial (late Eocene to early Oligocene Unit II), glacial marine (Unit II and late Pliocene and younger Unit I), and subglacial (Unit I) sediments. The ages of Units III and IV are yet to be determined and, once known, will resolve the current uncertainty in what part of the transition to full-scale Antarctic glacial conditions was recorded at Site 1166. Adequate materials have been collected for palynologic evaluation to determine the needed ages.

Site 1167: Continental Slope (Trough Mouth Fan)

Site 1167 is located in the middle of the Prydz Channel Trough Mouth Fan (Figs. 10, 17). Construction of the fan started in early to mid-Pliocene time when the Lambert Glacier formed a fast-flowing ice stream on the western side of Prydz Bay. The fan has grown most during episodes when the Lambert Glacier has grounded at the shelf edge, delivering basal debris to the fan apex. This material was then redistributed by sediment gravity flows and meltwater plumes. Models of trough mouth fan sedimentation suggest that thick siliciclastic units should correspond to peaks in Antarctic ice volume, whereas periods of reduced ice volume should be represented by hemipelagic sediments. Thus, the alternation of facies should reflect the number of times the East Antarctic Ice Sheet has expanded to the shelf edge in latest Neogene time.

Hole 1167A was cored with the advanced hydraulic piston corer (APC) system to refusal at 39.7 mbsf. Coring then proceeded with the extended core barrel (XCB) system to a total depth of 447.5 mbsf. Planned drilling time at the site was shortened by 42 hr because of icebergs and a ship schedule change, and the target depth of 620 mbsf (base of the Prydz Trough Mouth Fan) was not achieved. Four icebergs approached to within 0.1 nmi of the drill site, causing a total of 27 hr delay.

The sedimentary section at Site 1167 comprises a 447.5-m-thick sequence of clayey silty sands with dispersed rock clasts with minor beds of coarse sands, clays, and sandy clays. Two lithostratigraphic units are identified (Fig. 18).

Unit I (0 to 5.17 mbsf) is composed of olive and reddish brown clay and sandy clay with minor admixtures of biogenic components (e.g., as much as 2% diatoms and 1% sponge spicules). There are isolated beds of fine sand and rare limestones. Diffuse reddish brown color bands are present in several thin intervals. The transition to Unit II is gradational. Unit I records a period of hemipelagic deposition during the last interglacial, when fine particles, biogenic material, and IRD settled out of the water column.

Unit II (5.17–447.5 mbsf) makes up the majority of the section at Site 1167 and is composed of one major facies (II-1) and three minor facies. Facies II-1 is composed of interbedded, poorly sorted dark gray sandy silt, silty sand, clayey sand, and clast-poor diamicton. Numerous color alternations of dark gray and dark reddish gray with sharp contacts occur between 64 and 98 mbsf. Some decimeter- to meter-scale successions of clast-poor diamicton and gravel beds are noted. Limestones are common, with variable lithologies including granite, granite gneiss, garnet-bearing gneiss, metaquartzite, and sandstone. Dolerite, schist, conglomerate, and rare carbonized wood are also present. Sandstone and granite components vary systematically in the hole, with sandstone limestones common below 200 mbsf and granite limestones common above 200 mbsf. Facies II-2 is composed of gray, moderately sorted coarse sand. Grains are subrounded and predominately quartz, K-feldspar, and mafic minerals. The first occurrence of Facies II-2 downcore is at 179 mbsf. Facies II-3 is composed of dark gray clay with silt laminations, rare sand grains, and no limestones. Sharp contacts mark the top and base of this facies. Some silt laminae converge and indicate cross-bedding. Facies II-4 is composed of green gray clay with dispersed clasts, abundant foraminifers, and few nannofossils. The upper contact is sharp, and the lower contact is gradational to sharp.

Unit II (Facies II-1 and II-2) records deposition by mass transport, probably massive debris flows as evidenced by poor sorting, abundant floating clasts, little visible grading, and a lack of biogenic components. The debris flows most likely represent deposition during glacial periods when ice extended to the shelf break and could deliver large volumes of sediment to the upper continental slope. Individual flows cannot be identified visually. The thin intervals of fine-grained sediment (Facies II-3 and II-4) are similar in appearance and composition to muddy contourites observed at Site 1165 and, hence, may denote times when contour currents were active on the fan. The silt laminae and bioturbation in Facies II-3 are not consistent with turbidite deposition. Facies II-4 may record short intervals, possibly interglacials, when pelagic deposition dominated.

Sixteen lithologic varieties of limestones were cataloged, and they generally vary randomly in size, with only a small size increase downhole to 200 mbsf. Below ~160 mbsf, the number of limestones per meter remains fairly consistent, except for three intervals (160 to 210, 300 to 320, and 410 to 420 mbsf) where there are downward increases. Systematic variations in

concentration of sandstone and granite clasts (noted above) suggest that possibly two different source areas delivered material to Site 1167 at different times (Fig. 19).

X-ray diffraction analyses show that the total clay mineral content is relatively constant throughout the hole. XRD analyses of clay types give mixed results for Units I and II, with smectite more common in Unit I and at depths below 382 mbsf than elsewhere and illite found in all samples. Further detailed analyses are likely to clarify whether changes in illite-smectite ratios indeed relate to times of glacial advances.

Chronostratigraphy at Site 1167 is poorly controlled because of the unexpected paucity of siliceous microfossils; however, dates in Unit I are younger than 0.66 Ma, and a sample from ~215 mbsf seems to be of early or middle Pleistocene age. Foraminifers are present consistently throughout the section and include pelagic foraminifer shelf faunas in diamictons and in situ midbathyal faunas in a few samples. Changes in foraminifer faunas match closely changes detected in various lithological parameters. Age control at this time is not adequate to determine average sedimentation rates.

Magnetostratigraphic analyses identified the Matuyama/Brunhes boundary between 30 and 34 mbsf (Fig. 20). The magnetic polarity below 34 mbsf remains mainly reversed, possibly including the Jaramillo and Olduvai Subchrons. The concentration-dependent magnetic parameters (susceptibility and anhysteretic and isothermal remanent magnetization) indicate that magnetite concentrations have large-scale cyclic (tens to hundreds of meters) variations, not commonly seen (Fig. 20). The values increase abruptly uphole at ~208 mbsf, between 113 and 151.2 mbsf, and between 55 and 78.5 mbsf, followed by a nearly linear uphole decrease. Superimposed on the large-scale cycles are small-scale variations. The anhysteretic over isothermal remanent magnetization ratio indicates that the magnetic grain size changes uphole from finer to coarser at 217 mbsf. The origin of the large-scale cycles is not yet understood but is likely related to systematic changes in sediment provenance caused by changes in the volume of ice from different sources and the location of areas of maximum erosion during glacial periods.

Interstitial water profiles document downhole sediment diagenesis, mixing of distinct subsurface interstitial water intervals, and diffusional exchange with modern bottom seawater. From 0 to 20 mbsf, chlorinity and sulfate increase by ~3% over seafloor values, suggesting that high-salinity, last-glacial-maximum seawater is preserved (Fig. 21). Sulfate decreases downhole from the seafloor (30 mM) to 433 mbsf (24 mM) in a stepped profile, raising the possibility that a number of "fossil" sulfate reduction zones may also be preserved (Fig. 21). Dissolved manganese increases downhole from 15 to 20 mM between the seafloor and ~25 mbsf. Alkalinity decreases downhole from 3 to 1.3 mM between the seafloor and 40 mbsf before steadily increasing to 2 mM at 433 mbsf. From 0 to ~60 mbsf, dissolved downhole profiles of calcium (10 to 25 mM), magnesium (56 to 42 mM), potassium (12 to 2 mM) and lithium (30 to 5 mM), all suggest diagenetic silicate-clay reactions are occurring. Below 5 mbsf, dissolved silica concentrations are enriched slightly over modern bottom waters (~300 vs. ~220 mM), reflecting the absence of biogenic opal within the sediments. Calcium carbonate is a minor component in

the matrix sediments throughout the hole and is slightly higher in lithostratigraphic Unit II than in Unit I.

The concentration of hydrocarbon gases was at background levels (4–10 ppmv) for methane, and ethane was present at detection limits only in a few cores from deeper than 350 mbsf. The organic carbon content averages ~0.4 wt%, with no apparent trend with depth. Organic matter characterization by Rock-Eval pyrolysis indicates that all samples contain predominantly recycled and degraded thermally mature organic matter.

Sediment water content and void ratio decrease sharply with depth in lithostratigraphic Unit I, reflecting normal compaction. But, within Unit II, these properties were relatively uniform, except for a downhole decrease at 210 mbsf, where grain density and magnetic susceptibility values also decrease abruptly. *P*-wave velocities increase at this depth. Undrained shear strength values increase uniformly throughout the hole at a lower than typical rate, possibly because of the clay mineralogy combined with the high proportions of the silt and sand fraction of the sediment. There is no evidence of sediment overcompaction.

Wireline logging operations in Hole 1167A were attempted with the triple combo tool string. The tool string was lowered to 151 mbsf, where an obstruction halted the tool. A conglomerate interval was noted in the cores at this depth. Log data were collected from this depth to the base of pipe at 86.9 mbsf, covering an interval of 66 m. Time constraints, poor hole conditions, and problems encountered with the lockable flapper valve, resulted in a decision to switch to LWD in a new hole. Excellent spectral gamma ray and resistivity data were recorded to 261.8 mbsf before time ran out. Resistivity data show several clay and gravel-rich beds, with high gamma-ray values for a red bed interval at 60–90 mbsf, and low values between 90–120 mbsf and 215–255 mbsf. The change to low values may be due to a reduced concentration of granitic clasts or a change from a clay-rich to a sandier matrix.

Site 1167 is the first drill site to directly sample the sedimentary fans that are common on the upper continental slope around Antarctica, seaward of glacially carved sections of the continental shelf. The site reveals previously unknown large-scale (20 m to more than 200 m thick) cycles in magnetic susceptibility and other properties that are not yet fully explained but are likely due to systematic changes in the Lambert Glacier ice-drainage basin during Pleistocene and late Pliocene(?) time. Within the large cycles are likely many separate debris flows and interbedded hemipelagic muds that indicate times of individual advances and retreats of the ice front to, or near, the continental shelf edge. The debris flows are well represented in the cores, but the mud intervals are sparse and may either have not been recovered or have been removed by younger flows. Because of few age control points, it is not yet possible to determine sedimentation rates at Site 1167. If the rates are high, as we suspect from the limited available age dates, then almost all sediment during the latest Neogene glacial intervals sampled at Site 1167 were deposited as debris flows on the trough mouth fan and are not getting to the Wild Drift (Site 1165), where sediment rates are low. Alternatively, some of the fine component of the latest Neogene glacial sediment is being carried away by deep ocean currents.

Site 1165: Continental Rise (Wild Drift)

Site 1165 is situated on the continental rise offshore from Prydz Bay over mixed pelagic and hemipelagic sediments of the central Wild Drift (Figs. 10, 22A, 22B). The drift is an elongate sediment body formed by the interaction of sediment supplied from the shelf and westward-flowing currents on the continental rise. The site is in 3537 m of water and was selected to provide a record of sedimentation that extends back to the onset of contour current-influenced deposition on the rise. The main objective was to obtain a proximal continental rise record of Antarctic glacial and interglacial periods for comparison with other sites around Antarctica and with those of Northern Hemisphere ice sheets.

Prior to drilling, a single seismic-reflection profile was recorded across the location of Site 1165, using the ship's water-gun and digital recording system, to verify the location of the site. Three holes were drilled at the site. Hole 1165A consisted of a mudline core that was dedicated to high-resolution interstitial water sampling. Hole 1165B was cored with the APC to 147.9 mbsf (86.4% recovery) and deepened with the XCB to 682.2 mbsf (57.3% recovery). Hole 1165C was washed down to a depth of 54 mbsf, where a single core was taken at an interval that had been missed in Hole 1165B. Continuous RCB coring began at 673 mbsf and continued to a total depth of 999.1 mbsf, with 80% recovery. Coring operations were interrupted by five icebergs, which came to within 200 m of the drill site and caused a total loss of 98 hr. Hole 1165C was successfully logged with the triple-combo tool string from 176 to 991 mbsf and from 176 to 580 mbsf with the sonic tool.

Drilling at Site 1165 yielded a relatively continuous 999-m-thick sedimentary section of early Miocene- to Pleistocene-age terrigenous and hemipelagic deposits (Fig. 23) with only few minor (<2 m.y.) disconformities. Dispersed clasts (IRD) are present down to the bottom of the hole, but limestones are infrequent below 500 mbsf (lower Miocene). They both are relatively abundant above 300 mbsf (middle Miocene).

The sedimentary section is divided into three lithostratigraphic units that are characterized by cyclic variations between biogenic-bearing (lighter) and terrigenous-dominated intervals (darker). The cyclic variations in lithology are also recorded as visual color alternations, and cycles in spectrophotometer lightness factor, bulk density, magnetic susceptibility, and other laboratory and downhole log parameters to varying degrees. In general, cores get darker downhole as biogenic intervals become thinner relative to the thickness of terrigenous-bearing intervals. For the same reason, light-dark cyclicity is more prominent above ~400 mbsf. Darker units generally have higher bulk density, magnetic susceptibility, and organic carbon values. The sediment consists mostly of quartz, calcite, plagioclase, K-feldspar, and a mixture of clay minerals, as well as minor hornblende and pyrite. Silt-sized components are mainly quartz, but plagioclase, biotite, amphibole, and other heavy minerals are common.

Unit I (0–63.8 mbsf) consists of structureless brown diatom-bearing clay and clay. There are beds with minor diatom-bearing greenish gray clay that have dispersed sand grains, granules, and limestones. There is minor laminated silt and minor brown foraminifer-bearing clay.

Foraminifers comprise 5%–15% of sediment in the upper 13 mbsf. One interval within Unit I (20?–30? mbsf) is characterized by alternations between two facies like those of Unit II (i.e., Facies II-1 and II-2).

Unit II (63.8–307.8 mbsf) is characterized by alternations of two main facies, which differ in color and composition. Facies II-1 consists of structureless, homogeneous, greenish gray diatom clay, and Facies II-2 is mostly dark gray diatom-bearing clay with some intervals of scattered silt laminae. Many lower boundaries of Facies II-2 are sharp, and upper boundaries are transitional with bioturbation that increases upward into Facies II-1. Higher amounts of siliceous microfossils and ice-rafted debris (floating sand grains and pebbles) are found in Facies II-1 than II-2. Facies II-1 is characterized by lower grain density because of the higher diatom content. A third facies (II-3) is sometimes found and consists of several 15- to 40-cm-thick nannofossil chalk beds that have a sharp base and pass gradually up into Facies II-1. Within Unit II, three subunits are identified based on the different proportions of Facies II-1 and II-2. Subunit boundaries are at 160 and 252 mbsf and partially denote amounts of lonestones, with greater amounts of lonestones in Subunits IIA and IIC than in Subunit IIB.

Unit III (307.8–999.1 mbsf) comprises a section of thinly bedded planar-laminated claystone that is divided, like Unit II, into two main facies that differ in color, composition, and bedding characteristics. Facies III-1 consists of greenish gray, bioturbated, structureless clay and claystone and diatom-bearing clay and claystone with dispersed coarse sand grains and rare granule to pebble-sized lonestones. Facies III-2 is composed of dark gray, thinly bedded, planar-laminated clay and claystone with abundant silt laminae. Lonestone (dolerite, diorite gneiss, and mudstone) abundance in Unit III is low and decreases downhole.

In Facies III-1, the thickness of the greenish gray intervals is generally less than 1 m, and some intervals have higher concentrations of material as coarse as sand sized. The upper contacts are commonly sharp, laminae are rare, and bioturbation increases upward. Angular mud clasts and benthic foraminifers are present in this facies below 800 mbsf. Siliceous microfossil content is low.

Facies III-2 becomes increasingly fissile with depth and changes to very dark gray or black below 894 mbsf. Bioturbation is rare in Facies III-2, and light-color silt laminae are a conspicuous feature (average = 150–200 laminae/m). Many cross-laminated silt ripples are present, and ripples are more common below 673 mbsf than above. Microfossils are rare and seem to disappear completely below ~600 mbsf. Below 842 mbsf, laminae with calcite cement are present and sections of the core become increasingly cemented with likely authigenic carbonates. A change to darker-color claystones occurs at 894 mbsf, where fracture patterns also become curved.

In both Facies III-1 and -2, individual 0.5-cm-sized horizontal burrows (*Zoophycos*) are evident along with clusters of millimeter-sized burrows.

An excellent record of siliceous microfossils is found at Site 1165 down to 600 mbsf, where biogenic opal disappears because of an opal-A/opal-CT diagenetic transition. Neogene high-

latitude zonal schemes for both diatoms and radiolarians yielded identification of 21 diatom and 12 radiolarian biostratigraphic datums between 0 and 600 mbsf. Below 600 mbsf, age assignments are inferred from calcareous nannofossils, which are present in only a few discrete intervals with moderate to good preservation of assemblages that have low diversity. Nannofossils yield Pleistocene to lowermost Miocene ages. Benthic foraminifers are more common than planktonics, which are rare. The foraminifers indicate several intervals of redeposited material.

A magnetostratigraphy was determined for Site 1165 for the interval 0–94 mbsf and below 362 mbsf (Fig. 24). The magnetostratigraphic record and biostratigraphic ages, when combined, yield an age-versus-depth model that shows relatively rapid deposition in early Miocene time (~120 m/m.y.), somewhat slower deposition in middle to late Miocene time (~50 m/m.y.), and even slower deposition since late Miocene time (~15 m/m.y.) (Fig. 25). From magnetostratigraphy, the bottom of Hole 1165C (999.1 mbsf) has an age of ~21.8 Ma. The uncertainty in ages is larger below 600 mbsf, where only few biostratigraphic ages exist to constrain the paleomagnetic reversal stratigraphy.

Measurements of rock magnetic properties in the interval 114–370 mbsf indicate that magnetic mineral concentrations (i.e., concentrations of magnetite) drop significantly, with nearly a complete loss of magnetic intensity. Shipboard analysis suggests that this unusual loss of magnetic signal is caused by diagenetic dissolution of magnetite in the presence of high silica-rich pore-water concentrations. A zone of low grain density is observed in cores from part of this zone ~140 mbsf and may also coincide with the disappearance of magnetite.

The interstitial water profiles document downhole sediment diagenesis at Site 1165. Sulfate values decrease linearly from 30 to 2 mM in the interval from 0 to 150 mbsf, but increases occur in ammonium (20 to 384 μ M), phosphate (3 to 10 μ M) and alkalinity (3 to 8 mM) throughout the same interval because of destruction of organic matter. Ammonium increases (to 800 μ M), phosphate decreases (to 0), and alkalinity decreases linearly (to 1 mM at 999 mbsf) throughout the interval from 150 to 400 mbsf. Concentrations of dissolved silica increase from 522 μ M at the seafloor to a maximum of 1000 μ M at 200 mbsf and reflect the dissolution of abundant siliceous microfossils. Silica values decrease from 400 to 999 mbsf. The theoretical opal-A/opal-CT transition is at ~600 mbsf, based on measured downhole temperatures. A strong seismic reflection is observed at this depth. Below 150 mbsf, calcium and magnesium values correlate inversely, which suggests diagenetic control and an unidentified Ca-rich lithology below the drilled section. A decrease in potassium values below 50 mbsf and an increase in fine-grained K-feldspar, identified by XRD measurements, suggests an authigenic origin for feldspars.

Hydrocarbon gas contents of cores are low (<400 ppmv) within the sulfate reduction zone down to ~150 mbsf (Fig. 26). Below 150 mbsf, methane increases rapidly and reaches values of 20,000 to 40,000 ppmv between 270 and 700 mbsf, and 40,000–100,000 ppmv from 700 to 970 mbsf. These headspace gas measurements indicate only the residual gas in the pore water of cores after outgassing upon retrieval to the surface. The gas concentrations are equivalent to ~8

to 35 millimoles per liter (mM) dissolved CH₄ when adjusted for sample size variation, density, and porosity. Cores deeper than 700 mbsf may contain more gas because of increased lithification and retarded outgassing. Ethane is present in headspace gas samples deeper than 157 mbsf, and the C₁/C₂ value shows the expected decrease with depth for the observed geothermal gradient at this site (secant temperature gradient of 43.6°C/km). OC contents of Hole 1165 sediments are low (0.1 to 0.8 wt%), except for high organic carbon (1.8–2 and 1.3 wt%) beds at depths of 122 and 828 mbsf (Fig. 26). Cores from within the gas hydrate stability zone (seafloor to 460 mbsf) were examined immediately upon recovery, but no hydrates were observed.

Acoustic velocities and shear-strength measurements increase as a result of normal compaction (in the upper 500 mbsf) and diagenesis (with a greater effect below 600 mbsf). Horizontal *P*-wave velocities increase abruptly at 114 mbsf from ~1535 to 1575 m/s and then linearly from 114 to 603 mbsf. Other significant *P*-wave velocity increases occur at 692 mbsf, at 800 mbsf (to 2660 m/s), and 960 mbsf (to 2840 m/s). These abrupt increases are observed as reflections on seismic data.

Hole 1165C was logged with a single pass of the triple combo tool from 176 to 994 mbsf and a single pass of the sonic tool from 176 to 580 mbsf. Total gamma-ray and bulk-density log traces covary, suggesting that diatom-bearing strata (lower density) are present throughout the hole. The boundary between lithostratigraphic Units II and III at 305 mbsf is marked by a large fluctuation in total gamma-ray values, which suggests a shift in clay content at the boundary. The distinct silica- and calcite-cemented intervals observed in the cores are marked by peaks in most log traces.

Site 1165 provides paleontologic and sedimentologic evidence that numerous alternations or cycles between biogenic material and clay-sized terrigenous debris from Antarctica have occurred since earliest Miocene time (Fig. 27). The cyclicity observed in the lightness values for two intervals (83–100 mbsf and 107–123 mbsf; in lithostratigraphic Unit II) in the cores was analyzed for spectral content to evaluate the potential effect of Milankovitch periodicities on biogenic/terrigenous sedimentation cycles at this site (Fig. 27). For the shallower interval, significant spectral peaks are found at periods of 3.28, 1.45, 1.08, and 0.64 m thickness. A sedimentation rate of 3.5 cm/k.y. is reasonably well constrained for the interval and gives periods of 93.7, 41.5, 20.8, and 18.2 k.y., respectively. These periods are similar to the Milankovitch cycles of 100 k.y. (eccentricity), 41 k.y. (obliquity), 23 k.y. and 19 k.y. (precession), suggesting an orbitally forced origin for the light–dark cyclicity. For the deeper interval, significant spectral peaks are at 4.27, 1.55, 0.95, and 0.72 m, which have similar peak periodicity ratios to the upper interval, again suggesting an orbital origin for the deeper cycles. In the deeper interval, the sedimentation rate is less well constrained. But, by using the peak-to-peak ratios as a guide, an inferred sedimentation rate of 3.8 to 4.1 cm/k.y. would give the same periods as the shallow interval (i.e., 93.7, 41.5, 20.8, 18.2 k.y.). The observed lightness changes correlate also to variations in bulk density and magnetic susceptibility, indicating that the lightness (color) data likely document orbitally driven changes in the Site 1165 depositional environment since at least

early Miocene time. A similar approach has been used recently to detect orbital signals in upper Oligocene to lower Miocene sedimentary sequences drilled in the Ross Sea, Antarctica, by the Cape Roberts Project (Claps et al., in press). Milankovitch cyclicities have been reported for late Miocene-age and younger diatom-bearing hemipelagic and terrigenous sediments at ODP Site 1095 from a drift deposit, like the Wild Drift, adjacent to the Antarctic Peninsula (Shipboard Scientific Party, 1999).

In addition to the cyclic variations, significant uphole changes occurred at Site 1165 from early to late Miocene times (Units III and II), and include an eightfold decrease in average sedimentation rates from 12 to 1.5 cm/k.y., an increase in the total clay content, an increase in amount of sand-sized and lonestone IRD, and other changes (e.g., first appearance of glauconite) (Figs. 22, 25). The changes likely reflect shifts, in the onshore Prydz Bay region (sediment source area), to paleoenvironments that produced less terrigenous sedimentation, a lower-energy current regime, and more floating ice at Site 1165 starting in middle Miocene time. The uphole shift to increased clay (~305 mbsf) and first appearance of glauconite (~220 mbsf) heralds (1) a mid-Miocene change to erosion of sedimentary basins on the shelf and (2) subsequent inferred overdeepening of the shelf to the large water depths of today. Such deep-cut erosion would be by grounded glaciers crossing the continental shelf and dispersing icebergs with entrained sediment. The times of lowest sediment supply, in the latest Neogene (i.e., above 60 mbsf), have upward-decreasing silica contents (i.e., fewer diatoms and sponge spicules) and varied (cyclic?) IRD concentrations, which may reflect increasing extent of sea ice cover and ice sheet fluctuations. During latest Neogene time, a widely recognized period of intense Antarctic (and Arctic) glacier fluctuations, thick debris flows blanketed the adjacent continental slope (Site 1167), but little sediment was deposited on Wild Drift (Site 1165).

SUMMARY

The three sites proximal to the East Antarctic Ice Sheet drilled during Leg 188 across the Prydz Bay continental shelf, slope, and rise provide new evidence of long- and short-term variations in paleoenvironments (i.e., depositional, glacial, and inferred climate) extending from Holocene into Mesozoic times. The shelf site (Site 1166) documents the earliest stages of East Antarctic glaciation from inferred temperate climates (i.e., with vegetation) to transitional environments of proximal glaciers to full glacial and interglacial conditions with intermittently grounded glaciers on the shelf. Site 1167 on the slope samples the latest Neogene sediments that attest to the rapid deposition and variability of onshore erosion areas and glaciomarine depositional settings in front of grounded ice sheets during glacial–interglacial periods. On the continental rise, at Site 1165, the drilling record documents the long-term, lower to upper Miocene transition from temperate to cold-climate glaciation, with superimposed short-term glacier fluctuations since early Miocene time.

These sites document changing paleoenvironments (Fig. 28), with long-period changes that may mark the transition from more temperate times of wet-based onshore glacier systems with fluvial outwash (i.e., before 13–14 Ma; middle Miocene) to cold times of dry-based systems with overdeepened shelf and subglacial deposition (late Miocene and younger). The notable variability in IRD concentrations since middle Miocene time suggests that the transition varied between the temperate and cold glacier systems. The short cyclic variations (at Milankovitch periodicities) recorded by the gray/green (dark/light) facies observed at Site 1165 may track the persistent seaward-landward movements of onshore glaciers and their internal ice streams. The glacier systems provided more terrigenous sediments (gray facies) during times of glacial advances and less terrigenous sediment during periods of glacial retreat (interglacials; green facies).

Leg 188, together with previous (e.g., ODP Legs 119 and 178) and future Antarctic continental margin drilling transects, can provide the hard-earned proximal geologic samples needed to link the histories of the Antarctic Ice Sheet and the distal ocean-current and climate systems.

REFERENCES

- Abreu, V.S., and Anderson, J.B., 1998. Glacial eustacy during the Cenozoic: sequence stratigraphic implications. *AAPG Bull.*, 82:1385–1400.
- Allison, I.F., 1979. The mass budget of the Lambert Glacier drainage basin, Antarctica. *J. Glaciol.*, 22:223–235.
- Alonso, B., Anderson, J.B., Diaz, J.I., and Bartek, L.R., 1992. Pliocene-Pleistocene seismic stratigraphy of the Ross Sea: evidence for multiple ice sheet grounding episodes. In Elliot, D.H. (Ed.), *Contributions to Antarctic Research III*. Am. Geophys. Union, Antarct. Res. Ser., 57:93–103.
- Barker, P.F., Barrett, P.J., Camerlenghi, A., Cooper, A.K., Davey, F.J., Domack, E., Escutia, C., Kristoffersen, Y., and O'Brien, P.E., 1998. Ice sheet history from Antarctic continental margin sediments: the ANTOSTRAT approach. *Terra Antarct.*, 5:737–760.
- Barrett, P., 1999. Antarctic climate history over the last 100 million years. In Barrett, P., and Orombelli, G. (Eds.), *Proceedings of the Workshop: Geological Records of Global and Planetary Changes*. Siena, 1998. *Terra Antarct. Rep.*, 3:53–72.
- Barron, J., Larsen, B., et al., 1989. *Proc. ODP, Init. Repts.*, 119: College Station TX (Ocean Drilling Program).
- , 1991. *Proc. ODP, Sci. Results*, 119: College Station TX (Ocean Drilling Program).
- Barron, J.A., Baldauf, J.G., Barrera, E., Caulet, J.-P., Huber, B.T., Keating, B.H., Lazarus, D., Sakai, H., Thierstein, H.R., and Wei, W., 1991. Biochronologic and magnetostratigraphic synthesis of Leg 119 sediments from the Kerguelen Plateau and Prydz Bay, Antarctica. In Barron, J., Larsen, B., et al., *Proc. ODP, Sci. Results*, 119: College Station TX (Ocean Drilling Program), 813–847.
- Boulton, G.S., 1990. Sedimentary and sea level changes during glacial cycles and their control on glacial marine facies architecture. In Dowdeswell, J.A., and Scourse, J.D. (Eds.), *Glacial Marine Environments: Processes and Sediments*. Geol. Soc. Spec. Publ. London, 53:15–52.
- Budd, W., 1966. The dynamics of the Amery Ice Shelf. *J. Glaciol.*, 6:335–358.

- Budd, W., Cory, M.J., and Jacka, T.H., 1982. Results from the Amery Ice Shelf project. *Ann. Glaciol.*, 3:36–41.
- Claps, M., Niessen, F., and Florindo, F., in press. High-frequency analysis of physical properties from CRP-2/2A and implication for sedimentation rate. *Terra Antarct.*
- Cooper, A., Stagg, H., and Geist, E., 1991a. Seismic stratigraphy and structure of Prydz Bay, Antarctica: implications from Leg 119 drilling. In Barron, J., Larsen, B., et al., *Proc. ODP, Sci. Results*, 119: College Station TX (Ocean Drilling Program), 5–26.
- Cooper, A.K., Barrett, P.F., Hinz, K., Traube, V., Leitchenkov, G., and Stagg, H.M.J., 1991b. Cenozoic prograding sequences of the Antarctic continental margin: a record of glacio-eustatic and tectonic events. *Mar. Geol.*, 102:175–213.
- Denton, G.H., and Hughes, T.J. (Eds.), 1981. *The Last Great Ice Sheets*: New York (Wiley).
- Denton, G.H., Prentice, M.L., and Burckle, L.H., 1991. Cainozoic history of the Antarctic ice sheet. In Tingey, R.J. (Ed.), *The Geology of Antarctica*. Oxford Monogr. Geol. Geophys., 17:365–433.
- Domack, E., Jull, A.J.T., and Donahue, D.J., 1991. Holocene chronology for the unconsolidated sediments at Hole 740A: Prydz Bay, East Antarctica. In Barron, J., Larsen, B., et al., *Proc. ODP, Sci. Results*, 119: College Station, TX (Ocean Drilling Program), 747–750.
- Domack, E., O'Brien, P.E., Harris, P.T., Taylor, F., Quilty, P.G., DeSantis, L., and Raker, B., 1998. Late Quaternary sedimentary facies in Prydz Bay, East Antarctica and their relationship to glacial advance onto the continental shelf. *Antarct. Sci.*, 10:227–235.
- Fedorov, L.V., Grikurov, G.E., Kurinin, R.G. and Masolov, V.N., 1982. Crustal structure of the Lambert Glacier area from geophysical data. In Craddock, C. (Ed.), *Antarctic Geoscience*: Madison (Univ. Wisconsin Press), 931–936.
- Fielding, C.R., Woolfe, K.J., Howe, J.A., and Lavelle, M., 1998. Sequence stratigraphic analysis of CRP-1, Cape Roberts Project, McMurdo Sound, Antarctica. *Terra Antarct.*, 5:353–362.
- Flower, B.P., 1999. Cenozoic deep-sea temperatures and polar glaciation: the oxygen isotope record. In Barrett, P., and Orombelli, G. (Eds.), *Proceedings of the Workshop: Geological Records of Global and Planetary Changes*. Siena, 1998. *Terra Antarct. Rep.*, 3:27–42.

- Forsberg, C.F., Solheim, A., Elverhøi, A., Jansen, E., Channell, J.E.T., and Andersen, E.S., 1999. The depositional environment of the western Svalbard margin during the late Pliocene and the Pleistocene: sedimentary facies changes at Site 986. *In* Raymo, M.E., Jansen, E., Blum, P., and Herbert, T.D. (Eds.), *Proc. ODP, Sci. Results*, 162: College Station, TX (Ocean Drilling Program), 233–246.
- Goodwin, I., 1992. Holocene deglaciation, sea level change and the emergence of the Windmill Islands, Budd Coast, Antarctica. *Quat. Res.*, 40:70–80.
- Grobe, H., and Mackensen, A., 1992. Late Quaternary climatic cycles as recorded in sediments from the Antarctic continental margin. *In* Kennett, J.P., and Warnke, D.A. (Eds.), *The Antarctic Paleoenvironment: A Perspective on Global Change* (Pt. 1). Am. Geophys. Union, Antarct. Res. Ser., 56:349–376.
- Hambrey, M.J., Ehrmann, W.U., and Larsen, B., 1991. Cenozoic glacial record of the Prydz Bay continental shelf, East Antarctica. *In* Barron, J., Larsen, B., et al., *Proc. ODP, Sci. Results*, 119: College Station TX (Ocean Drilling Program), 77–132.
- Hambrey, M.J., and McKelvey, B., in press. Neogene fjordal sedimentation on the western margin of the Lambert Graben, East Antarctica. *Sedimentology*.
- Harris, P.T., and O'Brien, P.E., 1996. Geomorphology and sedimentology of the continental shelf adjacent to Mac. Robertson Land, East Antarctica: a scalped shelf. *Geo-Mar. Lett.*, 16:287–296.
- Harris, P.T., O'Brien, P.E., Sedwick, P., and Truswell, E.M., 1996. Late Quaternary history of sedimentation on the Mac. Robertson Shelf, East Antarctica: problems with ¹⁴C-dating of marine sediment cores. *Pap. Proc. R. Soc. Tasmania*, 130:47–53.
- Harris, P.T., Taylor, F., Pushina, Z., Leitchenkov, G., O'Brien, P.E., and Smirnov, V., 1998. Lithofacies distribution in relation to geomorphic provinces of Prydz Bay, East Antarctica. *Antarct. Sci.*, 10:227–235.
- Kuvaas, B., and Leitchenkov, G., 1992. Glaciomarine turbidite and current controlled deposits in Prydz Bay, Antarctica. *Mar. Geol.*, 108:365–381.
- Leitchenkov, G., Stagg, H.M.J., Gandjukhin, V., Cooper, A.K., Tanahashi, M., and O'Brien, P., 1994. Cenozoic seismic stratigraphy of Prydz Bay (Antarctica). *In* Cooper, A.K., Barker, P.F., Webb, P.-N., and Brancolini, G. (Eds.), *The Antarctic Continental Margin: Geophysical*

and Geological Stratigraphic Records of Cenozoic Glaciation, Paleoenvironments and Sea-level Change. Terra Antarct., 1:395–398.

Licht, K.M., Jennings, A.E., Andrews, J.T., and Williams, K.M., 1996. Chronology of late Wisconsin ice retreat from the western Ross Sea. *Geology*, 24:223–226.

McKelvey, B.C., and Stephenson, N.C.N., 1990. A geological reconnaissance of the Radok Lake area, Amery Oasis, Prince Charles Mountains. *Antarct. Sci.*, 2:53–66.

McLoughlan, S., and Drinnan, A.N., 1997. The sedimentary and revised stratigraphy of the Permian-Triassic Flagstone Bench Formation, Northern Prince Charles Mountains, east Antarctica. *Geol. Mag.*, 134:335–353.

Miall, A.D., 1986. Eustatic sea level changes interpreted from seismic stratigraphy: a critique of the methodology with particular reference to the North Sea Jurassic record. *AAPG Bull.*, 70:131–137.

Miller, K.G., Barrera, E., Olsson, R.K., Sugarman, P.J., and Savin, S.M., 1999. Does ice drive early Maastrichtian eustasy? *Geology*, 27:783–786.

Mizukoshi, I., Sunouchi, H., Saki, T., Sato, S., and Tanahashi, M., 1986. Preliminary report of geological geophysical surveys off Amery Ice Shelf, East Antarctica. *Mem. Nat. Inst. Polar Res. Spec. Iss. Jpn.*, 43:48–61.

O'Brien, P.E., De Santis, L., Harris, P.T., Domack, E., and Quilty, P.G., 1999. Ice shelf grounding zone features of western Prydz Bay, Antarctica: sedimentary processes from seismic and sidescan images. *Antarct. Sci.*, 11:78–91.

O'Brien, P.E., and Harris, P.T., 1996. Patterns of glacial erosion and deposition in Prydz Bay and the past behaviour of the Lambert Glacier. *Pap. Proc. R. Soc. Tasmania*, 130:79–86.

O'Brien, P.E., and Leitchenkov, G., 1997. Deglaciation of Prydz Bay, East Antarctica, based on echo sounder and topographic features. In Barker, P.F., and Cooper, A.K. (Eds.), *Geology and Seismic Stratigraphy of the Antarctic Margin* (Pt. 2). Am. Geophys. Union, Antarct. Res. Ser., 71:109–125.

Pickard, J. (Ed.), 1986. *Antarctic Oasis: Terrestrial Environments and History of the Vestfold Hills, East Antarctica*: Sydney (Academic Press).

Quilty, P.G., 1991. The geology of Marine Plain, Vestfold Hills, East Antarctica. *In* Thomson, M.R.A., Crane, J.A., and Thomson, J.W. (Eds.), *The Geological Evolution of Antarctica*: New York (Cambridge Univ. Press).

———, 1993. Coastal Neogene sections and their contribution to the ice sheet evolution debate. *In* Kennett, J.P., and Warnke, D.A. (Eds.), *The Antarctic Paleoenvironment: a Perspective on Global Change*. Am. Geophys. Union, Antarct. Res. Ser., 60:251–264.

Rebesco, M., Larter, R.D., Barker, P.F., Camerlenghi, A., and Vanneste, L.E., 1997. The history of sedimentation on the continental rise west of the Antarctic Peninsula. *In* Barker, P.F., and Cooper, A.K. (Eds.), *Geology and Seismic Stratigraphy of the Antarctic Margin* (Pt. 2). Am. Geophys. Union, Antarctic Res. Ser., 71:29–50.

Scott, R.F., 1905. *The Voyage of the Discovery*: London (Charles Scribners and Sons).

Shipboard Scientific Party, 1999. Leg 178 summary: Antarctic glacial history and sea-level change. *In* Barker, P.F., Camerlenghi, A., Acton, G.D., et al., *Proc. ODP, Init. Repts.*, 178: College Station, TX (Ocean Drilling Program), 1–58.

Smith, N.R., Zhaoqian, D.J., Kerry, K.R., and Wright, S., 1984. Water masses and circulation in the region of Prydz Bay, Antarctica. *Deep-Sea Res. Part A*, 31:1121–1147.

Solheim, A., Forsberg, C.F., and Pittenger, A., 1991. Stepwise consolidation of glacial sediments related to the glacial history of Prydz Bay, East Antarctica. *In* Barron, J., Larsen, B., et al., *Proc. ODP, Sci. Results*, 119: College Station TX (Ocean Drilling Program), 169–184.

Stagg, H.M.J., 1985. The structure and origin of Prydz Bay and the Mac. Robertson Shelf, East Antarctica. *Tectonophysics*, 114:315–340.

Tingey, R.J., 1982. The geologic evolution of the Prince Charles Mountains—an Antarctic Archean cratonic block. *In* Craddock, C. (Ed.), *Antarctic Geoscience*: Madison (Univ. Wisconsin Press), 455–464.

———, 1991. Commentary on schematic geological map of Antarctica, scale 1:10 000 000. *Bull.—Bur. Miner. Resour., Geol. Geophys. (Aust.)*, Rep. No. 238.

- Truswell, E.M., Dettmann, M.E., and O'Brien, P.E., 1999. Mesozoic palynofloras from the Mac. Robertson Shelf, East Antarctica: geological and phytogeographic implications. *Antarct. Sci.*, 11:239–255.
- Turner, B.R., 1991. Depositional environment and petrography of preglacial continental sediments from Hole 740A, Prydz Bay, Antarctica. In Barron, J., Larsen, B., et al., *Proc. ODP, Sci. Results*, 119: College Station TX (Ocean Drilling Program), 45–56.
- Turner, B.R., and Padley, D., 1991. Lower Cretaceous coal-bearing sediments from Prydz Bay, Antarctica. In Barron, J., Larsen, B., et al., *Proc. ODP, Sci. Results*, 119: College Station TX (Ocean Drilling Program), 57–60.
- Vanney, J.R., and Johnson, G.L., 1985. GEBCO bathymetric sheet 5.18 (circum-Antarctic). In Jacobs, S.S. (Ed.), *Oceanology of the Antarctic Continental Shelf*. Am. Geophys. Union, Antarct. Res. Ser., 43:1–3.
- Vorren, T.O., and Laberg, J.S., 1997. Trough mouth fans—palaeoclimate and ice sheet monitors. *Quat. Sci. Rev.*, 16:865–881.
- Warnke, D.A., Marzo, B., and Hodell, D.A., 1996. Major deglaciation of east Antarctica during the early late Pliocene? Not likely from a marine perspective. In Poore, R.Z. and Sloan, L.C. (Eds.), *Climates and Climate Variability of the Pliocene*. Marine Micropaleontol., 27:237–251.
- Webb, P.N., Harwood, D.M., McKelvey, B.C., Mercer, J.H., and Stott, L.D., 1984. Cenozoic marine sedimentation and ice-volume variation on the East Antarctic Craton. *Geology*, 12:287–291.
- Wise, S.W., Jr., Breza, J.R., Harwood, D.M., Wei, W., and Zachos, J.C., 1992. Paleogene glacial history of Antarctica in light of Leg 120 drilling results. In Wise, S.W., Jr., Schlich, R., et al., *Proc. ODP, Sci. Results*, 120: College Station, TX (Ocean Drilling Program), 1001–1030.
- Wong, A.P.S., 1994. Structure and dynamics of Prydz Bay, Antarctica, as inferred from a summer hydrographic data set [M.S. thesis]. Univ. Tasmania.

FIGURE CAPTIONS

Figure 1. The Lambert Glacier drainage basin, East Antarctica, showing the location of the Gamburtsev Mountains. Ice surface elevations are in meters (modified from Hambrey, 1991). Gl. = Glacier.

Figure 2. Model of trough mouth fan deposition. **A.** During periods of maximum ice advance, basal debris is delivered to the shelf edge and redistributed by sediment gravity flows and meltwater plumes. **B.** During interglacial conditions, the outer shelf is reworked by iceberg ploughing and biogenic input from the water column.

Figure 3. Bathymetric features of and ODP sites in Prydz Bay, Antarctica. Contours are in meters below sea level. The outer edge of the Amery Ice Shelf is shown for the years 1964 (black) and 1991 (green/gray).

Figure 4. Generalized map of circulation in the Prydz Bay region (modified from Smith et al., 1984). The direction of flow is indicated by arrows. Site 1165 is located on the margin of the Antarctic Divergence, a series of cyclonic gyres at the boundary between the Antarctic Circumpolar Current (ACC) and the Polar Current. These major currents move in opposite directions and extend into Antarctic deep water.

Figure 5. Pre-Mesozoic geology of the Lambert Glacier drainage basin and Prydz Bay region after Tingey (1982) and Federov (1982). Late Proterozoic metamorphism in the northern Prince Charles Mountains, Mac. Robertson Land, and Ingrid Christensen Coast are mostly granulite facies. The southern Prince Charles Mountains metasediments are generally chlorite grade in some outcrops displaying primary sedimentary structures. Not shown are Mesozoic and Eocene basic igneous dykes in the Beaver Lake area.

Figure 6. Structure contour map of the top of basement in Prydz Bay. Contours are in milliseconds two-way travelt ime below sea level. A northeast-trending, faulted ridge separates the Prydz Bay Basin from the outer shelf.

Figure 7. Top Lower Cretaceous structure contour map (Surface PS.2B of Cooper et al., 1991a). Contours are in milliseconds two-way travelt ime below sea level.

Figure 8. Sketch profile of seismic sequences drilled during Leg 119, based on Line BMR 33-21. PS.1 is composed of Neogene topset and foreset beds, PS.2A is Paleogene glacial and preglacial sediment, PS.2B is lower Cretaceous nonmarine sediment, PS.4 is undated nonmarine red beds, and PS.5 is basement.

Figure 9. Isopach map of postsurface PP12 sediments. Contours are in milliseconds two-way traveltime; dashed line indicates shelf edge. Deposition is concentrated in the Prydz Channel Fan with relatively thin subglacial sediment on Four Ladies Bank, several patches of diatom ooze in Svenner Channel, and a morainal bank on the western side of the bay. Elsewhere, post-PP12 sediments are present but are too thin to be resolved on seismic records.

Figure 10. A. Overview map of the primary Leg 188 drill sites with respect to port of origin (Fremantle) and final port (Hobart). **B.** Map of East Antarctic coastline between 50°E and 90°E, showing the location of Prydz Bay, Mac. Robertson Land, Antarctic stations, Leg 119 drill sites (light gray circles), and Leg 188 drill sites (dark gray circles).

Figure 11. Seismic reflection profile BMR 33-23P3 over Site 1166 showing lithostratigraphic units, ages, rock types, paleoenvironmental interpretation, the schematic section, and downhole-logging units. SP = shotpoints; TD = total depth.

Figure 12. Composite stratigraphic section for Site 1166 showing core recovery, a simplified summary of lithology, lithostratigraphic unit boundaries, and age. Gamma-ray and resistivity curves are derived from downhole logs along with minerals identified by XRD, which shows the percentage of the most abundant minerals. Note: Lithology patterns have been added to this figure.

Figure 13. Plots showing biostratigraphic age control and magnetostratigraphic polarity intervals for Site 1166. FO = first occurrence; LO = last occurrence. The inclinations obtained from split cores are compared with inclinations from stepwise-demagnetized discrete samples (red/gray squares). Polarity is shown on the log to the right. Black represents normal and white represents reverse polarity intervals.

Figure 14. Downhole wireline logs from Site 1165 showing density, porosity, resistivity, and sonic velocity curves, with the logging units marked. The core index property measurements of density and porosity and the lithostratigraphic units from core analysis are also shown. LWD = logging while drilling.

Figure 15. Representative examples of Formation MicroScanner (FMS) resistivity images from Hole 1166A, with lithologic descriptions, porosity, density, gamma ray, and caliper and resistivity curves from downhole logging. APLC = accelerator porosity sonde near-array limestone porosity corrected (decimal fraction); RHOM = corrected bulk density (g/cm^3).

Figure 16. Conceptual diagrams for the setting of the Prydz Bay region from preglacial (scene 1) to the initiation of glaciation with marine transgressions (scenes 2, 3, and 4) to full glaciation with ice sheets on the overdeepened continental shelf (scene 5).

Figure 17. Seismic reflection profile AGSO 49/0901 over Site 1167. SP = shotpoints.

Figure 18. Site 1167 lithostratigraphic units, facies, and interpretation. In “Recovery” column, black = recovered; gray = not recovered.

Figure 19. Distribution and frequency of sandstone vs. granite/igneous limestones in Hole 1167A. A shift from largely sandstone clasts to granite clasts occurs uphole at ~200 mbsf.

Figure 20. Plots showing magnetostratigraphy, magnetic susceptibility, and the ratio of anhysteretic and isothermal remanent magnetization (ARM/IRM) for Site 1167. The inclinations from split cores are compared with inclinations from stepwise-demagnetized discrete samples (red/gray squares). The horizontal lines and the labels on the magnetic susceptibility plot indicate intervals with different magnetic properties.

Figure 21. Plots of chloride and sulfate interstitial water values with depth at Site 1167.

Figure 22. Seismic reflection profiles across Site 1165. **A.** Regional profile across the Wild Drift. The regional horizon PP12 can be traced beneath the continental slope and is the base of the Prydz Bay Trough Mouth Fan. **B.** Profile recorded over the drill site by the *JOIDES Resolution*'s water gun seismic system upon approach to the site. Lithostratigraphic units and lithology are also shown.

Figure 23. Composite stratigraphic section for Site 1165 showing core recovery, a simplified summary of lithology, lithostratigraphic unit boundaries, and age. Also shown are the distribution of limestones and dispersed clasts, mineral abundances identified by XRD, the percentage of diatoms and sponge spicules from smear slides, and color reflectance. See Figure 12 for lithology and mineral legends. The bar graph shows the distribution of isolated limestones (>5 mm) downhole. The vertical bars on the right side of the column show the distribution of dispersed grains and granules (<5 mm). X-ray diffraction shows the percentage of most abundant minerals. This graph was plotted using the methods of Forsberg et al. (1999). In the smear-slide graph, solid line = diatoms; dashed line = sponge spicules. The thin line in the color reflectance plot shows the reflectance percent downhole. The thick line is a 200-point moving average.

Figure 24. Magnetostratigraphy for Site 1165.

Figure 25. Age-depth plot for Site 1165 based on biostratigraphy and magnetostratigraphy. FO = first occurrence; LO = last occurrence.

Figure 26. Organic gases and carbon in Holes 1165B (open symbols) and 1165C (solid symbols). **A.** Concentrations of methane (C_1), ethane (C_2), and propane (C_3) gases with depth. **B.** Percentage of organic carbon with depth.

Figure 27. Example of the cyclicity (at Milankovitch periodicities; see text) observed in Site 1165 cores, with spectra of spectrophotometer-lightness and gamma-ray (GRA) bulk density values. **A.** Three sections for Core 188-1165B-14H with core photo (left), model (center), and lightness curve. **B.** Lightness and bulk density values, with maximum entropy spectra showing peaks (in depth) at periods of 4.27, 1.55, 0.95, and 0.72 m, equivalent to approximate time intervals of 93.7, 41.5, 20.8, and 18.2 k.y. at a sedimentation rate of 3.8 to 4.1 cm/k.y.

Figure 28. Conceptual diagrams showing the long-term shift from temperate to cold conditions across the continental margin at Prydz Bay, from times of wet-based glaciers with fluvial systems to those of dry-based(?) ice sheets in maximum glacial–interglacial conditions. During the transition to cold times, short-term seaward-landward shifts in glaciers (double arrow) may explain the cyclic gray/green sedimentation patterns with Milankovitch periodicities (i.e., Site 1165; early Miocene and younger times).

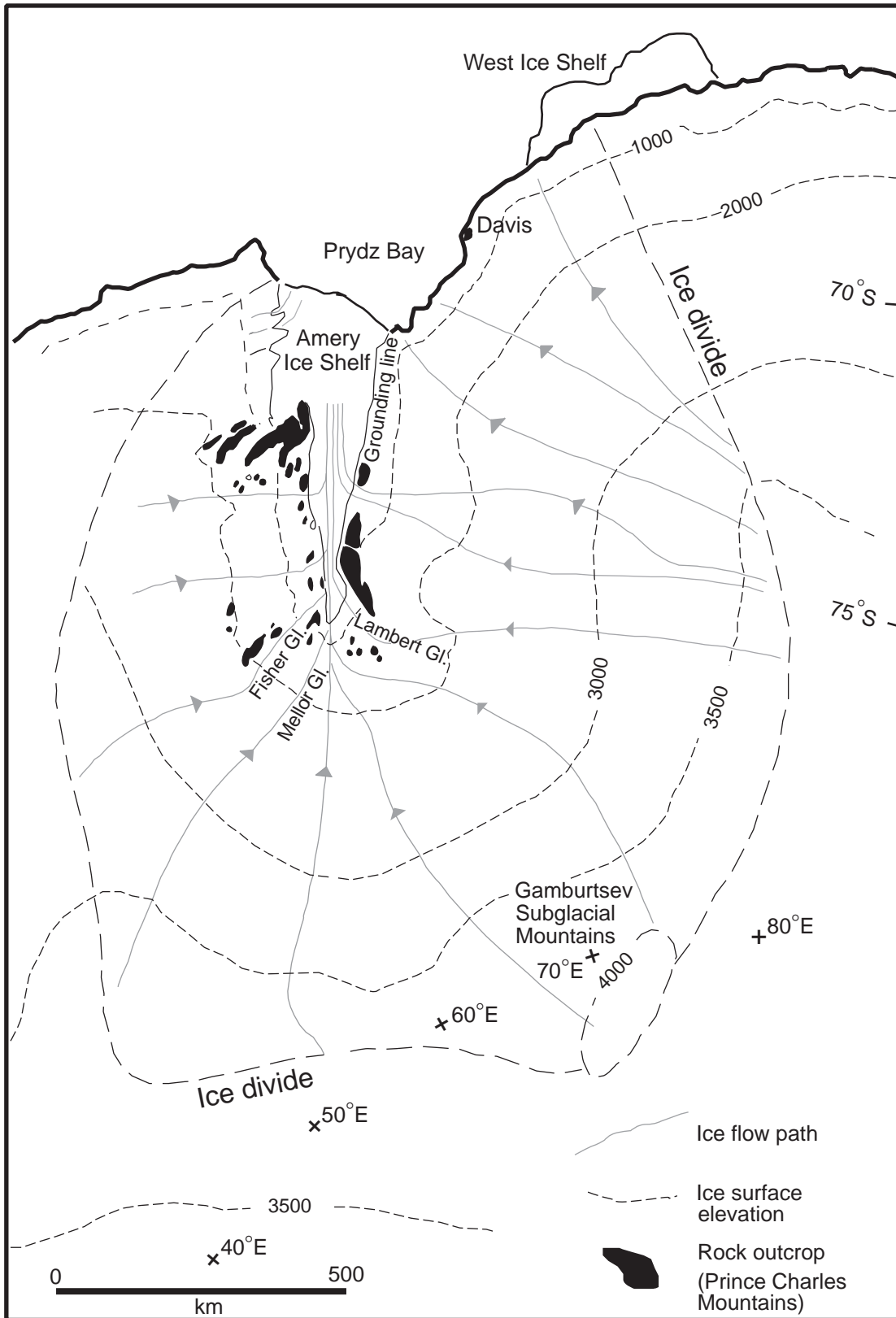
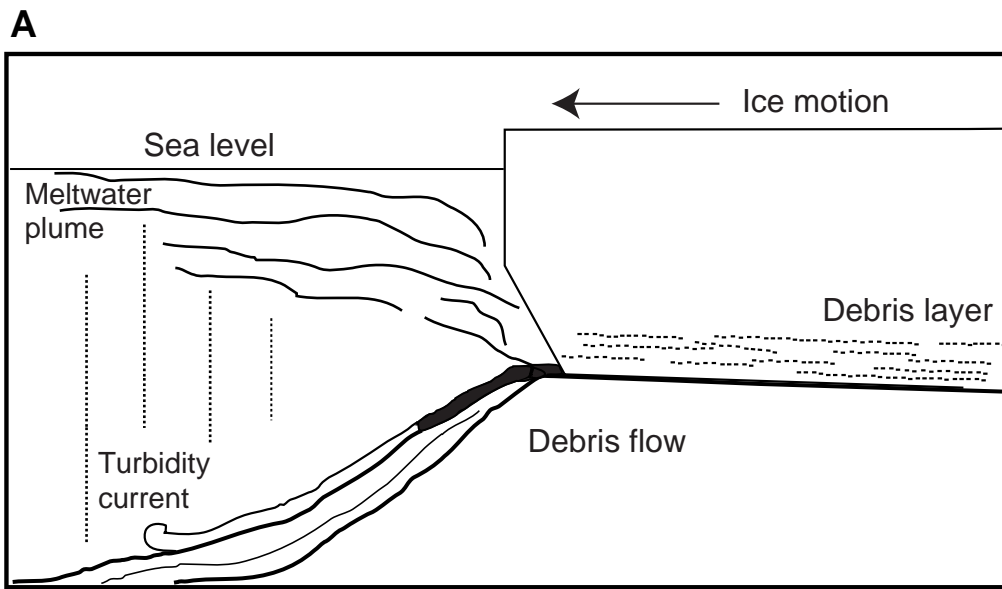
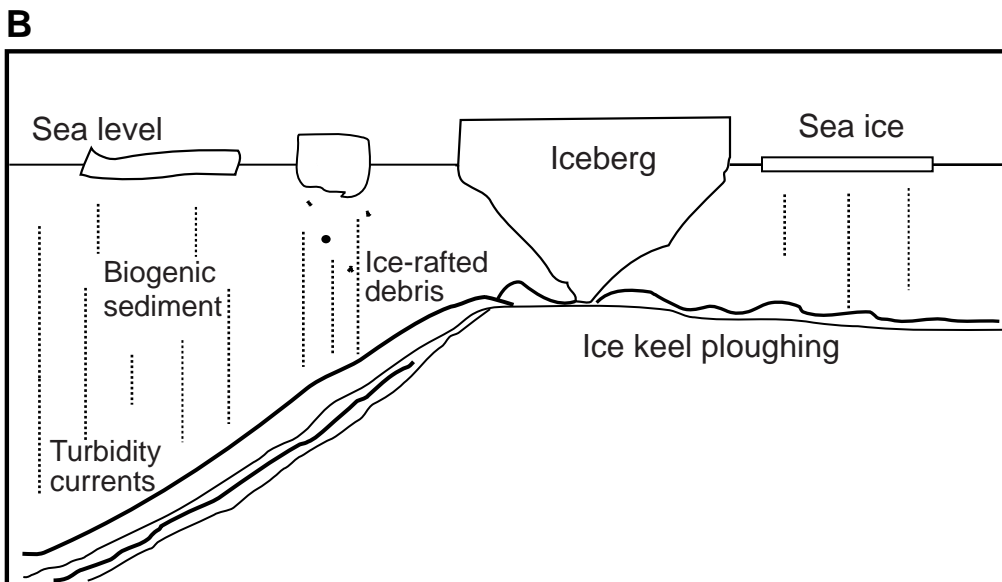


Figure 1



Glacial maxima - Ice grounded at shelf edge



Interglacial conditions - High sea level, ice near coast

Figure 2

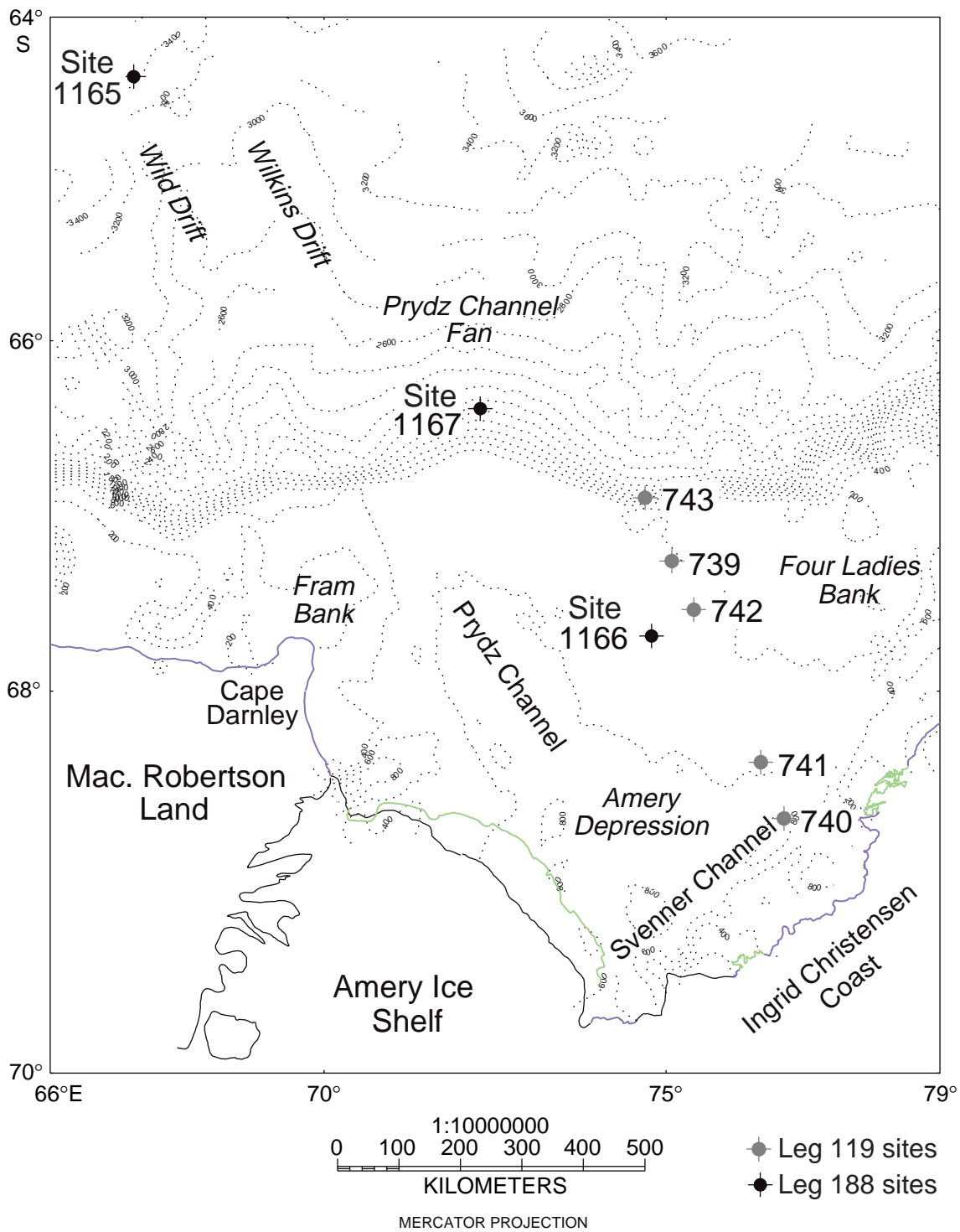


Figure 3

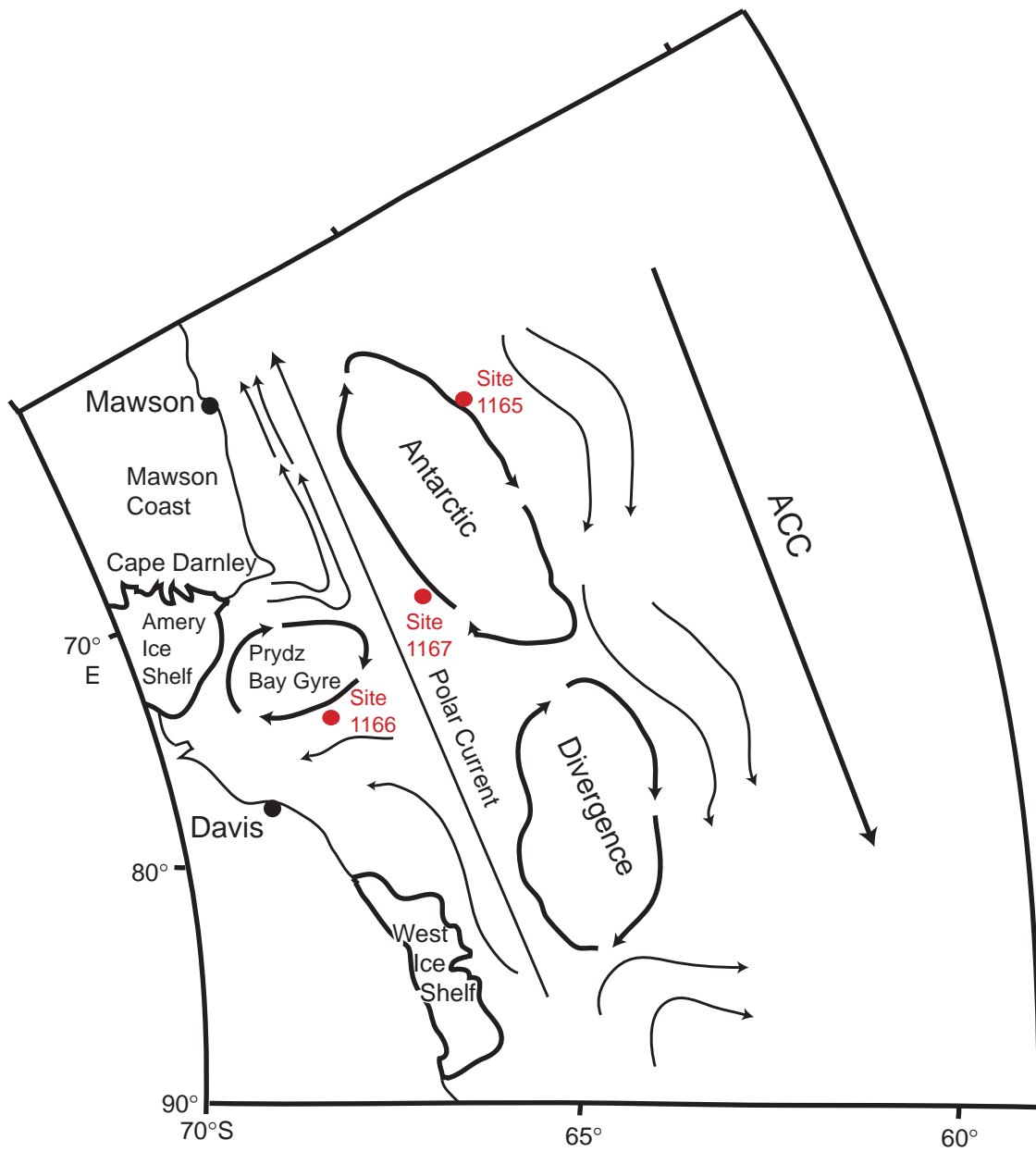


Figure 4

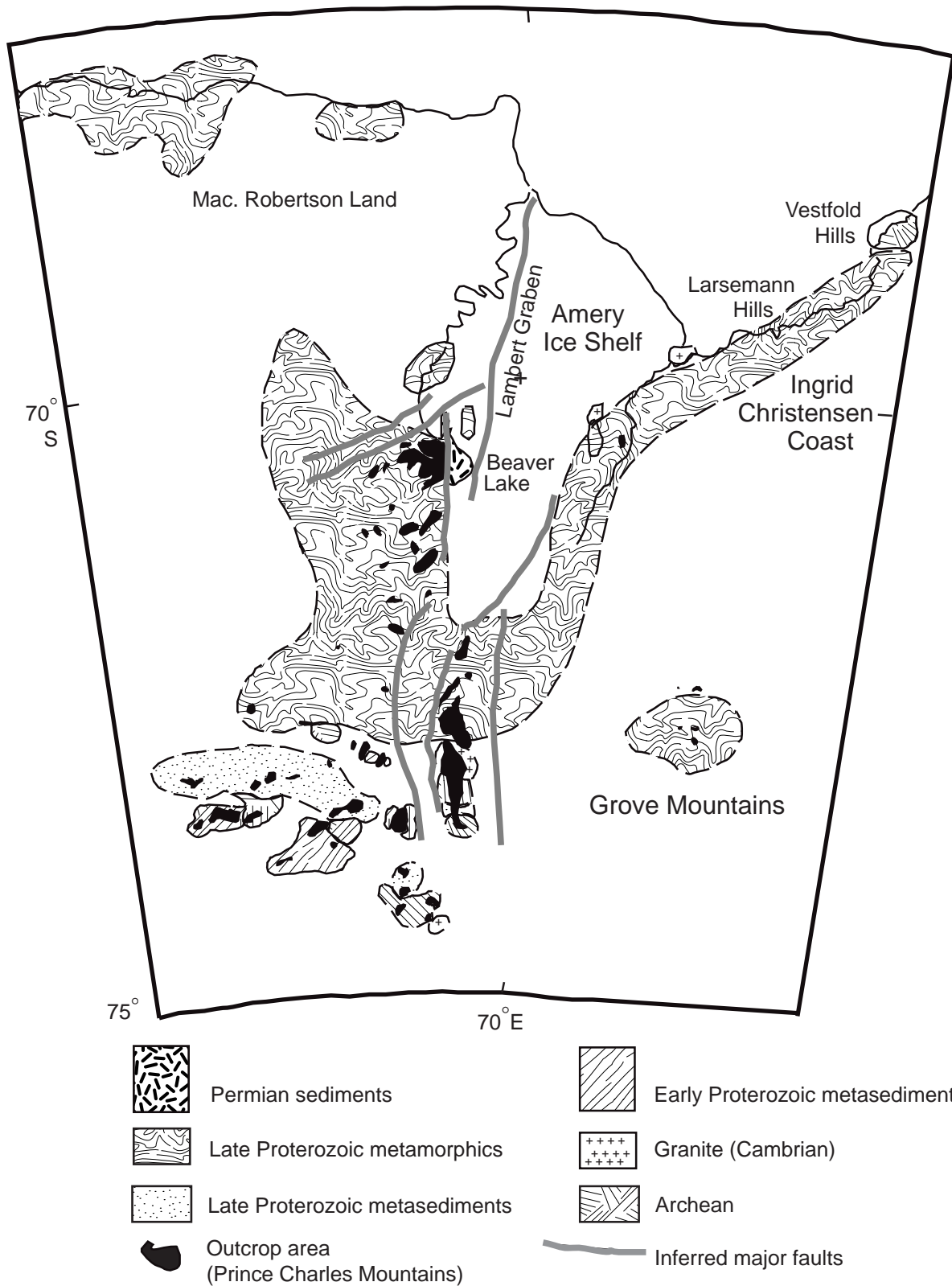


Figure 5

PRYDZ BAY

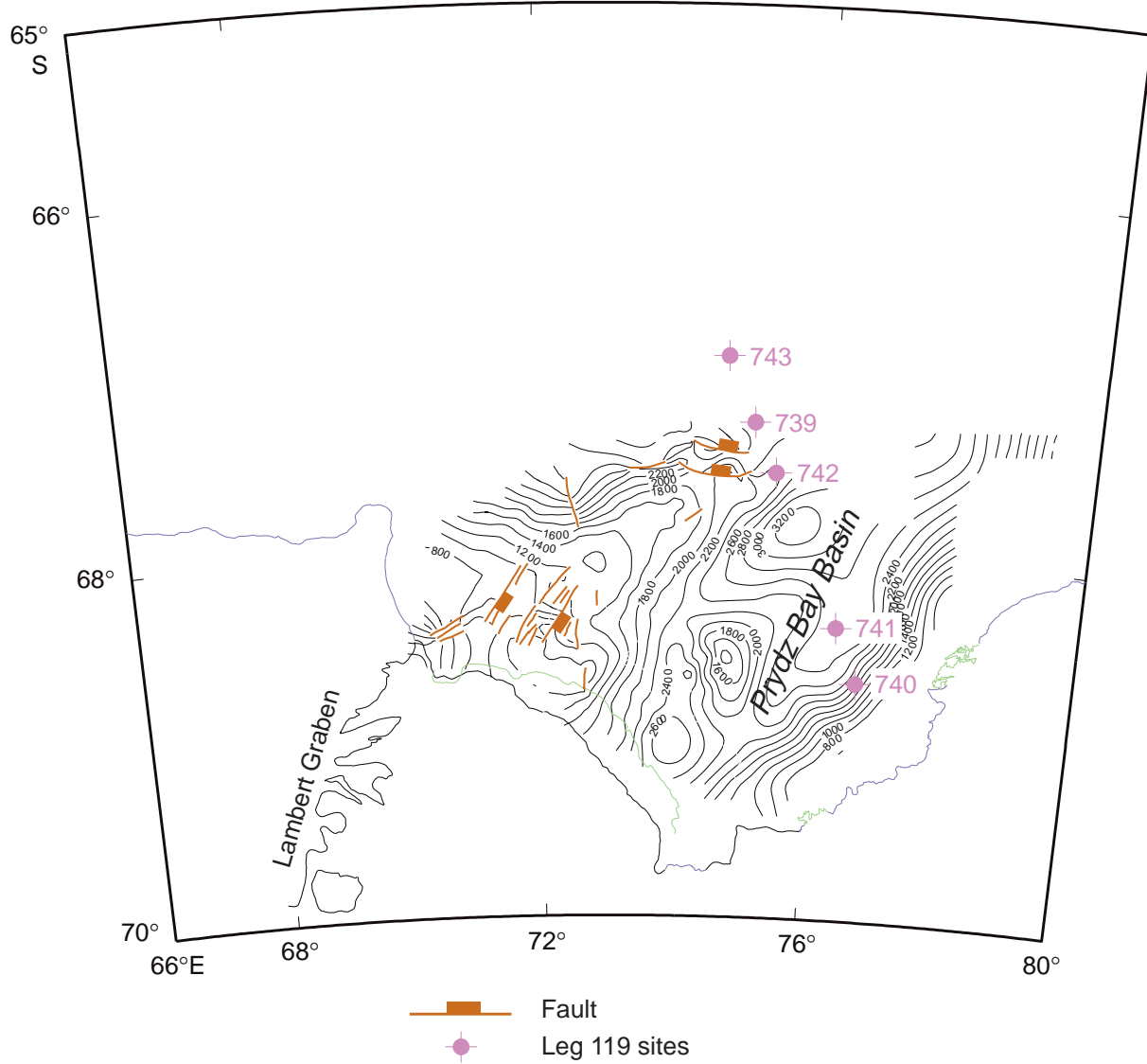


Figure 6

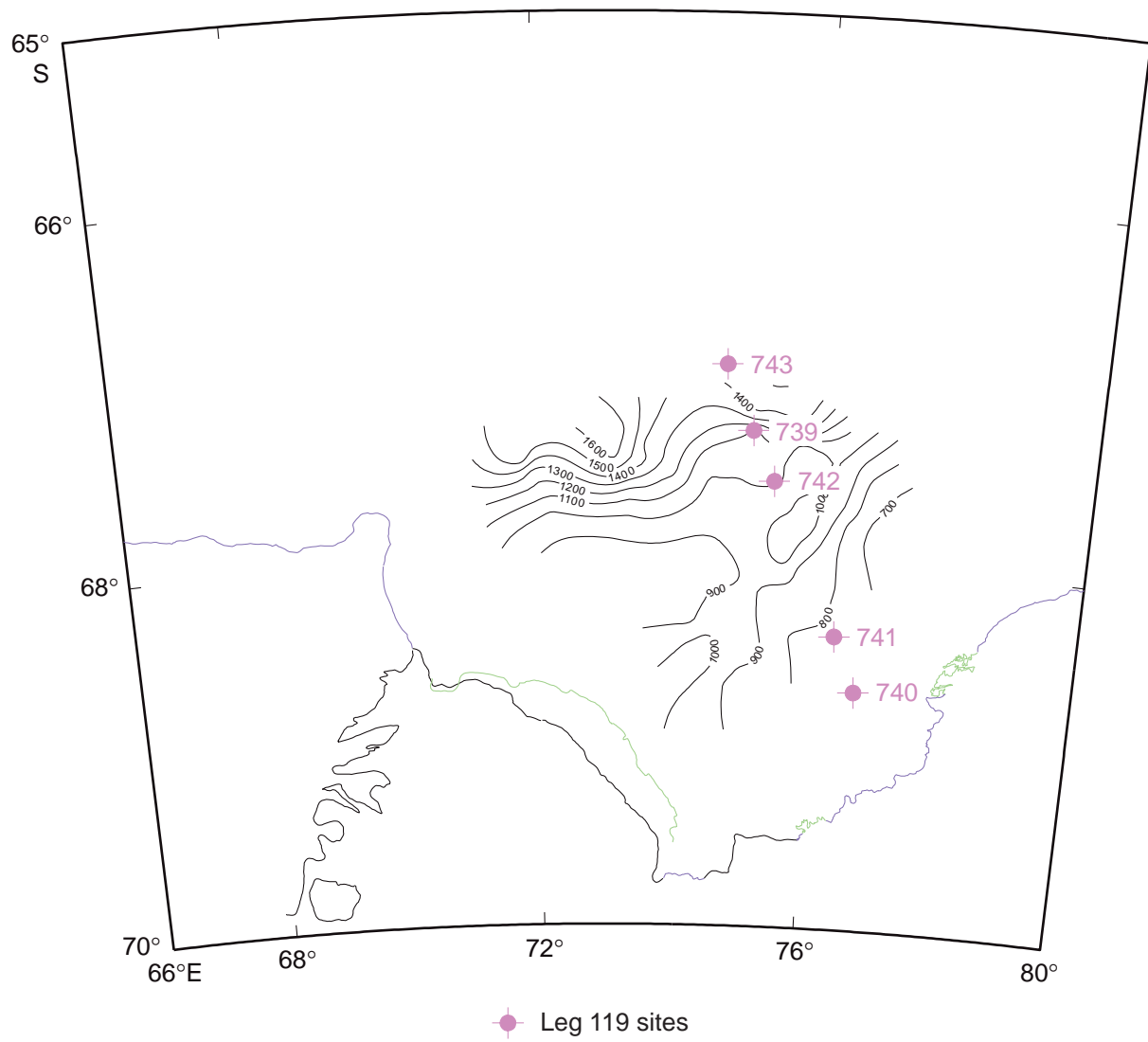
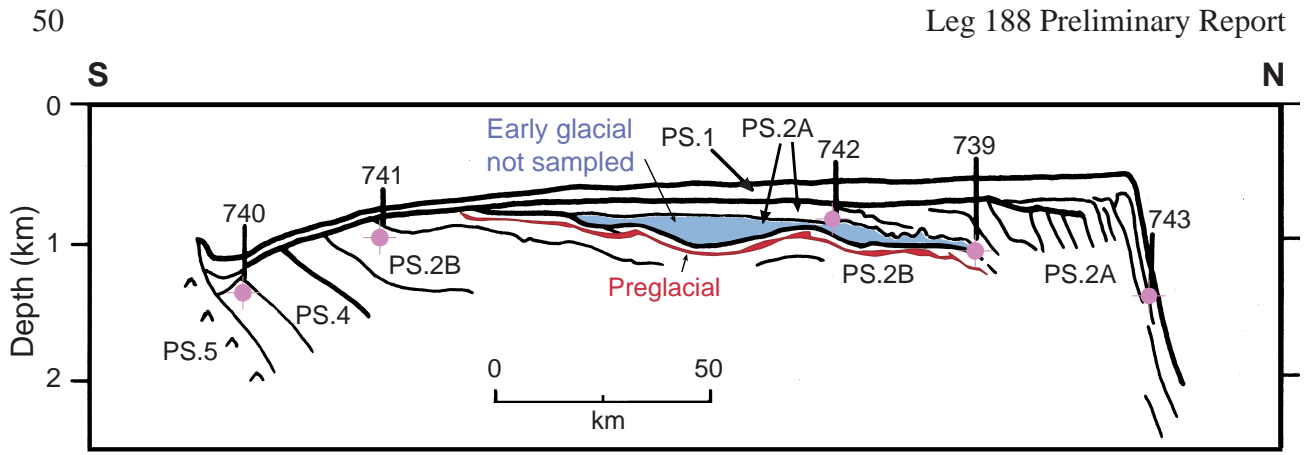


Figure 7



● Leg 119 sites

Figure 8

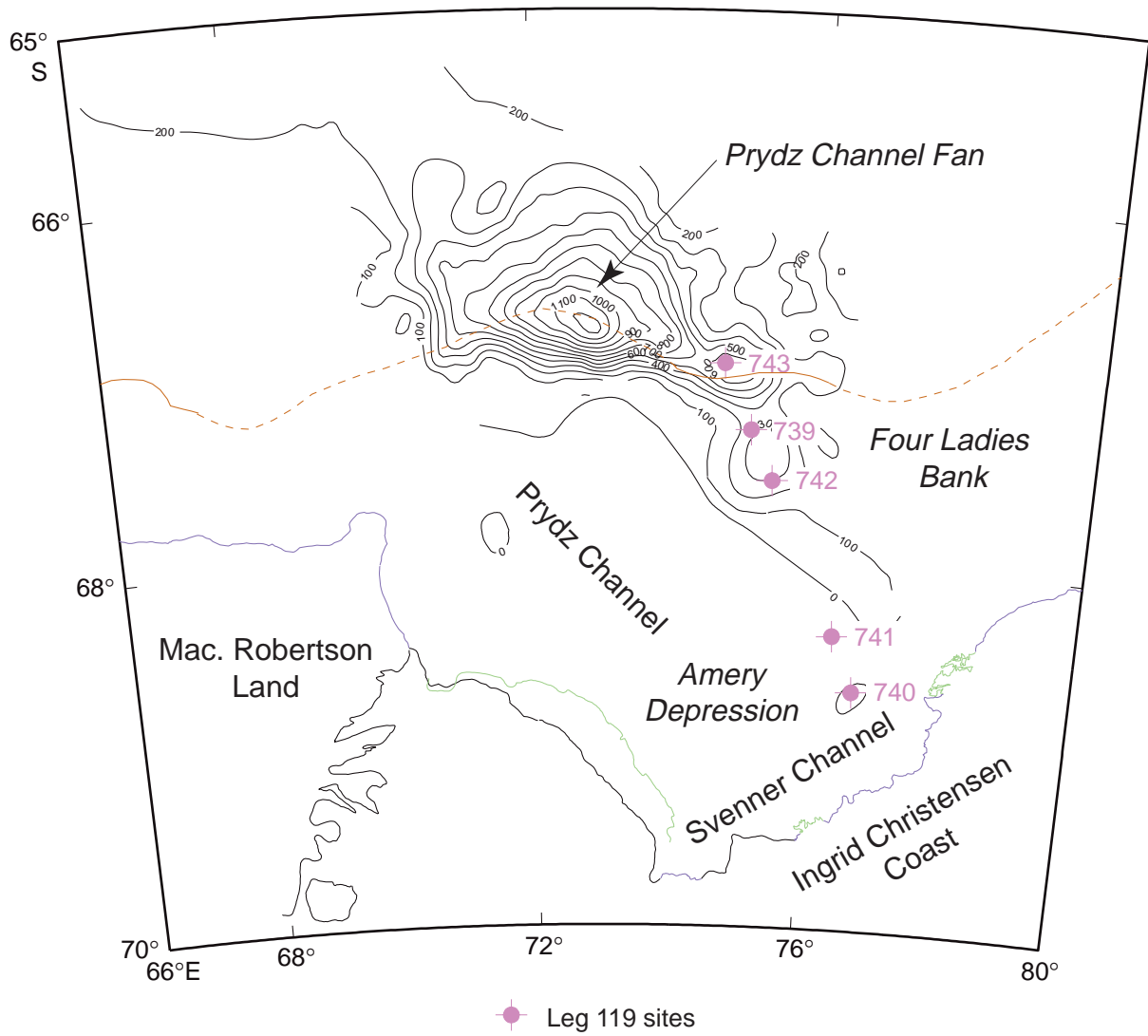
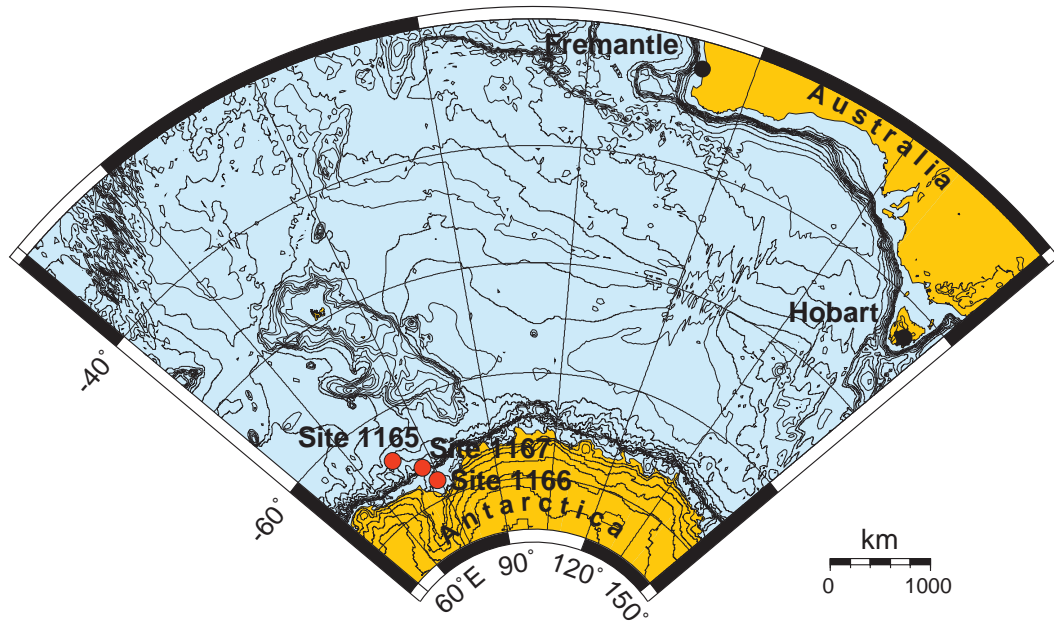


Figure 9

A



B

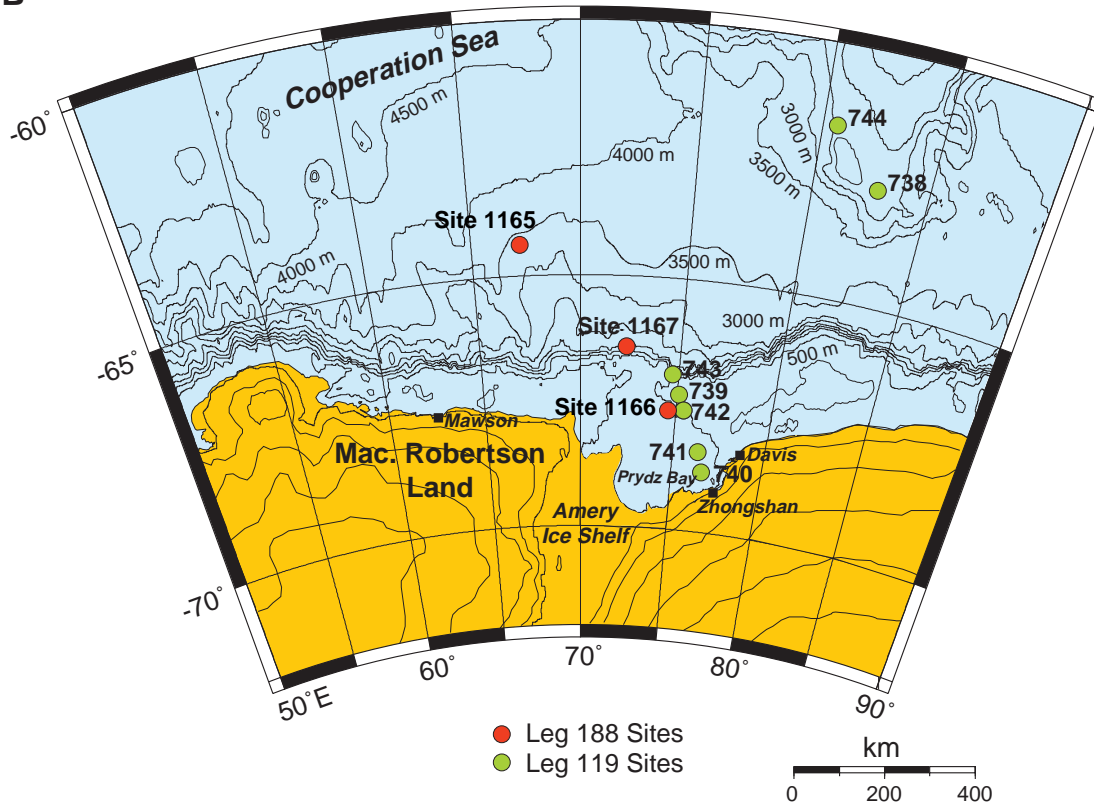


Figure 10

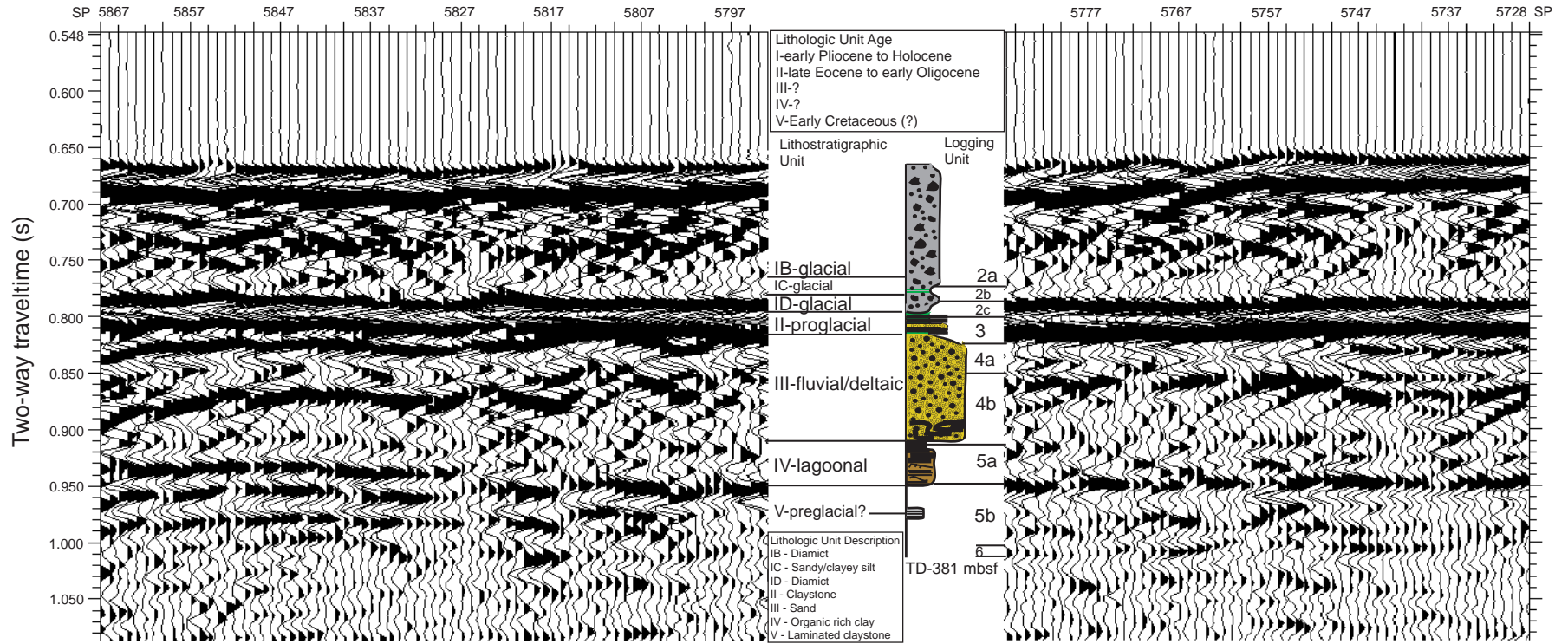


Figure 11

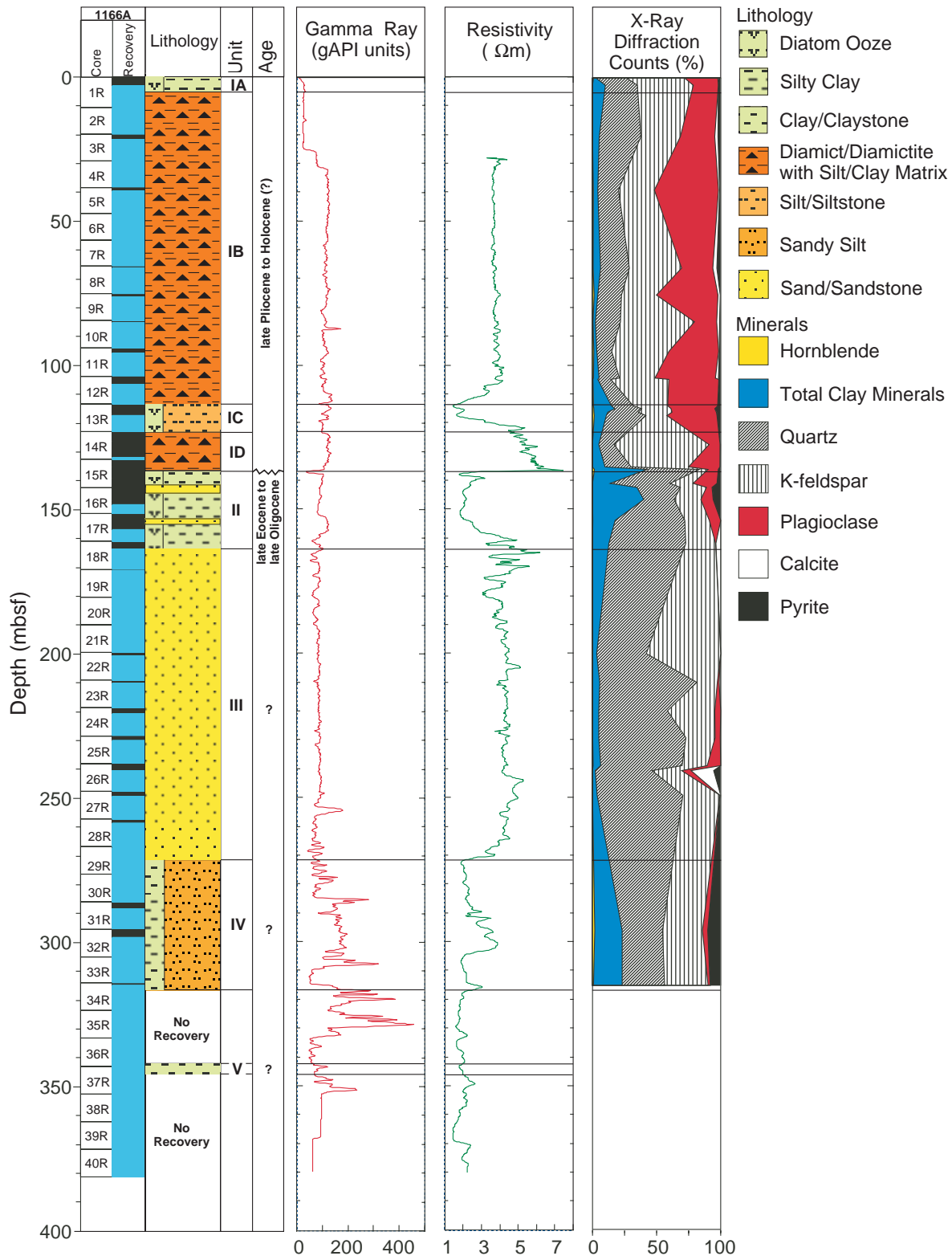


Figure 12

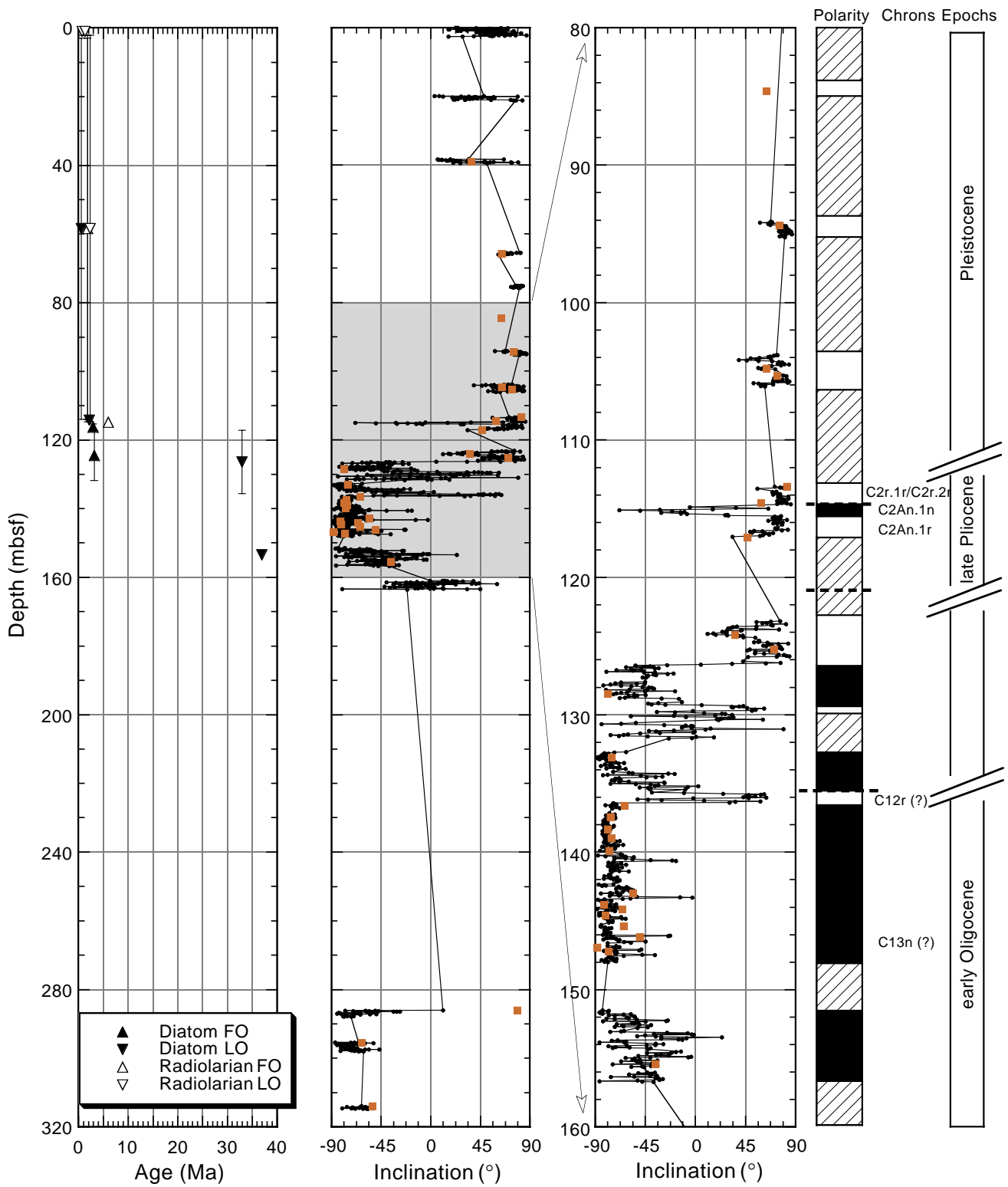


Figure 13

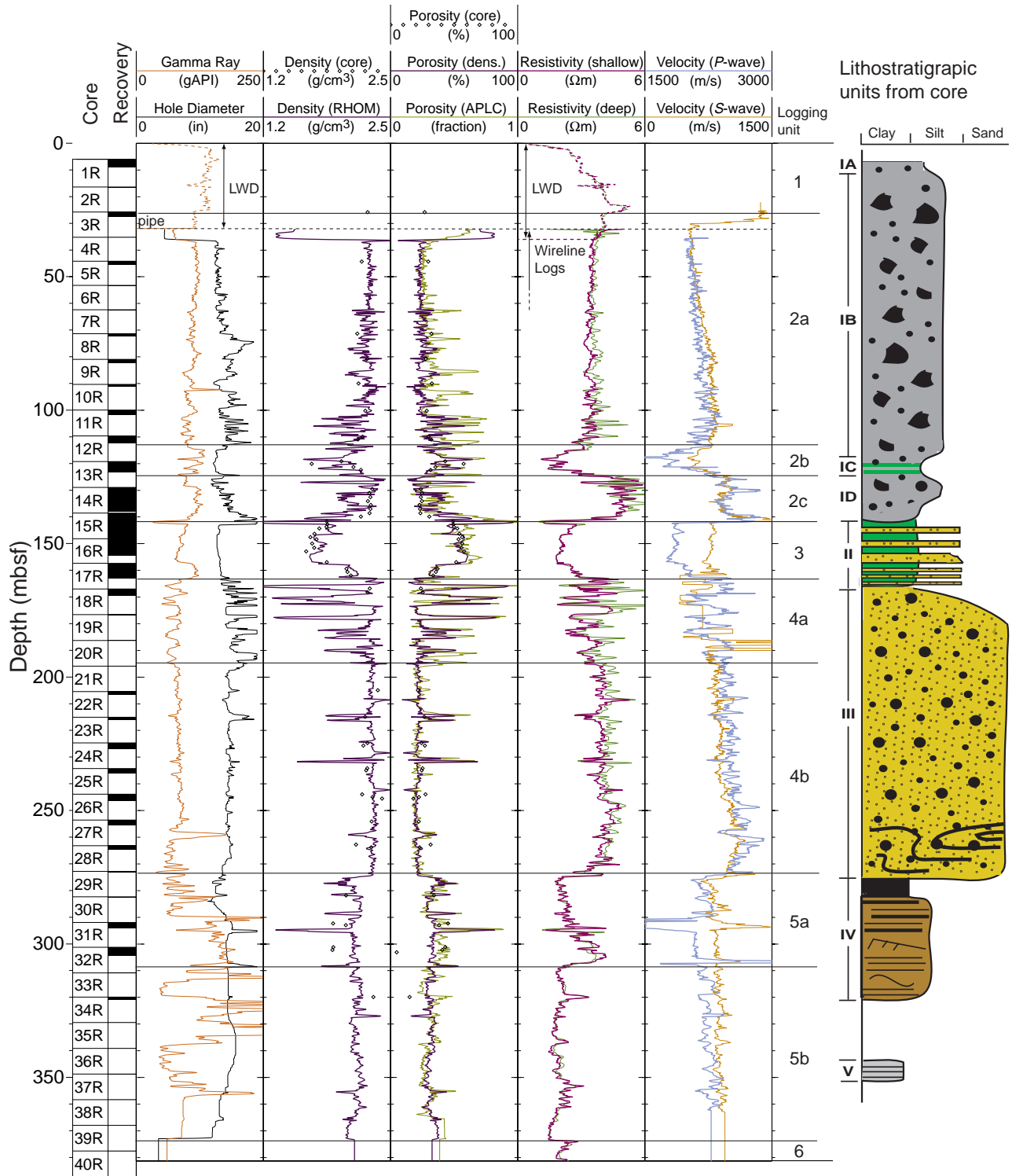


Figure 14

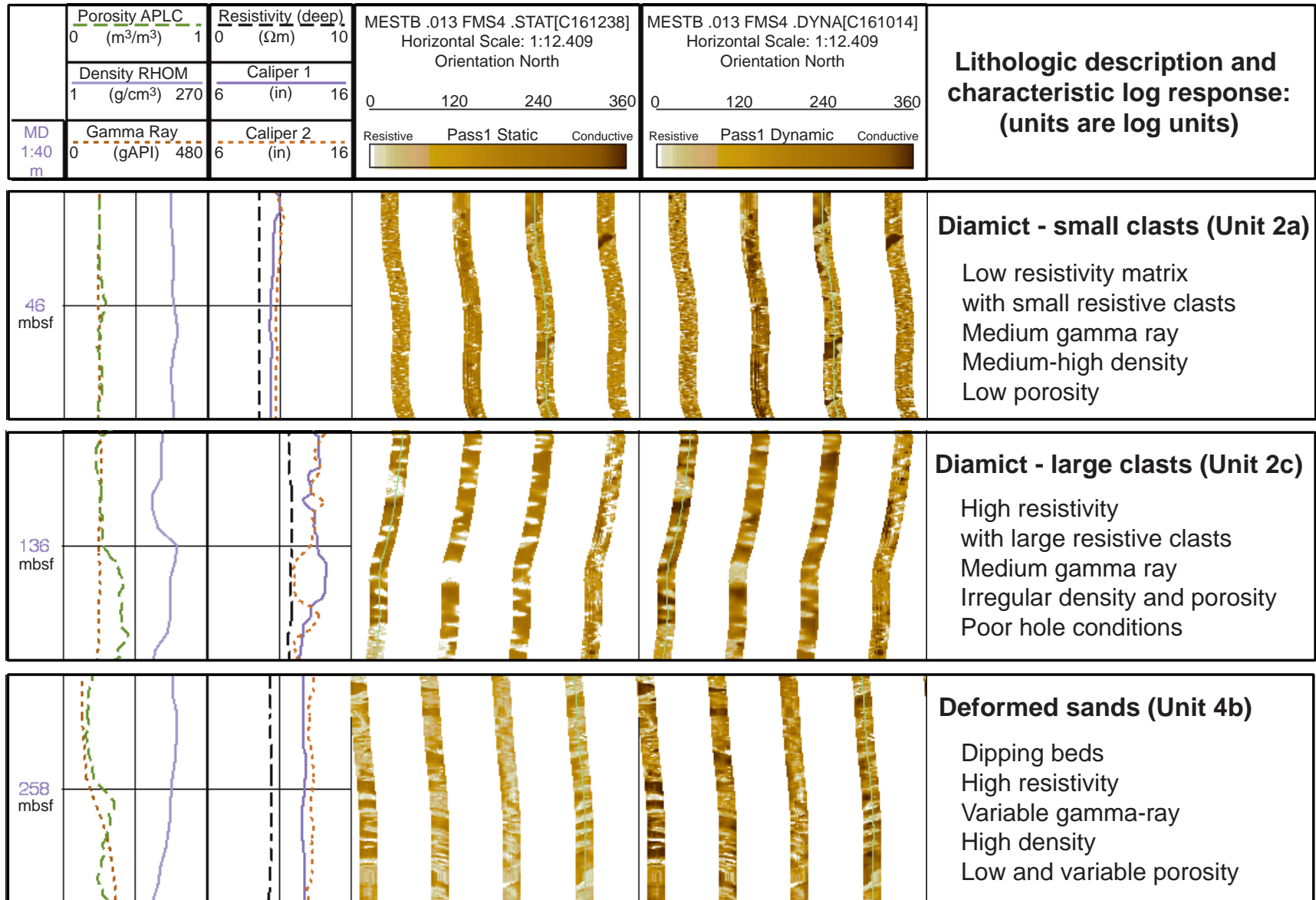
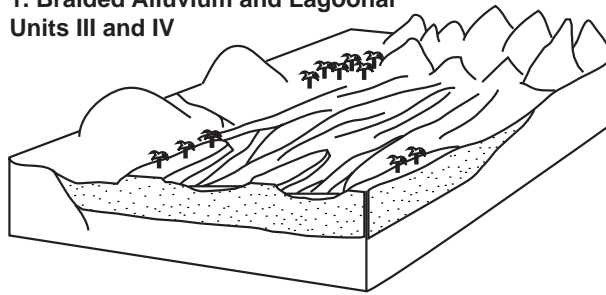
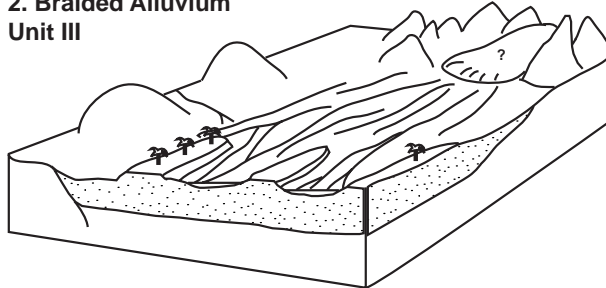


Figure 15

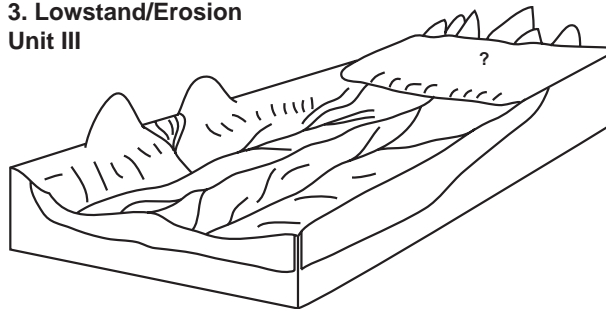
**1. Braided Alluvium and Lagoonal
Units III and IV**



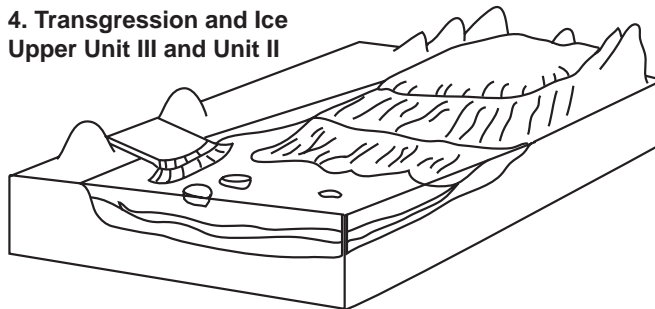
**2. Braided Alluvium
Unit III**



**3. Lowstand/Erosion
Unit III**



**4. Transgression and Ice
Upper Unit III and Unit II**



**5. Ice Sheet Development
Unit I**

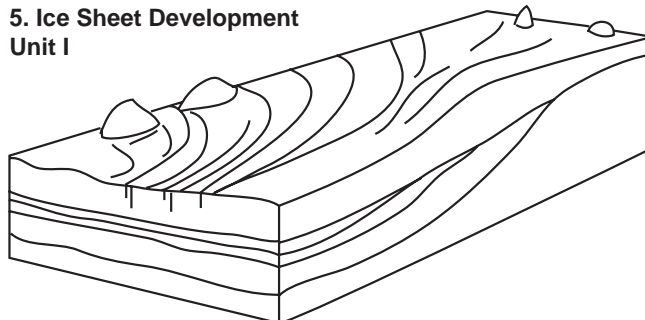


Figure 16

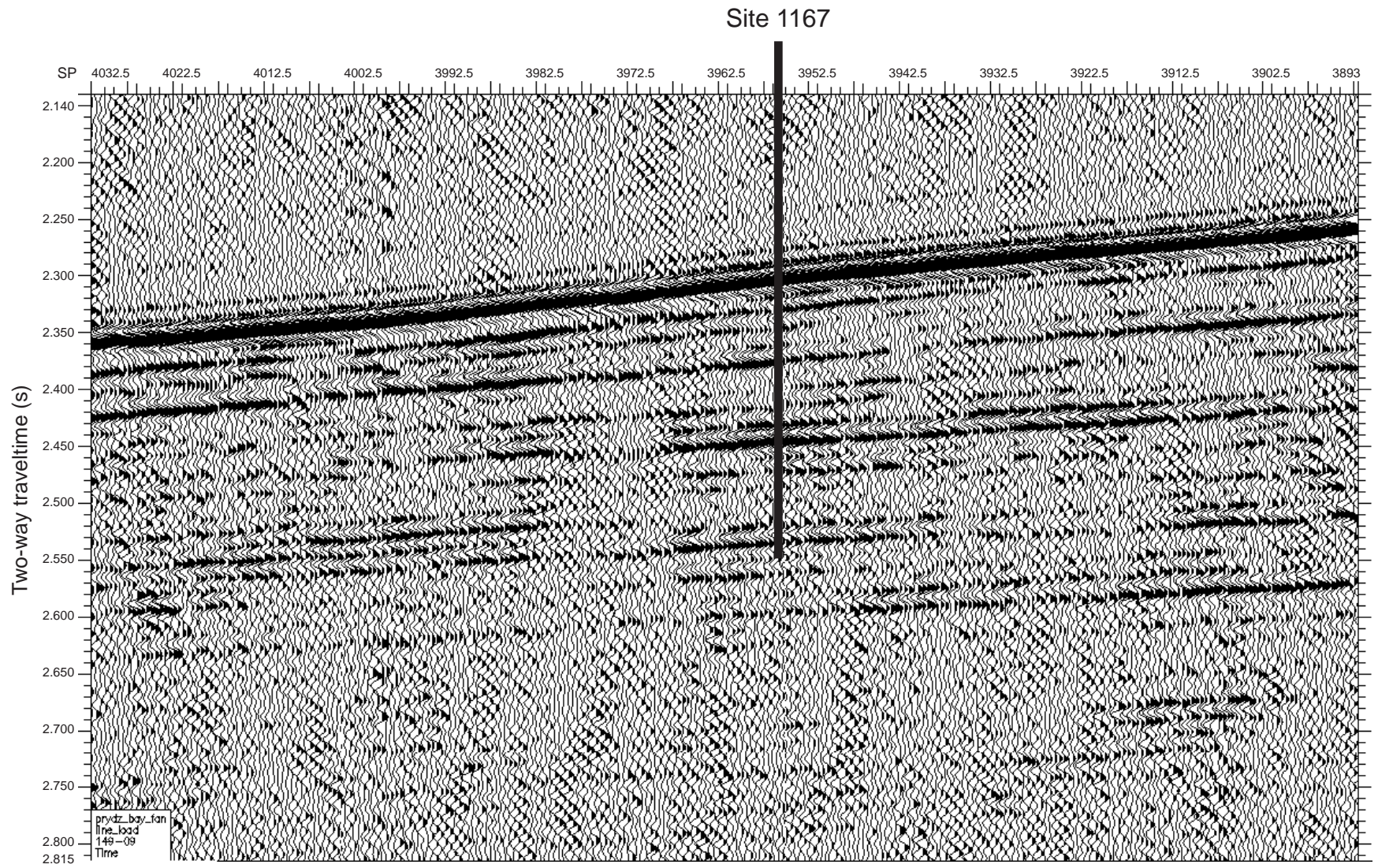


Figure 17

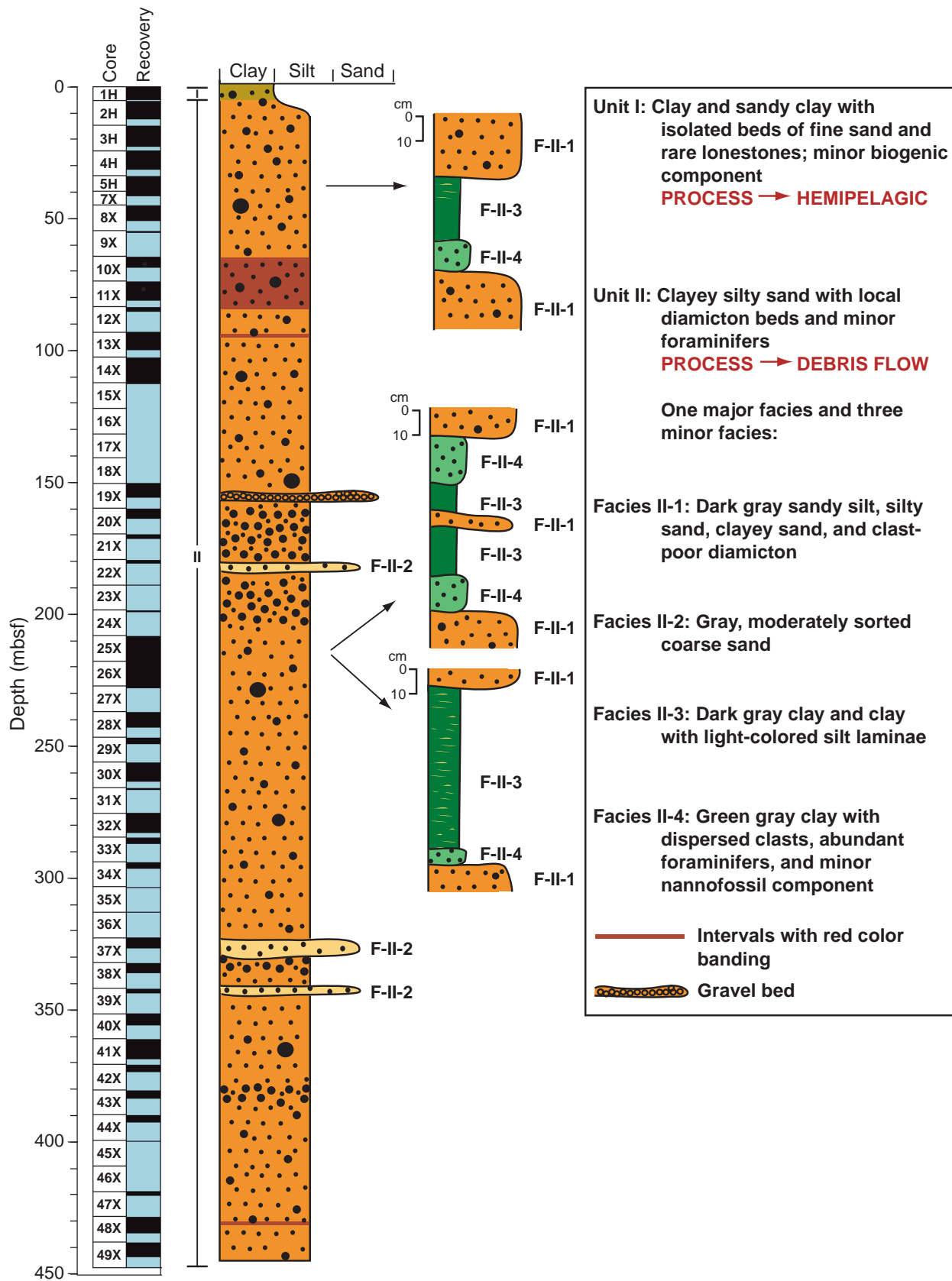


Figure 18

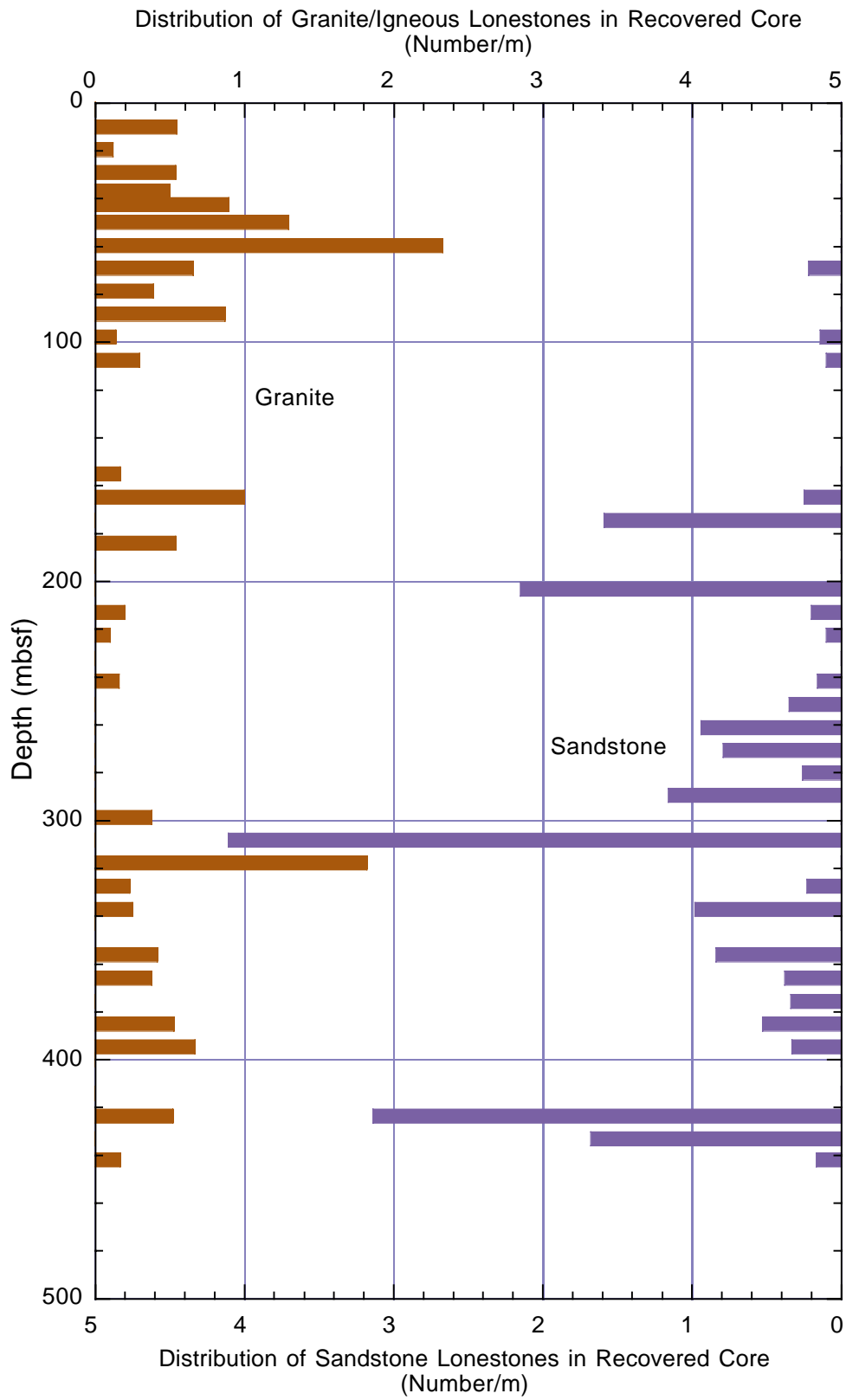


Figure 19

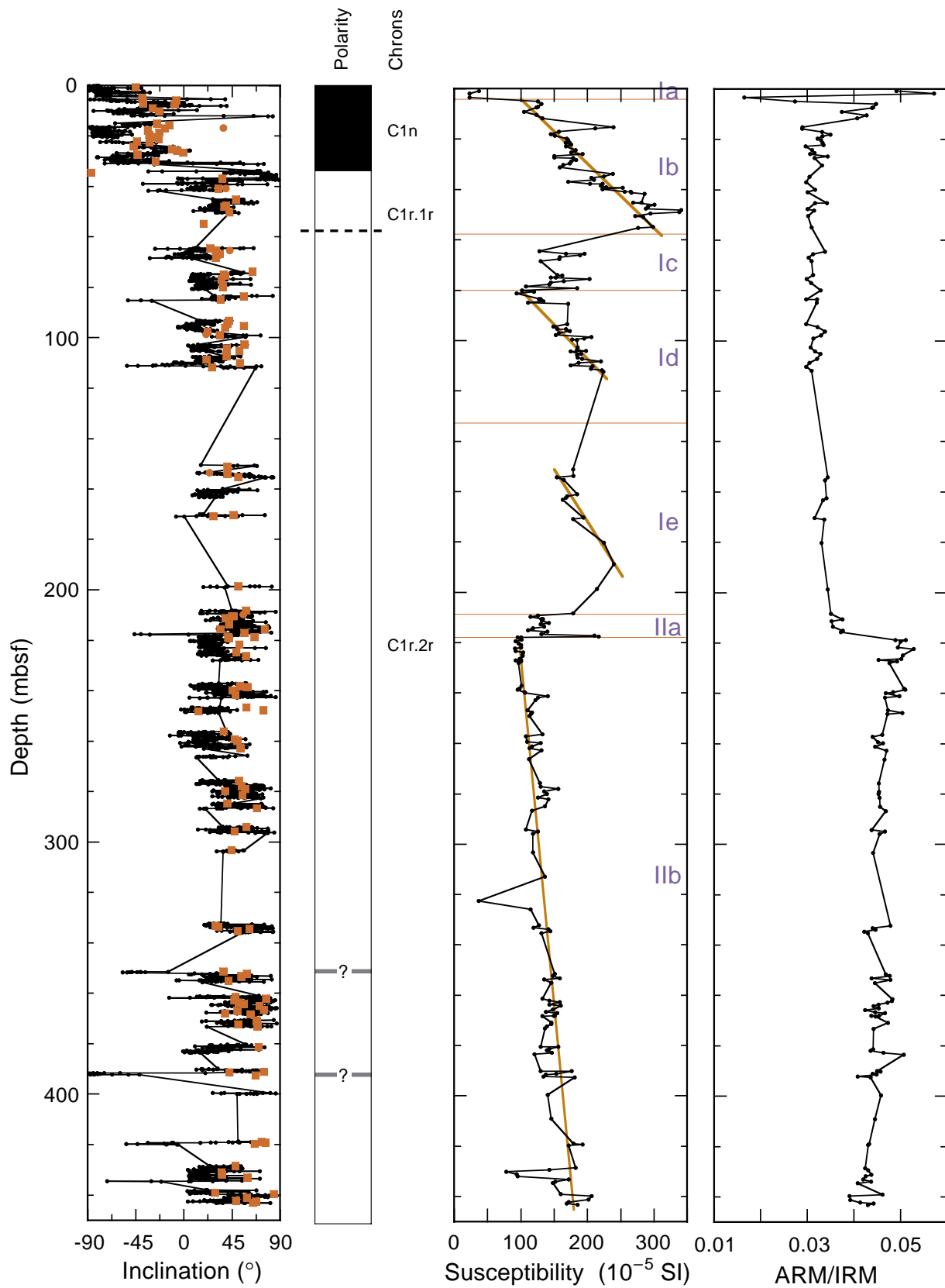


Figure 20

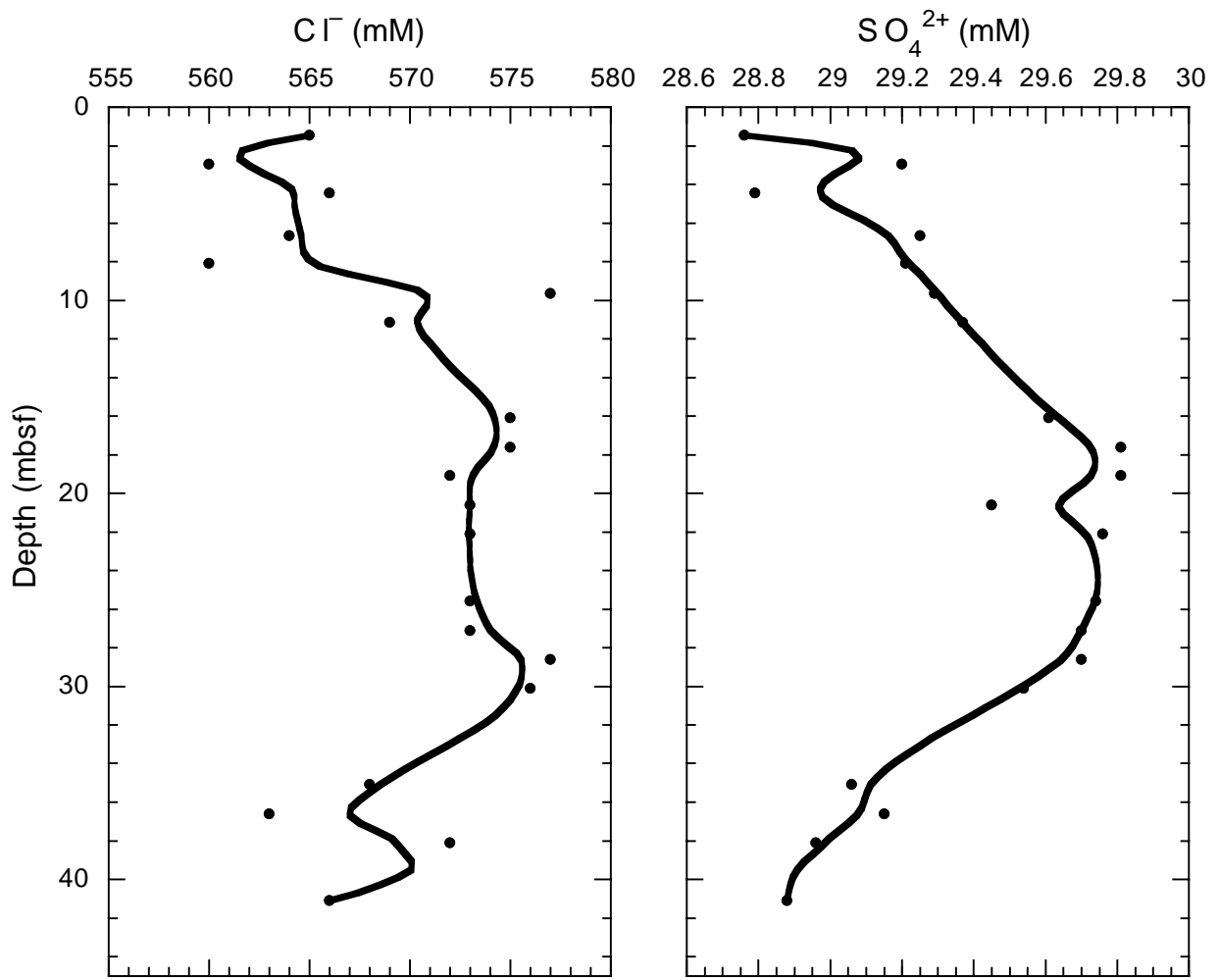


Figure 21

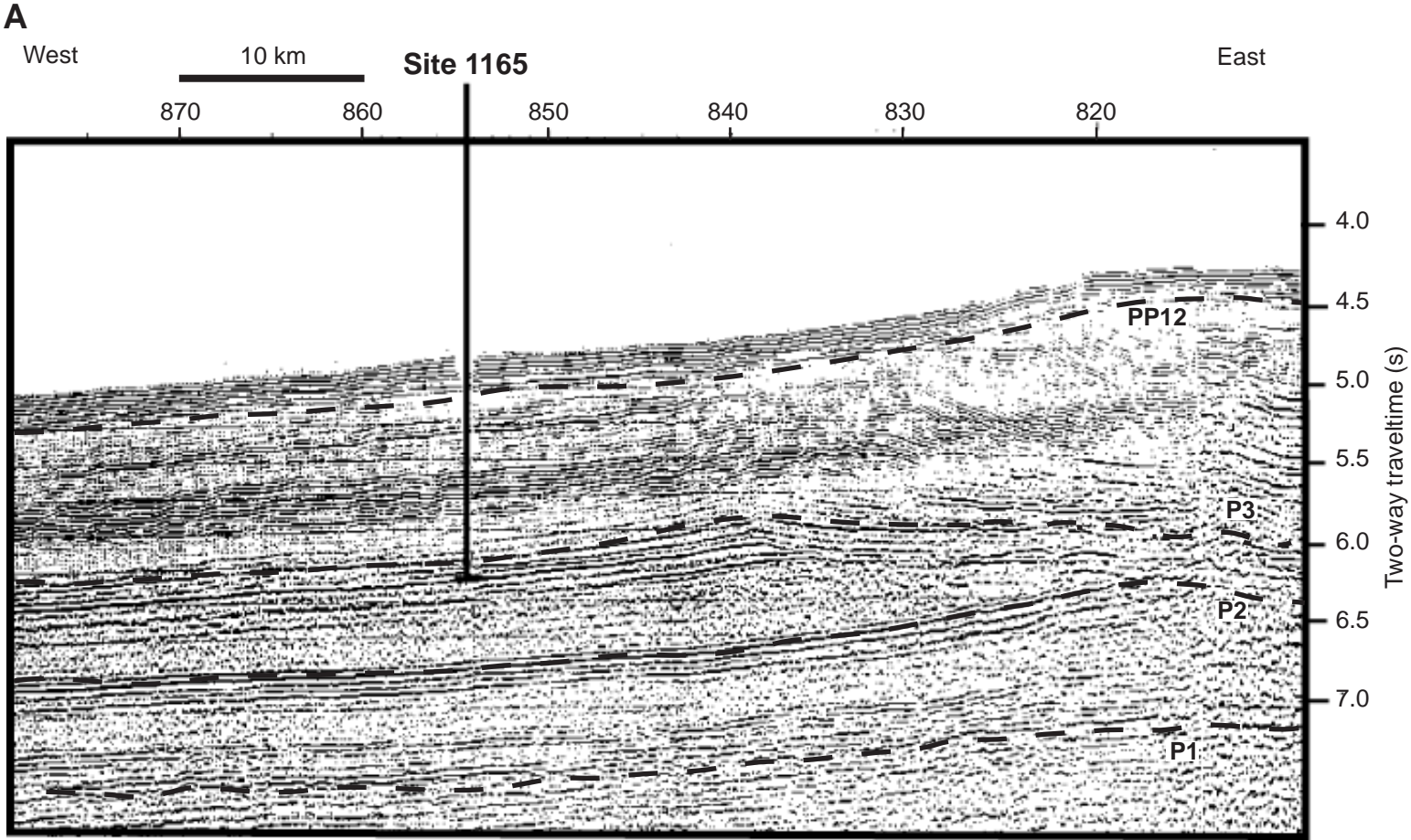
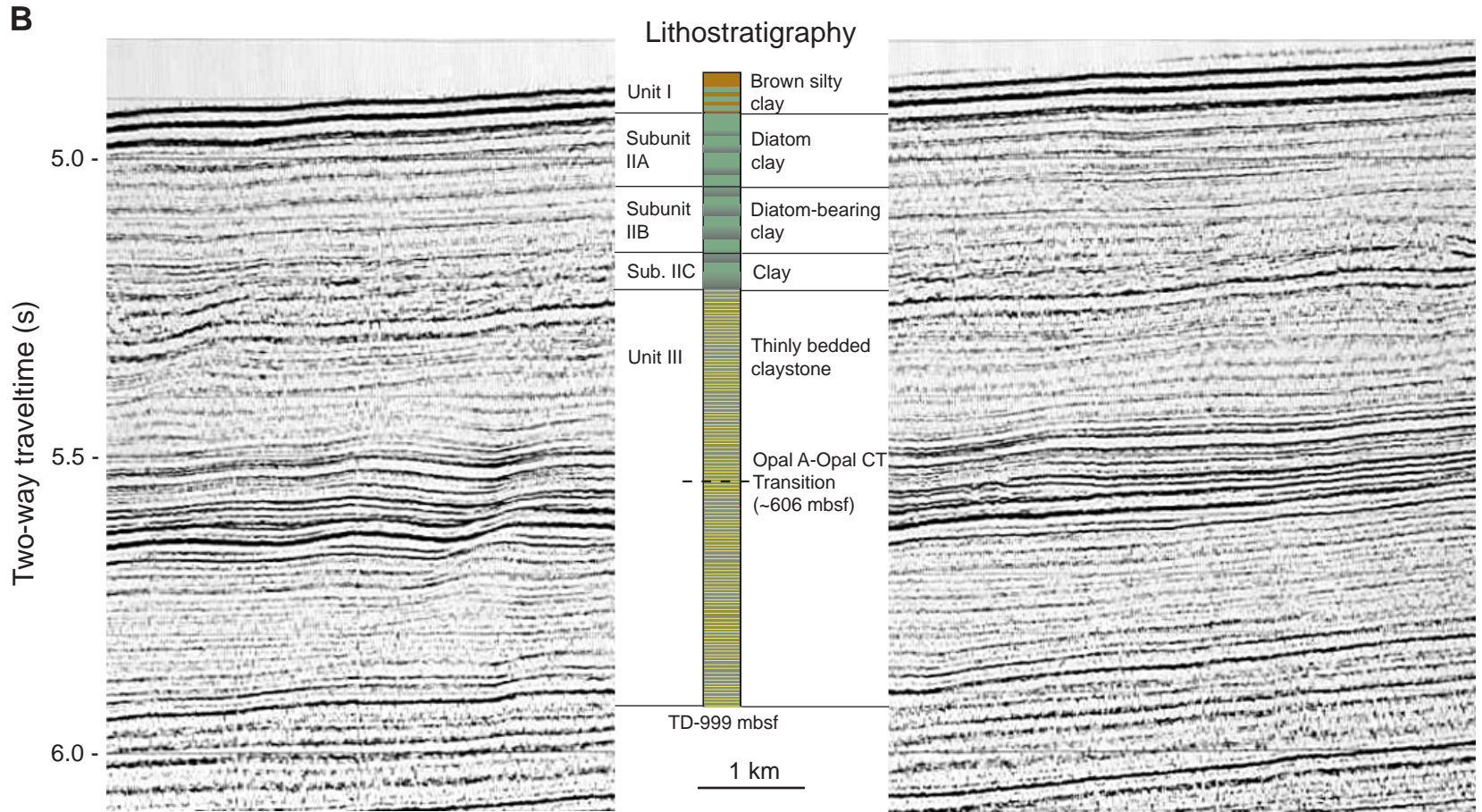


Figure 22A



Unit 1: upper Pliocene to Pleistocene

Unit II: middle to upper Miocene

Unit III: lower to middle Miocene

Figure 22B

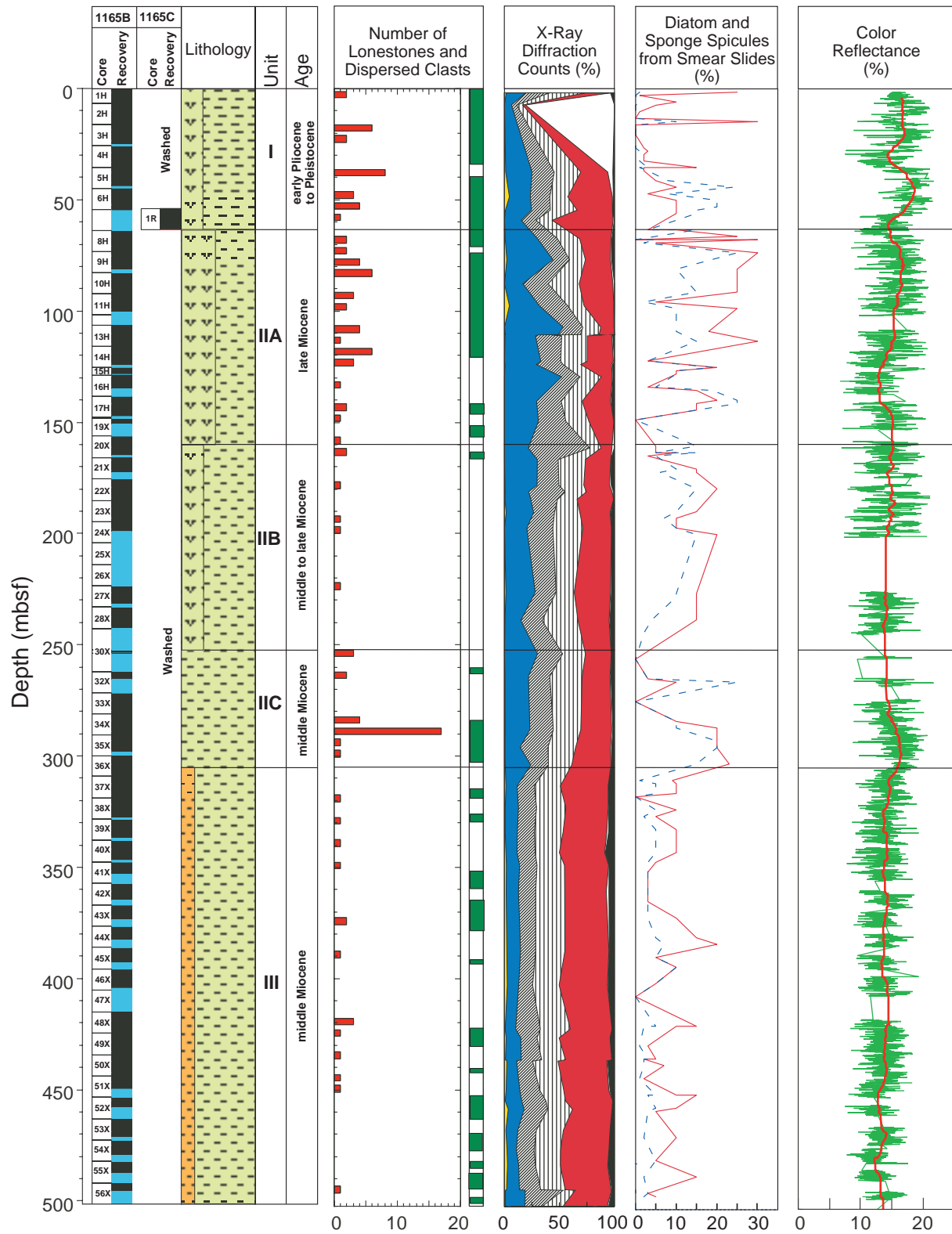


Figure 23

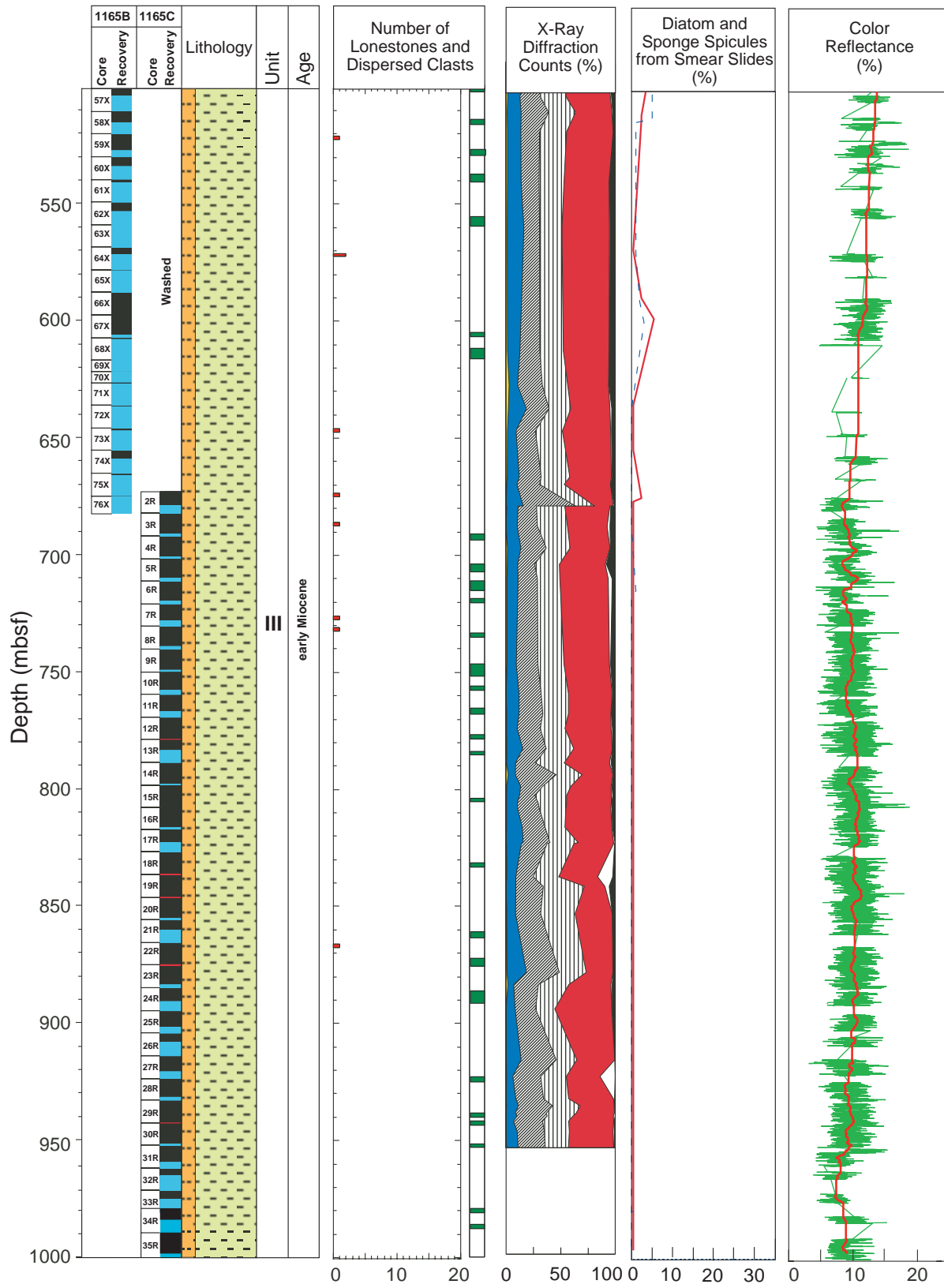


Figure 23 (Cont.)

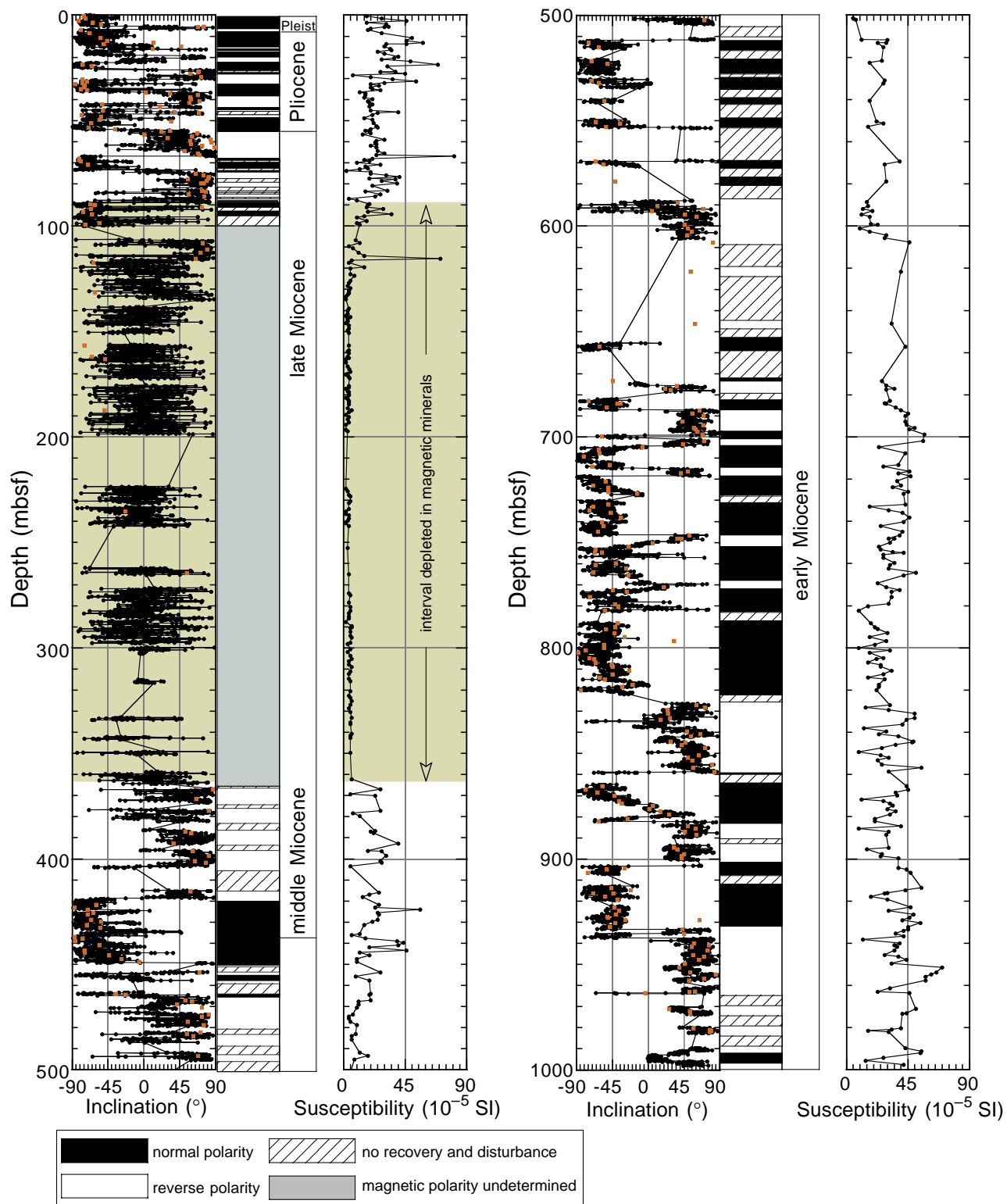


Figure 24

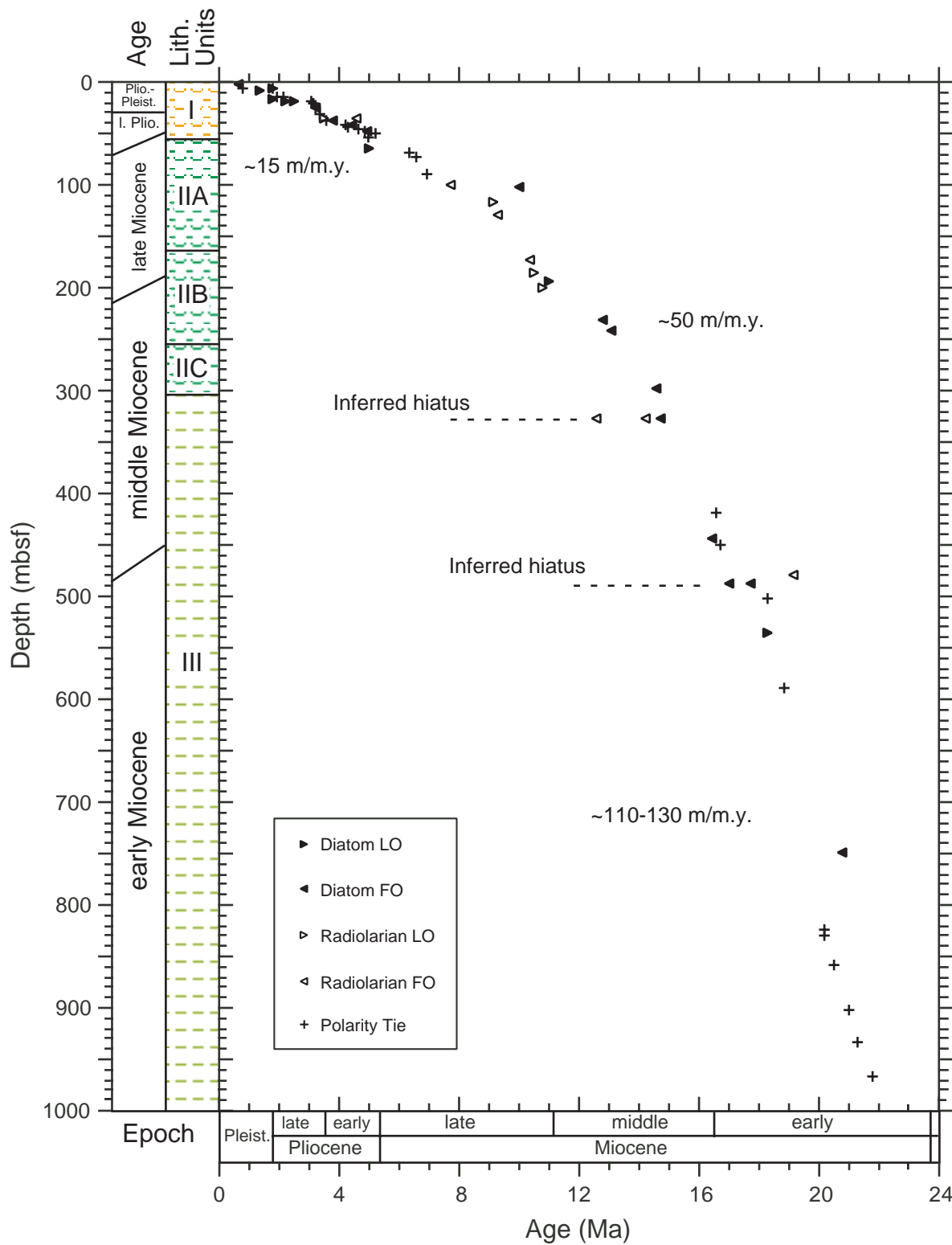


Figure 25

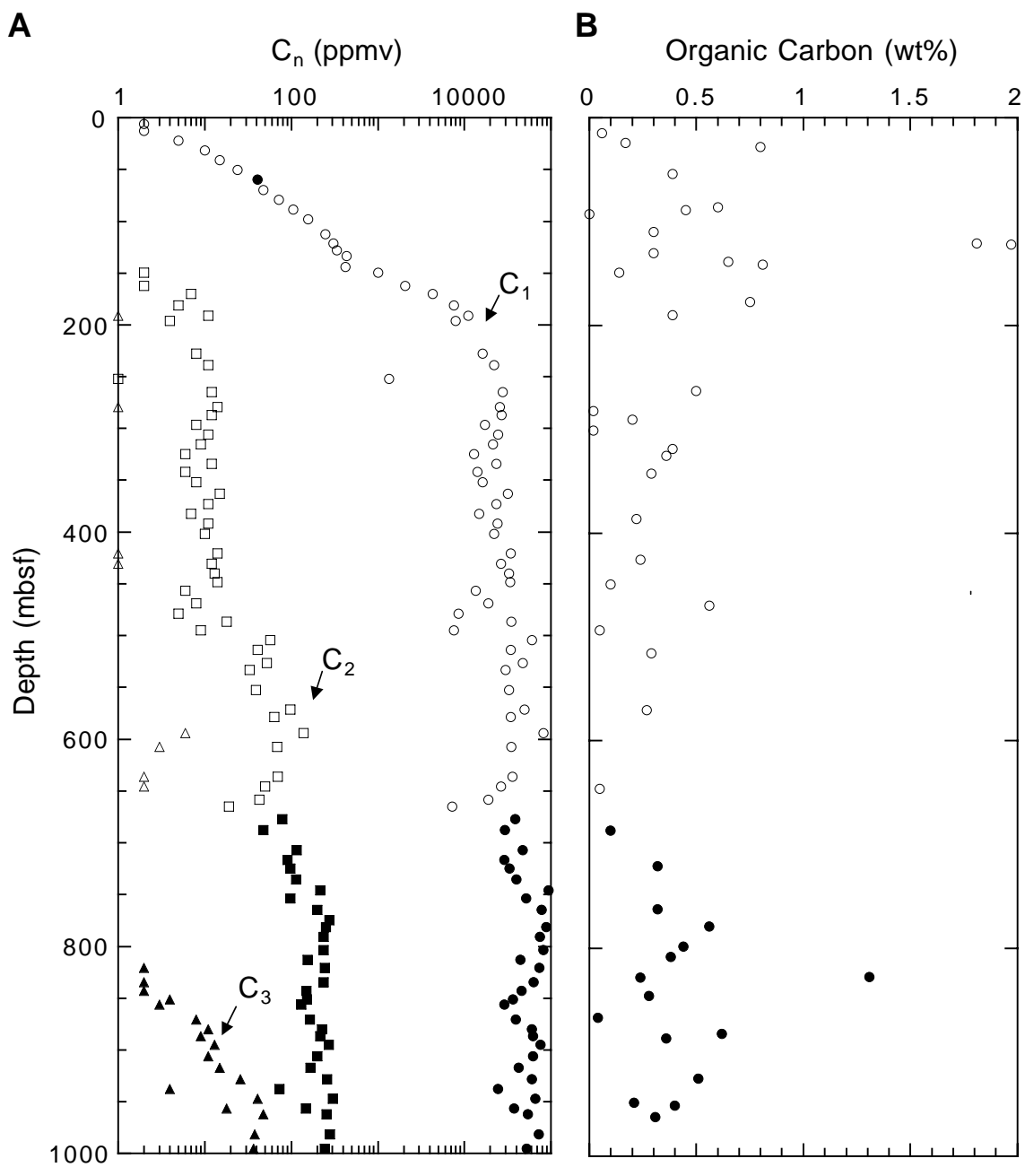


Figure 26

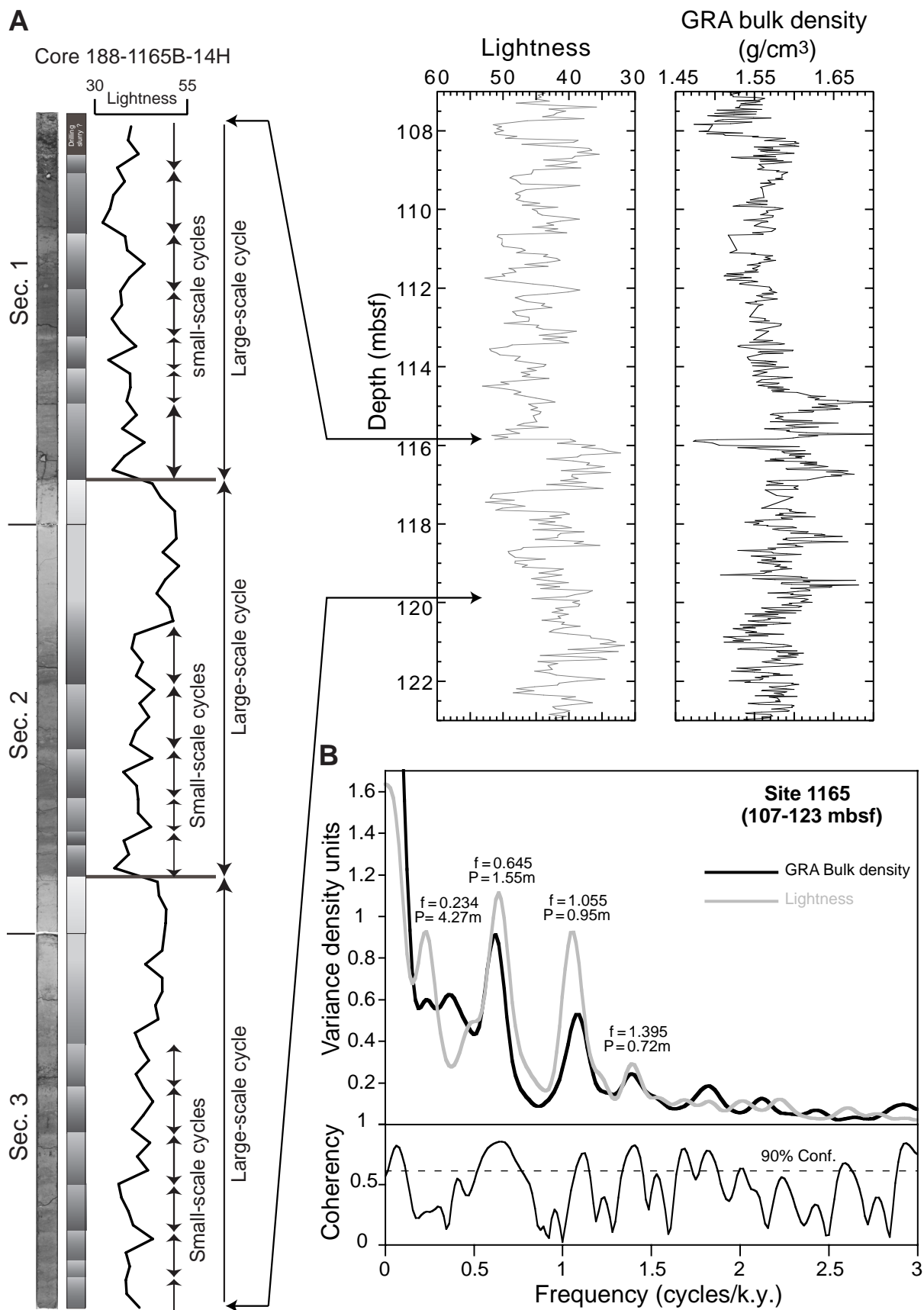
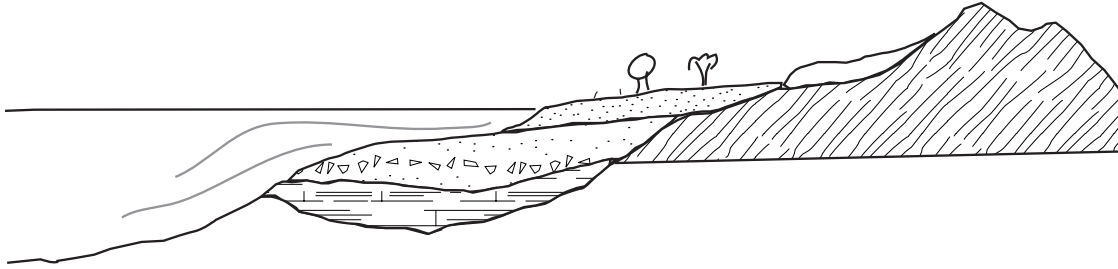
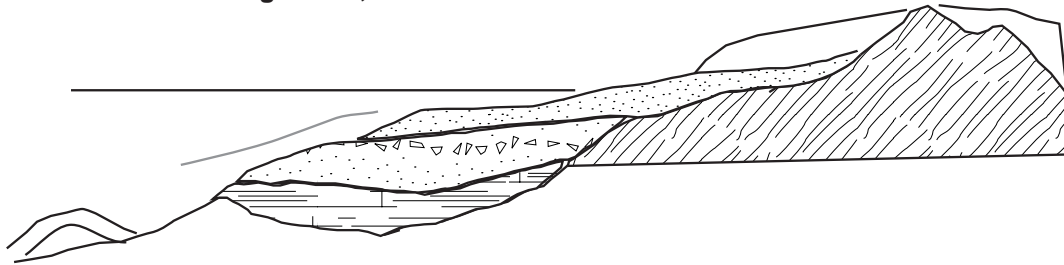


Figure 27

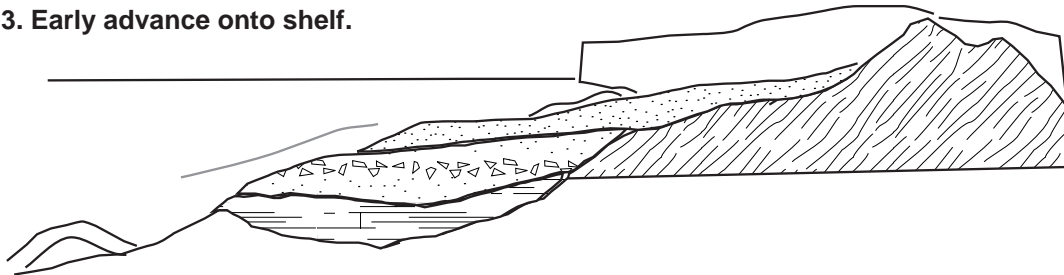
1. Glacial onset, fluvial outwash, vegetation.



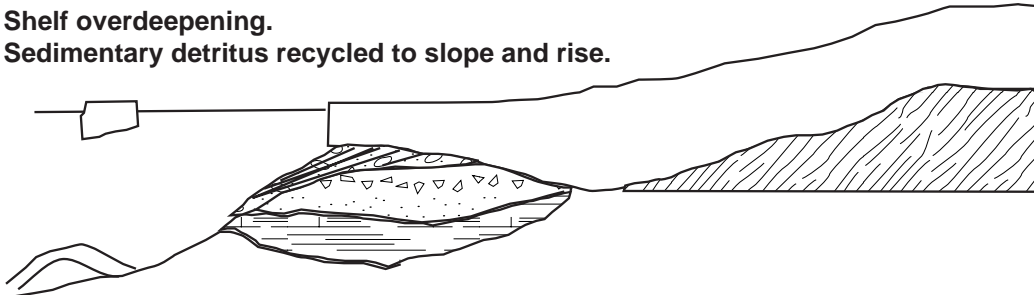
2. Small continental glaciers, fluvial outwash.



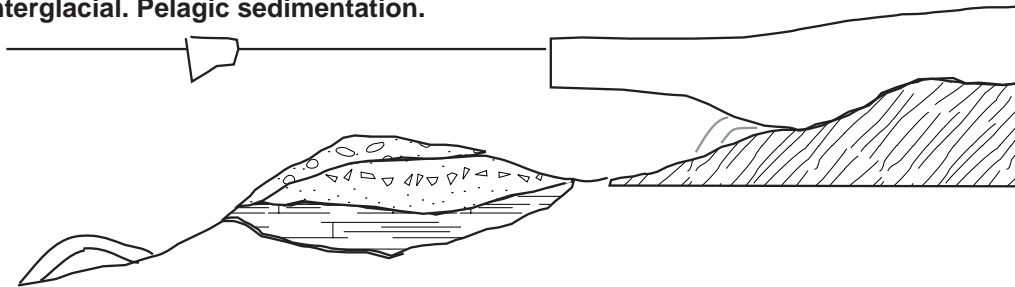
3. Early advance onto shelf.



**4. Shelf overdeepening.
Sedimentary detritus recycled to slope and rise.**



5. Interglacial. Pelagic sedimentation.



Temperate
+
Transitional
+
Cold polar

Figure 28

OPERATIONS SYNOPSIS¹

PORT CALL

Leg 188 began on 10 January 2000 at 1027 hr with passage of the first line ashore to Berth “E” of Victoria Quay, Fremantle, Australia. After a six-day port call the last line was released at 0606 hr on 16 January from the pier, and the *JOIDES Resolution* transited to a location off Rottnest Island for shallow-water positioning testing. Approximately 8 hr was spent testing two custom-built Nautronix positioning beacons in ~30 m of water. By 1800 hr on 16 January 2000, the *JOIDES Resolution* was under way at full speed to the first site of Leg 188.

Fremantle to Site 1165

The 2676-nmi sea voyage to proposed site PBD-12B was accomplished at an average speed of 9.6 kt in 12 days. Several severe (force 10/12) gales were encountered en route. The storms led to several course changes and speed reductions that were due to sea state. At times the vessel was rolling 10°–15° and pitching 6°–8°. Seas of 12 m and swells as high as 3 m were not uncommon. Conditions began to improve considerably near 60°S latitude.

At 0930 hr on 28 January 2000, the vessel slowed down to 6 kt while the seismic equipment was deployed. The objective was to conduct a single-channel seismic survey to confirm the precruise survey line. The seismic survey was concluded by 1400 hr on 28 January, and the seismic equipment was retrieved.

SITE 1165

Hole 1165A (Proposed Site PBD-12A)

A beacon was dropped on the Global Positioning System (GPS) coordinates of Site 1165 at 1500 hr 28 January 2000. Once the hydrophones and thrusters were deployed and the vessel settled on location, the corrected precision depth recorder depth referenced to the dual elevator stool indicated a seafloor depth of 3552.4 meters below rig floor, equivalent to 3541.3 meters below sea level (mbsl).

Hole 1165A was spudded using the advanced hydraulic piston corer (APC) at 0450 hr on 29 January 2000. The hole was scheduled for a single mudline core, which recovered 5.43 m of sediment and placed the drill pipe–measured seafloor depth at 3537.0 mbsl. The bit was pulled clear of the mudline, and the hole was abandoned at 0515 hr.

¹The Operations and Engineering personnel aboard the *JOIDES Resolution* during Leg 188 were ODP Operations Manager Michael Storms, ODP Operations Engineer Deryll Schroeder, Schlumberger Engineer Steven Kittredge, and Anadrill Engineer Peter Sammann.

Hole 1165B

An offset was not deemed necessary, and Hole 1165B was spudded at 0610 hr on 29 January 2000. The APC bit was positioned at 3534.95 mbsl and the water depth was established at 3537.65 mbsl, based on recovery of the mudline core. APC coring continued through 18H to a depth of 148.3 mbsf. Piston coring was abandoned at that depth because of a continuing problem with jammed liners and poor recovery. Adara temperature tool measurements were taken at the mudline and at the depth of Cores 4H, 7H, 10H, and 14H. Data from the position of Core 7H could not be retrieved. Coring proceeded using the extended core barrel (XCB). Operations were suspended when iceberg Nora approached to within 2.0 nmi of the drill site. Core 29X was recovered from a depth of 252.4 mbsf, and the drill string was pulled up to 50 mbsf. At 1630 hr on 30 January 2000, the iceberg had moved to a distance of 2.6 nmi on a course that was taking it directly away from the drill ship. XCB coring resumed at 1800 hr on 30 January. Coring proceeded with excellent results through Core 67X to a depth of 607.3 mbsf. The XCB system was pushed in hard material beyond its normal use to a depth of 682.2 mbsf (Core 76X) because it was assumed that the hard formation might be penetrated in a few tens of meters. Unfortunately, the steadily declining rate of penetration and poor core recovery indicated that this was not the case. The last XCB core was recovered on 3 February at 1500 hr, and the decision was made to terminate coring in Hole 1165B in favor of rotary core barrel (RCB) coring. The hole was displaced with 18.8 bbl of cement, and the pipe was tripped back to the surface. The rotary table was cleared at 0530 hr on 4 February, ending Hole 1165B.

Hole 1165C

The vessel was offset 50 m to the west, and Hole 1165C was spudded at 1805 hr on 4 February. The seafloor depth was established as 3537.55 mbsl. The hole was washed down to a depth of 54.0 mbsf, where Core 1R was taken from 54.0 to 63.6 mbsf, recovering an interval missed in Hole 1165B. A center bit was deployed, and the hole was drilled down to a depth of 673.0 mbsf. Continuous RCB coring began at that depth and continued until 1445 hr on 6 February, when iceberg Mona came to within 4 nmi of the drill site. Core 5R was recovered, the drill pipe was pulled back to a depth of 75.1 mbsf, and a free-fall funnel (FFF) was deployed.

Mona approached within 2.1 nmi before moving on a path away from the ship. The pipe was tripped back in the hole at 0500 hr on 7 February, and RCB coring resumed at 1015 hr. A total of 19.25 hr was lost as a result of the approach of iceberg Mona. Continuous RCB coring continued until iceberg Lea headed toward the drill site on a southeasterly course. At 2015 hr on 8 February, coring had to be suspended after recovering Core 13R from a depth of 893.6 mbsf. Lea was moving rapidly toward the drill site at a speed of 0.7 kt and with a closest point of approach of 1.0 to 3.0 nmi, depending on the assumed course. The drill string was pulled to a depth of 75.1 mbsf. At 0600 hr on 8 February, the iceberg reversed course to north-northwest and sped up to 0.3 kt. Lea appeared to be moving away by 1115 hr on 8 February and was no longer considered a threat to drilling operations. The drilling assembly was run to bottom, and at 1515

hr on 9 February continuous RCB coring resumed. A total of 19.0 hr was lost due to the first encounter with iceberg Lea.

Coring proceeded with excellent results until Lea turned around and headed back toward the location, closing to within 5.0 nmi. Coring was suspended with the recovery of Core 32R from a depth of 970.2 mbsf, and the drill string was pulled to a depth of 75.1 mbsf. Lea moved to within 0.5 nmi of the ship's position at 2015 hr on a course and bearing likely to bring it even closer to the drillship. The decision was made to pull the drill pipe clear of the seafloor and to move the ship 0.7 nmi away from the location. Lea passed within 200 m of Site 1165. Ultimately Lea moved away, and the ship moved back over the location. Hole 1165C was reentered at 0250 hr on 11 February, the pipe was run to bottom, and coring resumed by 0915 hr. A total of 25.0 hr was lost as a result of the second encounter with iceberg Lea.

Only one core (33R) was cut before another iceberg, Bertha, approached to within 5.0 nmi of Site 1165. The drill string was pulled to the surface for the third time. Before Bertha moved out of range, another smaller, apparently wind-driven iceberg, Bertie, moved into the safety zone. At 1145 hr on 12 February, Bertie was at 3.7 nmi away from the location and moving away. The drill string was run back into the hole. A total of 28.0 hr was lost because of icebergs Bertha and Bertie.

Cores 34R and 35R were recovered before coring ended at a total depth of 999.1 mbsf. The pipe was raised to 89.7 mbsf, and preparations for logging were made.

Logging Operations in Hole 1165C

The first suite of logging tools was ready to be deployed at 0915 hr on 13 February. A 2-hr interruption was caused by an iceberg that was headed to the location from a distance of 3.9 nmi but changed course abruptly away from the drill site. The first logging string, the triple combination tool (triple combo), was deployed at 1200 hr. The triple combo string was composed of the dual-induction tool model E (DITE), high-temperature lithodensity sonde (HLDS), neutron array porosity sonde (APS), and high-temperature natural gamma sonde (HNGS). Unfortunately, the winch operator was unable to lower the tools past 118.3 mbsf. All attempts to pass beyond the tight spot or ledge were futile, and the decision was made to recover the logging tools and lower the drill string three additional stands to 175.9 mbsf. This time the tools reached 991.3 mbsf, or 7.8 m above the total depth of the hole. Good logs were recovered from this run, and the tools were recovered at 2400 hr.

The tools for the second logging run consisted of the Formation MicroScanner (FMS), digital sonic imager, and natural gamma tool. This string was run in the hole at 0215 hr on 14 February; however, a restriction in the hole prevented passage beyond 580.3 mbsf. A complete hardware failure prevented any FMS data from being collected. Sonic and natural gamma data were successfully obtained from the upper part of the hole. Hole 1165C was abandoned by setting a 30-m balanced plug cement.

The pipe trip from the seafloor commenced at 1315 hr, and by 2030 hr on 14 February the rig floor was secured, the thrusters were raised, the beacons were recovered, and the ship was under way for Site 1166.

Transit to Site 1166 (PBS-9B)

Based on satellite images from the National Ice Center (Washington, D.C.) and reports we had received from the *Hakurei-Maru*, a research vessel that had been operating in the area a week before our approach, it was unlikely that the primary shelf site (PBS-2A) would be ice free. Our plan was to locate the shelf site as far to the west as the ice would allow by heading for proposed site PBS-9A and proceed from there to the west toward proposed sites PBS-8A, PBS-7A, and possibly PBS-1A. During the transit into Prydz Bay, with ice floes to either side of the vessel, it became clear that it was unlikely that sites farther to the west would be ice free enough for drilling. The decision was therefore made to drill at site PBS-9A. Unfortunately, we discovered that a large iceberg was located directly over the selected drill site. As we were rapidly approaching our survey way point, we decided to move the site 3 nmi to the northwest. Permission for the new drilling location, dubbed PBS-9B, was requested by telephone and fax and granted during the approach to the site. The site survey ended before reaching the drill site because one water gun froze up and the other water gun broke an air hose. There was not enough time to fix these problems because the ship had to be on location before dark, in view of the close proximity of numerous icebergs and ice floes in the area.

SITE 1166

Hole 1166A

Hole 1166 was spudded with the RCB at 0745 hr on 16 February. Continuous RCB coring proceeded to a depth of 199.5 mbsf, when the passage of a significant low-pressure system led to a deterioration of weather conditions and sea state. Drilling operations were halted at 2130 hr on 17 February because shallow-water operating guidelines were in effect limiting our operating environment to <2 m heave and wind gusts of <40 kt. When an iceberg reached to within a distance of 0.6 nmi, the decision was made to pull the drill string clear of the seafloor. A FFF could not be deployed because of the hard seafloor. The drill string was raised to a safe height and the vessel was offset 1.0 nmi, allowing the iceberg to move directly over the vacated drill site. As the iceberg and the low-pressure cell moved across Site 1166, conditions had improved enough by 0630 hr on 19 February to deploy the subsea camera and reenter Hole 1166A. The reentry operation took a mere 13 min without the aid of a guide cone or funnel. A total of 38 hr was lost because of the storm.

The reentry showed that the seafloor was 6.7 m higher than identified by the driller's blind tag with the bit at the start of the hole. Observations with the television camera showed a seafloor

depth of 480.0 m. Continuous RCB coring resumed and continued to a depth of 381.3 mbsf. Overall recovery for the hole was 18.6%.

In preparation for logging the bit was released, the hole was displaced with sepiolite logging mud, and the drill string was tripped to the logging depth of 41.2 mbsf. The hole was logged with a full suite of sensors (seismostratigraphic suite, lithoporosity suite, FMS suite, and the geological high-sensitivity magnetic tool) from 41.2 to 377.3 mbsf. All logging runs were successful. By 0745 hr on 21 February, the logging sheaves had been rigged down and the wireline logging program was completed.

The hole was abandoned with a 21.5-bbl plug of cement, and the drill pipe was pulled clear of the seafloor and tripped back to the ship. At 1600 hr on 21 February, the rotary table was clear, ending Hole 1166A.

Hole 1166B

Hole 1166B was planned as a test of the measurement- and logging-while-drilling (M/LWD) tools. This included the transmission of data in real time by using a downhole turbine-driven mud pulsing unit.

The drill string was tripped to bottom, and Hole 1166B was spudded at 0020 hr on 22 February. The seafloor depth was determined to be 480.0 mbsf, and the first hard layer was contacted at 485 mbsf. Drilling proceeded very slowly for the first 25 m. Very little weight could be put on the drill string until at least the M/LWD tools were buried beneath the seafloor. The hole was terminated at a depth of 42.5 m because the objectives of the test had been met and the ability to pulse back data in real time was confirmed.

The hole was displaced with heavy mud, and the drill pipe was pulled clear of the seafloor by 1020 hr. The beacon was released and recovered aboard at 1050 hr. The pipe was back aboard ship and the M/LWD tools rigged down by 1330 hr on 22 February, and the *JOIDES Resolution* was under way for the final site of Leg 188.

SITE 1167

Hole 1167A (PBF-6A)

The 97-nmi voyage to Site 1167 was accomplished at an average speed of 11.4 kt. The vessel approached the GPS coordinates of the site on 22 February at 2200 hr, and a beacon was deployed at 2238 hr. Hole 1167A was spudded with the APC at 0925 hr on 23 February. The seafloor depth was established from the recovery of the first core at 1651.3 mbsl. APC coring advanced without incident, but with varying recovery (77% to 103%) to 39.7 mbsf. APC refusal was reached when the core barrel of Core 6H did not achieve a full stroke and was recovered empty and partially bent. A successful Adara tool heat-flow measurement was taken at the mudline and on Core 5H. Coring with the XCB system resumed at 1445 hr with Core 7X and

continued through Core 21X to a depth of 179.2 mbsf, when operations had to be suspended because of an approaching iceberg. After pumping a 30-bbl sepiolite mud sweep, the pipe was pulled to 42.6 mbsf while the movement of the iceberg was monitored. The iceberg came to within 0.1 nmi before sliding past the drill site. The decision was made to run back to bottom and resume coring by 1000 hr, when the iceberg had reached a range of 0.3 nmi and was moving away from the drill site. XCB coring was resumed and continued until Core 28X was recovered from a depth of 246.5 mbsf. Yet another iceberg approached the drill site at 2345 hr on 24 February. This iceberg came to within 0.5 nmi of the vessel. The iceberg was monitored for an hour, during which time it passed the drill site and was moving away. The drill string was again run to bottom with the top drive still in place. At a depth of 161.7 mbsf the driller noted 25,000 lb of downward drag. Light reaming was required to reach bottom. A core barrel was deployed, and at 0600 hr on 25 February XCB coring resumed.

Coring operations were short lived, however, when another iceberg arrived on the scene. After recovering Core 34X from a depth of 303.2 mbsf, the drill string was once again pulled back to the seafloor, with the end of the pipe placed at 42.6 mbsf.

The plan was to deploy a FFF once the pipe was at a safe depth below the seafloor. This plan had to be changed when the iceberg increased its approach speed and changed course, moving directly toward Site 1167. The decision was made to not deploy the FFF and to remain in position to pull the remaining drill pipe free of the seafloor should the need occur.

On 25 February at 2145 hr, the iceberg had moved to a distance of 1.5 nmi from the drill site and was continuing away at a rapid rate. The decision was made to deploy the FFF at this point because more icebergs were in the vicinity. The drill string was once again run into the hole. As before, the driller encountered an obstruction at 168.7 mbsf, resulting in 25,000 lb of down drag and requiring light reaming to reach the bottom.

Coring continued to Core 49X to a total depth of 447.5 mbsf. Recovery and rate of penetration were extremely variable throughout the coring cycle as we intermittently drilled through coarse sand and gravel beds and encountered occasional dropstones. The decision was made to halt coring operations short of the 620 mbsf objective to conserve adequate time for wireline logging and LWD operations, and to meet the 15-hr early departure from the site required as an additional transit-time contingency.

Logging Operations in Hole 1167A

In preparation for logging, the XCB bit was placed at a depth of 86.9 mbsf, and the Schlumberger wireline sheaves were rigged up. The first suite of logging tools to be deployed was the triple combo consisting of the DITE, HLDS, APS, and HNGS. The tools were deployed on 27 February at 1905 hr; however, they could only be lowered to a depth of 148.7 mbsf, or 61.7 m below the end of the pipe. This short section was logged back to the bit. The tool could not be retracted back into the pipe without circulating the rig pumps to open the flapper valve.

While the logging tools were being recovered, it was decided that further wireline logging efforts had to be abandoned. The logging tools were laid out, and by 2400 hr on 27 February the Schlumberger wireline sheaves were rigged down. The hole was filled with a 30-m cement plug, and the pipe was pulled clear of the seafloor by 0215 hr. The bit cleared the rotary table at 0825 hr, ending Hole 1167A. Total time lost because of icebergs and ice-related problems amounted to 26.75 hr at Hole 1167A.

Hole 1167B

The vessel was offset 50 m to the northwest for a dedicated M/LWD hole. After waiting on weather for 4.25 hr, the drill string was tripped to the bottom and Hole 1167B was spudded at 2100 hr on 28 February. Drilling with the M/LWD system proceeded smoothly throughout the night with excellent results. The time allocated for this operation ran out at 0930 hr on 29 February, and drilling was halted at a depth of 261.8 mbsf. All M/LWD systems and the real time data telemetry equipment performed perfectly.

The hole was displaced with 66 bbl of bentonite gel mud, and the pipe was recovered, clearing the seafloor at 1110 hr on 29 February. During the pipe trip, the positioning beacons were released and recovered. While we attempted to release the third beacon, the portable command unit cable was sucked into the No. 6 thruster well. The cable was severed immediately, and the transducers head was lost. As a result beacon No. 3 could not be released. The hydrophones and thrusters were retracted, and the drilling equipment was secured for transit. At 1730 hr on 29 February 2000, the vessel departed the last site of Leg 188.